Evaluation of Short Term Aging Effect of Hot Mix Asphalt Due to Elevated Temperatures and Extended Aging Time

by

Rubben Lolly

A Thesis Presented in Partial Fulfillment
of the Requirements for the Degree
Master of Science

Approved April 2013 by the
Graduate Supervisory Committee:

Kamil Kaloush, Chair
Wylie Bearup
Claudia Zapata
Michael Mamlouk

ARIZONA STATE UNIVERSITY

May 2013

ABSTRACT

Heating of asphalt during production and construction causes the volatilization and oxidation of binders used in mixes. Volatilization and oxidation causes degradation of asphalt pavements by increasing the stiffness of the binders, increasing susceptibility to cracking and negatively affecting the functional and structural performance of the pavements. Degradation of asphalt binders by volatilization and oxidation due to high production temperature occur during early stages of pavement life and are known as Short Term Aging (STA). Elevated temperatures and increased exposure time to elevated temperatures causes increased STA of asphalt.

The objective of this research was to investigate how elevated mixing temperatures and exposure time to elevated temperatures affect aging and stiffening of binders, thus influencing properties of the asphalt mixtures. The study was conducted in two stages. The first stage evaluated STA effect of asphalt binders. It involved aging two Performance Graded (PG) virgin asphalt binders, PG 76-16 and PG 64-22 at two different temperatures and durations, then measuring their viscosities. The second stage involved evaluating the effects of elevated STA temperature and time on properties of the asphalt mixtures. It involved STA of asphalt mixtures produced in the laboratory with the PG 64-22 binder at mixing temperatures elevated $25^{O}F$ above standard practice; STA times at 2 and 4 hours longer than standard practices, and then compacted in a gyratory compactor. Dynamic modulus (E*) and Indirect Tensile Strength (IDT) were measured for the aged mixtures for each temperature and duration to determine the effect of different aging times and temperatures on the stiffness and fatigue properties of the aged asphalt mixtures.

The binder test results showed that in all cases, there was increased viscosity. The results showed the highest increase in viscosity resulted from increased aging time. The results also indicated that PG 64-22 was more susceptible to elevated STA temperature and extended time than the PG 76-16 binders.

The asphalt mixture test results confirmed the expected outcome that increasing the STA and mixing temperature by 25°F alters the stiffness of mixtures. Significant change in the dynamic modulus mostly occurred at four hour increase in STA time regardless of temperature.

DEDICATION

To my mother and father Victoria Akakpo and Jacob Loli who always gave me love and care, and to my wife ShaRonda and children Saraia, Samaya and Ryeland whose sacrifice and support always gave me energy and encouragement to persevere.

ACKNOWLEDGEMENTS

My first gratitude goes to God, the Father Almighty, who gives me strength and wisdom to seek knowledge and understanding, and without whom my life will have no meaning.

Secondly I would like to thank my advisor and Chair of my committee Dr. Kamil E. Kaloush, whose encouragement, support and patience helped me complete this thesis project. His perspectives and guidance enabled me to attain my goals for the master program.

I would also like to thank Dr. Wylie Bearup whose exemplary leadership and knowledge encourages me to yearn for excellence. Thanks to Dr. Claudia Zapata and Dr. Michael Mamlouk who have been part of my education and given me invaluable knowledge through my education at ASU. The knowledge they gave will always be part of me and be part of the gateway to new ideas and possibilities in life and I will remain grateful to them for that. I thank Dr Waleed Zeiada who supported me and spent valuable time with me in the lab and sharing his knowledge of the intricacies of conducting dynamic modulus testing to ensure the success of this project. None of this work would have been possible without his help.

I thank the Arizona Department of Transportation (ADOT), the Arizona Pavements Materials conference committee and Bob McGennis for proposing this study and providing support through the study. Thank you to David Ramsey and all my colleagues in Advanced Pavements Research Group, their friendship, support and assistance made the difficult times short-lived. Lastly I thank my coworkers at the City of Phoenix and friends whose support sacrifices gave me added reason to complete this process. Their contributions are immeasurable and of immense value to me through my graduate study and I am thankful for that.

TABLE OF CONTENT

Page

Page

Page

LIST OF TABLES

Table Page

Table Page

LIST OF FIGURES

Figure Page

Figure Page

Figure Page

Figure Page

INTRODUCTION

Background

Construction of asphalt pavements involves the production of the asphalt mixtures at temperatures prescribed by asphalt binder manufactures. The temperature is necessary to enable softening of the asphalt to a viscosity that enables coating of the aggregates. After an asphalt mixture is produced, it is transported to the construction site to be placed and compacted into an asphalt pavement. Placement and compaction of asphalt pavements require minimum temperatures for the construction of a quality and good performing pavement.

After an asphalt mix is produced, it is transported to the construction site in trucks. Between the time of loading a truck at the production plant and transporting it to the construction site, the asphalt mixes will continue to lose some heat. This loss of heat from the mix can, sometimes, results in the mixes arriving at the construction site with temperatures below specified lay down and compaction temperature. Such cases cause loads of asphalt mixes to be rejected causing waste of material, delays in construction scheduling and the risk of disputes resulting from delays in the completion of projects.

Particularly in cooler temperature regions or seasons with harsher weather conditions, or areas where construction sites are farther away from asphalt production plants, the loss of temperature can be even more of a problem and affects quality control parameters for pavement construction such as compaction and air voids. In addition to the difficulty in achieving or maintaining compaction temperatures in cooler seasons, most agencies require minimum surface temperatures before allowing paving to occur. For example, in the 2012

Maricopa Association of Governments (MAG) uniform standard specifications for construction, a minimum surface temperature of 45°F and rising is required to allow paving operation to proceed. This leads to paving operations that are halted, delayed or shut down during the winter months. To overcome these delays and waste associated with constructions shut downs, contractors have proposed that hot mix asphalt be produced at higher than prescribed temperature as long as compaction densities or target air voids and binder contents are achieved in the field.

However, the concern with elevated temperatures is that they may further degrade the asphalt binder to a level beyond that caused by normal production temperatures; thus increasing the degree of short term aging to a level that may adversely affect the performance of the asphalt pavement. Several research studies have shown that the volatilization and oxidation are the biggest contributors to the hardening (aging) process of asphaltic binders (Clark, R.G. 1958)

These mechanisms are enhanced at elevated temperatures hence increasing the aged properties of the binders in the mixture. In some instances, longer hauling distance means that the hot mix asphalt will be subjected to elevated temperature for a longer period of time, possibly causing further hardening. The combined effect of elevated temperature and longer exposure time may cause excessive short term aging and adversely affect the performance of the pavement.

This research study aimed on quantifying how much further aging occurs beyond normal mixing temperatures and exposure times of asphalt mixes. The quantification is achieved by measuring viscosities of aged binders as well as measuring the dynamic modulus and the

indirect tensile strength properties of laboratory manufactured, aged and compacted asphalt mixtures.

Objectives

The objective of this study was to investigate the effect of elevated temperatures and extended exposure time on short term aging properties of asphalt binders and mixtures. The objectives were achieved in two stages. The first stage involved determining the short term aging properties of the binders conduct by laboratory aging of two Arizona binders and measuring the viscosities and penetration. The second stage involved aging loose mixtures at different temperatures and aging times. The aged samples were compacted and then their dynamic modulus and indirect tensile strengths were measured. The results were compared to establish correlations between the properties of the differently aged samples and their laboratory performance, upon which conclusions was drawn.

Scope of Work

The scope of work for this project was divided into two main parts. During the first part, Two Arizona performance graded virgin (unmodified) asphalt binder (PG 64-22 and PG 76-16) were aged in Rolling Thin Film Oven (RTFO) using ASTM D2872 test protocol. The samples were supplied by Holly Asphalt in collaboration with the Arizona Department of Transportation (ADOT). The binders were aged at 322^{o}F and 350^{o}F, with aging times of 85 minutes for both binders, and aging time of 170 minutes on the PG 64-22 binder. The aged binders were then tested to measure their viscosities, penetration and softening point. Based on the result, the PG 64-22 binder was selected for the second stage of the research study.

The second phase of the research study consisted of aging laboratory produced asphalt mixtures in their loose state then compacted into gyratory plugs. The loose samples were aged at 300°F and 310°F and aging times of 4, 6 and 8 hours. The effects of aging on the properties of the samples were determined by characterizing the compacted aged mixtures. Dynamic Modulus (E*) using AASHTO test protocol (AASHTO TP-62-07) was measured to determine the stiffness characteristics. Indirect Tensile Strength (IDT) using ASTM test method (ASTM D6931-07) was measured and the fracture energy calculated to determine the fatigue characteristics of the aged samples.

LITERATURE REVIEW

Introduction

The testing procedures were determined prior to starting this study. However a literature review was conducted to assess work done on short aging of asphalt binders and asphalt mixtures. A summary of the literature review and the testing protocols used in this study is presented in this section.

Short term aging of asphalt binders refers to the hardening of asphalt that occurs during mixing, storing, transporting and placement operations. This hardening is a result of the volatilization and loss of lighter aromatic fractions from the binder due to exposure to high temperature, leaving behind larger and stiffer fraction asphaltenes. Several factors affect how much aging of the asphalt binder occurs during this process. The extent of aging during mixing operation depend on the mixing temperature, the type of asphalt and other material used to produce the mix, mixing time and storage time. During transportation, the atmospheric temperature and haul distance affect the rate and amount of cooling. During lay down operations, waiting time of haul trucks and ground surface temperature also affect the amount and the rate of cooling. Generally higher temperature and longer exposure time to high temperature results in a greater degree of deterioration of asphalt binders and stiffening of asphalt mixtures. Temperature and the type of asphalt are important factors responsible for short term aging operations (Mirza, 1993). It is generally known that softer (low stiffness) binders are more affected by higher temperature than harder (higher stiffness) binders.

The reason for heating asphalt binders to high temperatures during mix production is to produce viscosities that will enable the coating of dry aggregates and also achieve minimum lay down temperatures. The 2009 Shell Handbook recommends that the best practices for

providing coating viscosity while limiting aging due to elevated temperatures is to use the minimum temperatures necessary to attain required coating viscosities (2009 Shell Handbook). It acknowledges the practice of mixing hot mix asphalt (HMA) at elevated temperatures to address the need for maintaining adequate lay down temperatures under conditions of low ambient temperatures and long hauling distances. The shell handbook however stated that the increased temperatures will "considerably accelerate the rate of bitumen oxidation which will decrease the viscosity of the bitumen. Thus a significant proportion of the reduction in viscosity achieved by increasing the mixing temperature will be lost because of additional oxidation of the bitumen" (2009 Shell Handbook). It recommends the use of lowest mixing temperatures and minimum mixing times.

Binder Aging Studies

Many researchers have studied the oxidation effect of high temperature on the behavior of asphalt binders and the subsequent effects on the performance of pavements. Oxidative hardening of asphalt binder causes the deterioration of many desirable properties that measure performance of asphalt mixes (Huang and Grimes, 2010). In their research to determine the effect of aging temperatures on the rheological and chemical properties of asphalt binders, Huang and Grimes found that a linear relationship existed between the physical properties and change of chemical properties due to oxidative aging. They measured the complex modulus (G*) of asphalt binders after subjecting them to short term aging (RTFO) followed by long term aging in a pressure aging vessel (PAV), and used the G* versus phase angle plot to characterize the rheological properties of the asphalt mixes. They concluded that regardless of oxidation time-temperature combination used to produce a mix, a plot of G* versus phase angle showed a correlation with the oxidative aging products

formed during aging (Huang and Grimes, 2010). Although their work measure long term aging, Huang and Grimes work demonstrated the detrimental effect of oxidative aging on asphalt mix properties.

The effect of short term aging on asphalt binders is measured in the laboratory by the Rolling Thin Film Oven Test (RTFOT), which exposes the binder to continuous heat and air flow that promotes oxidation to cause aging. Asphalt binders are organic bituminous substances hence are affected by the presence of oxygen, ultra violet radiation and changes in temperature resulting in increased penetration increase in softening point and viscosity (Airey and Brown, 1998). Airey and Brown also reported from test results that bitumen experienced a decrease in aromatics and an increase in asphaltenes and resins as well as changes in their chemical composition due to aging process (oxidative hardening) caused by RTFOT. Their test measured the rheological changes that occurred after the short and long term aging using Penetration, Softening Point, Viscosity and Dynamic Shear Rheometer test on the binders. They also measured the percentage changes in saturates, aromatics, resins and asphaltenes using Iatroscan thin film chromatography. Their results showed a decrease in aromatics and an increase in asphaltenes.

As mentioned earlier mixing time as well as longer time of exposure to high temperatures during transportation to construction sites affects the oxidative hardening of asphalt bonders. Lee et al (2007) conducted a research to compare the aging effect of RTFOT and Short Term Oven Aging (STOA) in the lab and in the field. They measured viscosity on the premise that increased viscosity of the binders resulted in an increase in the large molecular size (LMS) particles thus increasing the stiffness of the asphaltic binders. They measured this

change in viscosity by the method of gel permeation chromatography (GPC). They also conducted the RTFOT at five different times (70, 85, 100,115, and 240 min) and evaluated effects of these five aging times to simulate the short-term aging of asphalt binders in the laboratory. Their results are shown in Figure 1 and Figure 2 below. They found that longer aging time resulted in increased LMS ratio, higher viscosity and high failure of asphaltic binders.

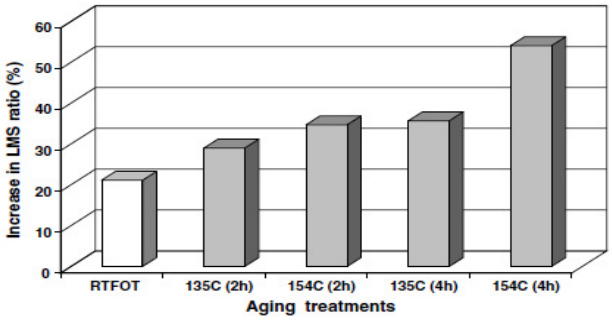

Figure 1: Aging effect (increase in LMS ratio) by Short-Term Aging Treatments in the Laboratory.

Source; (S.-J. Lee et al. / Construction and Building Materials August 2007)

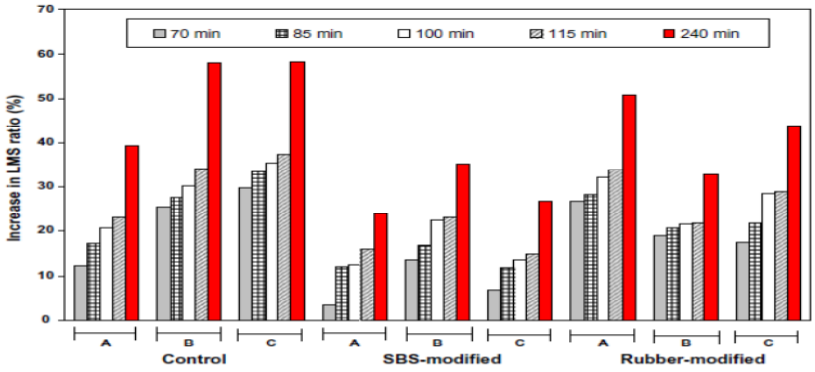

Figure 2: Aging Effect (increase in LMS ratio) by Aging Time in the RTFOT.

Source; (S.-J. Lee et al. / Construction and Building Materials August 2007)

The effect of binder properties alone is insufficient to completely evaluate the effect of aging in an asphalt mixture. Aging of asphalt mixture in the field is significantly influenced by the

several factors relating to the mix such as heat applied to the mixture during production, initial void ratio and densification of the mixture under traffic among other factors. Therefore relying on the laboratory simulation of the binder alone to simulate the aging of the asphalt mixture is impossible (Brown et al, 2009). Brown et al go on to mention that, binder testing is still important because it serves as a means to identify and eliminate binders that will age too quickly.

Binder Aging

The Rolling Thin Film Oven Test (RTFOT) method is used to simulate hardening of asphalt binders in the laboratory. The RTFOT conditions are not identical to those found during actual mixing but has proven to correlate the amount of hardening during the test and that observed in the conventional batch mixer (Airey and Brown, 1998). The rolling thin film oven test was first adopted in 1970 as ASTM D2872 (Airey and Brown, 1998). It simulates the hot mix process by bringing a heated asphalt film into contact with hot air allowing the oxygen in the air to induce the oxidative aging process while enabling the heating process to volatilize the lighter component of the asphalt bitumen.

The RTFOT procedure is prescribed by ASTM the designation ASTM D2872. It involves pouring 35 grams of asphalt into each of eight RTFOT glass bottles that are placed horizontally in a vertically rotating shelf located in an oven maintained at 163^{o}C during the test. The shelf rotates at a speed of 15 revolutions per minute. The open mouth of the bottle faces outward towards a nozzle blowing air at the rate of 4L/min. The test is run for 85 minutes after which asphalt binder is scraped from the bottles and tested for their properties.

Binder Testing

Testing methods used to measure the consistency of asphalt are the Brookfield rotational viscosity test, penetration test, and softening point test. The Brookfield Rotational Viscosity Test measures viscosity directly while the softening point and penetration tests measure viscosity indirectly using correlations from the test result.

The Brookfield test determines viscosity by measuring the resistance of the binder to shearing forces imparted by a rotating spindle inserted into the liquid binder rotating at a constant rate.

The summary description of the steps involved is presented. The chamber and selected spindle is preheated until the desired temperature is attained for at least 15 minutes. The asphalt samples is then poured into the sample chamber and inserted into a temperature control chamber heater. The spindle is then inserted into the asphalt sample to a depth that completely immerses the measuring unit of the spindle and it is attached to a rotational viscometer. Before measuring the temperature of the sample, it is brought to the target temperature within 30 minutes and allowed to equilibrate for 10 minutes. The viscometer is set to rotate the spindle at the desired rate and then it is started. The viscosity readings are allowed to stabilize for another five minutes. Three viscosity measurements are taken at 1 minute intervals for a total of three minutes then averaged together (ASTM D4402-06).

Penetration test involves the following steps as prescribed by ASTM. A sample of the binder in poured into a container so that the depth of the sample is at least 120% the expected needle penetration depth. Depending on the size of the container, the sample is cooled between 45 minutes to 2 hours. It is then conditioned by placing it in a water bath at the target temperature for another 45 minutes to 2 hours depending on the size of the sample.

The conditioned sample is next placed in a transfer dish filled with water from the temperature bath and placed under the penetrometer apparatus. The apparatus consists of a needle and spindle assemblage weighing approximately 50g that moves vertically without measurable friction. The assemblage is attached to a measuring device that can measure the depth of penetration and equipped with a timed release. The diameter of the needle is 1mm with a truncated tip. Additional weights of approximately 50g and 100g can be added to the needle assemblage depending on the testing conditions. Before starting the test, the needle is cleaned and placed flush against the surface of the binder in the sample container, and the measuring dial is set to zero. The needle is then released for 5 or 60 seconds, depending on temperature. The amount of drop of the needle is measured as the penetration number taken as 1pen = 0.1mm. Three measurements are taken and averaged as the penetration number for the sample (ASTM-D5-06).

The penetration measurements can be converted to viscosity using the following equation developed by Witczak and Mirza in 1995;

$\log\eta = 10.5012 - 2.2601 * \log(pen) + 0.00389 * (\log(pen))^2$, Where η is the Viscosity in poise (P) and Pen is the measured average penetration loading in 0.10mm.

The third test used to measure binder viscosity is the softening point test. It gives the indication of the tendency of the materials to flow under elevated temperature. In this test the binder is first poured into shouldered designed rings of approximately 23mm in diameter filled to a level above the brim. Excess binder over the top of the ring is cut to bring the binder is flush with the top and bottom of the ring. Ball guides are placed around the ring which is placed in a ring holder and assembly. The rings are then suspended in a glass water

bath containing distilled water at a temperature of 5±1°C. The binder samples and steel balls with diameter of 9.5mm and mass of 3.50g each are then conditioned for 15 minutes. After conditioning the steel balls are placed to rest at the center of the binders sample in the ring through the ball guides. The glass bath is then placed on hot plate and heated the bottom at a constant rate of 5°C/minute using the hot plate until it deforms and flows to touch a brass shelf placed below the ring assembly. The temperature at which the deformed sample touches the brass shelf at the bottom of the assembly shelf is recorded as the softening point of the binder. The softening point is the temperature at which the binder has a viscosity of 13,000 poise, cannot support a steel ball placed on it and begins to flow. (ASTM D36/D36M-09).

Short Term Mixture Aging Studies

Short Term Aging in the field is simulated in the laboratory using the Short Term Oven Aging (STOA) procedure which involves heating a loose mix in a forced draft oven for 4 hours at a temperature of 135°C (275°F) and has been validated in various past studies such as Bell, C.A., Weider, A.J., Fellin, M.J. reported in SHRP-A-390 (1994).

Research conducted by the University of California at Berkeley in conjunction with Oregon State University and Austin Research Engineers, Inc. evaluated the influence of aging in the performance test result of asphalt pavements. They concluded that 4 hours short-term aging adequately represents the effect of aging due to mix production and construction stages when the mix is in the loose state (HRP-A-417, 1994). They evaluated the effect of short-term aging by conducting resilient modulus and indirect tensile strength test on laboratory produced compacted samples that were subjected to 4-hrs of STOA in their loose state and then were followed by seven-day, long-term aging period of compacted samples. Their

results were then compared to samples that were not aged before long-term aging. Validation of their results was achieved by field testing new and young (4 years old) pavement sites using eight different types of asphalts dependant on their susceptibility to aging categorized into low, medium and high susceptibility to aging. They concluded that the short-term aging procedure produces a two-fold change in resilient modulus.

Azari (2011) conducted research to analyze the effect of laboratory short-term aging conditioning on the mechanical properties of asphalt mixtures. She conditioned asphalt samples at 145°C at half-hour intervals from zero to six hours and measured the dynamic modules at 4°C, 20°C, 40°C, and 45°C. Azari then constructed master curves for all the mixing times from 0 to 6 hours at 30 minutes intervals and compared the results. She concluded based there was a positive correlation between conditioning time and the dynamic modulus of the samples. Azari then performed a Scheffé analysis for conditioning time variations at the reference frequency of 10Hz on dynamic modulus values predicted from the master curve for the aged and un-aged samples and compared the results. The results of the Scheffé analysis indicated that for each pair of samples (aged versus un-aged) the effect of conditioning time was significant for the dynamic modulus and also concluded that the minimum conditioning time to measure changes in dynamic modulus of the mixture due short-term aging conditions was 3.5 hours.

When aged, asphalt mixtures tend to become stiffer and affect their performance. Stiffening of the mix should be considered a benefit due the enhanced load distributing and resistance to permanent deformation of the stiffened asphalt, however stiffening results in embrittlement of the HMA with reduced capacity to resist cracking and increased moisture

susceptibility. Baek, Underwood, and Kim, (2012) studied the effect of oxidative aging on the dynamic modulus and fatigue performance of asphalt mixtures. They subjected an asphalt mixture to four different degrees of aging including short-term aging procedure at 135°C for 4 hours and 85°C for 2 days, 4 days and 8 days. They then performed dynamic modulus and fatigue performance tests to characterize the linear viscoelastic and damage properties of the aged mixtures. They incorporated these properties into a comprehensive Visco Elastic Continuum Damage (VECD) analytical model enabling them to predict the affect of asphalt pavements in service and aging in hot and cold climates. Their findings show that the major effect of aging on the asphalt mixture is embrittlement which is manifest through increase in stiffness. Embrittlement has a noticeable effect on the damage growth in pavements which accumulates through the whole pavement structure (Baek, Underwood, and Kim, 2012). They also concluded that the stiffness of asphalt mixtures increases with aging time.

IDT and Fracture Energy Study

The reason for measuring indirect tensile strength is to characterize the resistance to low temperature cracking of hot mix asphalt concrete (Christensen, D. W., Bonaquist, 2004). Generally, stiffer samples have higher IDT strengths than weaker samples. However mixtures with higher resistance to fracture have higher fracture energy because they have better viscoelastric properties. In lower temperature conditions it is preferable to have a mixture with relatively lower tensile strength but higher fracture energy to help reduce the amount and extent of cracking in colder temperatures. Stiffer samples with lower resistance to fracture tend to perform poorly in cold temperature condition. Asphalt mixtures subjected to excessive aging are likely to become stiffer with higher tensile strength but are

also more brittle due to the loss of viscous components of the asphalt in the mix. Therefore excessively aged samples tend to resist cracking more rapidly especially in cold temperature when they are most brittle.

Standard Laboratory Short Term Aging (STA) Procedure of Asphalt Mixtures

The standard procedure for aging asphalt mixtures in the laboratory is carried out under AASHTO R30 - Mixture Conditioning of Hot-Mix Asphalt (HMA). This procedure is meant to represent the aging that occurs in the asphalt mixture caused by the construction activity. It is applied only to lose mix. During short term aging, the lose mix is place in a pan, and spread to an even thickness ranging between 1 to 2 in. (25 and 50 mm). The mixture and pan are then placed in a forced-draft oven for 4 hours ± 5 minutes at a temperature of 275 ± 5°F (135 ± 3°C). The mixture is stirred at 60 ± 5 minutes intervals so as to maintain uniform conditioning throughout the sample. For this study the above procedure was used on the mixes at temperature of 275°F and 300°F and aging times of 4 hours, 6 hours and 8 hours. Once the aging is completed the material is placed in an oven at 185°F for 15 minutes in the aging pan after which the required amount is placed in a mold and conditioned for another 15 minutes. The conditioned sample is then compacted in a gyratory compactor to produce a cylindrical compacted plugs with a diameter of 150mm (6 inches) and height of 170mm. Cylindrical cores specimens of 150-mm height and 100-mm diameter are then cored out from the plugs and used for dynamic modulus and indirect tensile strength testing.

Procedure for Dynamic Modulus $|E^*|$ Testing of Asphalt Mixtures

The dynamic modulus $|E^*|$ is the absolute value of a complex number relating stress to strain of a viscoelastic material that is subjected to a sinusoidal loading. It represents the time (frequency) dependent stiffness characteristics of a material. The test temperature of

the $|E^*|$ test protocol represents the temperature range of the environment in which the pavement will perform. The loading frequency of the $|E^*|$ test represents the speed of vehicles that will traverse the pavement during service.

The test procedure used to determine the dynamic modulus is designated in the AASHTO standards as a test protocol 62 (AASHTO TP 62) which requires the test to be performed on three replicates of each mix and the resulting dynamic modulus from each replicate averaged as the dynamic modulus for the mix. The test is performed with a Servo hydraulic machine. The procedure involves applying a controlled sinusoidal (haversine) axial compressive stress to a specimen of asphalt concrete plug with a diameter of 100mm (4 in) and a height of 150mm (6 in). The sinusoidal stress is controlled to produce strains smaller than 150 micro-strains enabling to the best possible degree a linear response through the material across temperatures. The stress is applied at samples equilibrium temperatures of -10°C, 4.4°C, 21.1°C, 37.8°C and 54.4 °C (14°F, 40°F, 70°F, 100°F and 130°F). At each temperature the load is applied at frequencies of 25 Hz, 10 Hz, 5 Hz, 1 Hz, 0.5 Hz, and 0.1 Hz. The applied stress is measured and, by means of linear variable differential transformers (LVDT), the resulting recoverable axial strain response of the specimen is measured. This is used to calculate the dynamic modulus and phase angle. The sequence of testing begins with the lowest temperature and proceeds to the highest. At a given temperature, the testing began with the highest frequency of loading and proceeded to the lowest. A rest period of at least 60 seconds is allowed between frequencies to allow the sample to preserve its properties being measured over the testing temperature and frequencies. Figure 3 shows a typical set up of the dynamic modulus test. The measured $|E^*|$ is used to develop a master curve for predicting the stiffness performance of a pavement.

Figure 3 : Set up for Dynamic Modulus Testing

Procedures for Dynamic Modulus Data

Development of Master Curves from $|E^*|$ Test

The basic Theory of Linear Viscoelasticity Concepts and Equations.

The evaluation of complex modulus tests requires an understanding of the fundamental concepts of linear viscoelasticity described as follows;

For the one-dimensional case of a sinusoidal loading, the equation of the stress can be represented by

$$\sigma_t=\sigma_o \sin(\omega t) = \sigma_o e^{i\omega t} \quad (1)$$

Where;

σ_t is the stress at any given time

σ_o is the stress amplitude

ω is the angular velocity

ω if related to the frequency by equation 2 as

$$\omega=2\pi f \quad (2)$$

The resulting steady state strain can be written as:

$$\varepsilon_t = \varepsilon_o \sin(\omega t - \phi) = \varepsilon_o e^{i(\omega t - \phi)} \quad (3)$$

Where;

ε_o is the strain amplitude

Ø is the phase angle that relates to the time lag of the strain relative to the stress. It gives an indication of the viscous-elastic properties of the material.

Ø = 0º for a purely elastic material and Ø = 90º for a pure viscous material.

The absolute value of the dynamic modulus is defined by the ratio of the stress to strain amplitudes

The in-phase component is used to define the storage modulus as follow:

$$E' = \frac{\sigma_o \mathrm{Cos}(\phi)}{\varepsilon_o} \quad (4)$$

The out-of phase components are used to define the loss modulus:

$$E'' = \frac{\sigma_o \mathrm{Sin}(\phi)}{\varepsilon_o} \quad (6)$$

From equations 2 and 3 the complex modulus, E*(*i*ω), can be defined by the equation:

$$E^*(\omega) = \frac{\sigma^*}{\varepsilon^*} = \frac{\sigma_o}{\varepsilon_o} e^{i\omega} = E' + iE'' \quad (7)$$

Where

E' is the real part the storage modulus and iE'' *is* the imaginary part is the loss modulus.

The absolute value of the complex modulus defines the dynamic complex modulus given by equation 8 as

$$|E^*| = \frac{\sigma_o}{\varepsilon_o} \quad (8)$$

Where:

$|E^*|$ = dynamic Modulus (psi), σ_0 = stress amplitude (psi), ε_0 = strain amplitude ($\mu\varepsilon$) shown in figures 4 and 5.

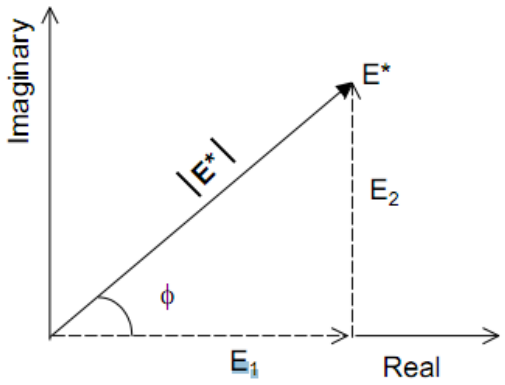

Figure 4: Real versus Imaginary Modulus Plot

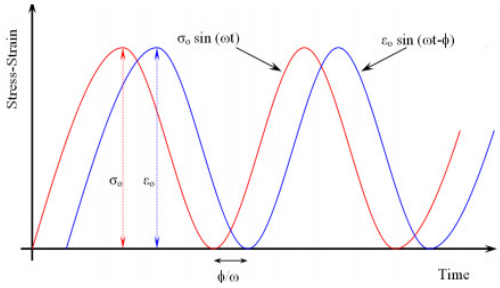

Figure 5: Stress and Strain in Dynamic Loading

The dynamic modulus obtained in the lab test is calculated by dividing the measure stress amplitude by the measured strain amplitude.

Shift Factors and Master Curves

In order to completely analyze and model the dynamic modulus test data a master curves needs to be generated. The data obtained from the test is used to construct the

master for the mixture. The master curve of the asphalt mixture is constructed to allow comparisons to be made over extended ranges of frequencies or temperatures without having to run the test at the extended temperatures again. It also allows the temperature and frequency dependent characteristics of the asphalt mix to be captured.

The master curve is generated using the time-temperature superposition principle also known as time temperature equivalence principle. The superposition principle allows the lab data collected at different temperatures and frequencies to be shifted horizontally relative to a reference temperature or frequency allowing the alignment of the various curves to conform to a single master curve. With this principle modulus values or behavior of the material at high test temperatures but lower frequencies or at low temperatures but higher frequencies can be obtained. Figure 6 shows a sample master curve of an asphalt mixture obtained in this project.

The Shift Factor

The shift factor, $\alpha(T)$, determines the amount of horizontal shift required at a given temperature to shift the measure dynamic modulus to fit the predictive sigmoidal function. The shift factor is given by equation 9 as follows;

$$f=\frac{f_r}{a(T)} \Rightarrow a(T)=\frac{f_r}{f} \qquad (9)$$

Where

f_r = frequency of loading at reference temperature

f = frequency of loading

$a(T)$ = Shift factor as a function of temperature

T = Temperature

The master curve for a material can be constructed using selected reference temperature to which all data are shifted and at which the shift factor $\alpha(T) = 1$. The reference temperature to for project to which all the data was shifted is 70°F.

The master curve of the dynamic modulus is defined by a non-linear sigmoidal function given by equation 10 as follows;

$$\text{Log}|E^*| = \delta + \frac{\alpha}{1+e^{(\beta+\gamma(\log f_r))}} \quad (10)$$

Where;

f_r = frequency of loading at reference temperature

δ= Minimum value Dynamic Modulus

$\delta+\alpha$ = Maximum value Dynamic Modulus

β,γ = Parameters describing the shape of the sigmoid function

The curve of the sigmoidal function of the dynamic modulus master curve describes the observed physical behavior of the asphalt mixture.

Procedure for Indirect Tensile (IDT) Strength Testing of Asphalt Mixtures

The indirect tensile strength test is used to determine the fatigue characteristics of an HMA mixture and the relative potential for rutting, moisture damage and cracking. The test is also based on the assumption that the material is homogeneous, isotropic and elastic. Even though none of these assumptions are practically true, estimates of the properties obtained based on these assumptions are useful in estimating the relative properties of HMA mixtures (Brown et al 2009).

The IDT test is performed in accordance with ASTM designation of ASTM D6931-07 Indirect Tensile (IDT) Strength of Bituminous Mixtures. During the test procedure a

cylindrical sample of the mixture with a determined height is conditioned to ±1°C of the test temperature for minimum periods between 30 minutes and 120 minutes depending on the method of conditioning. The sample is then placed on a loading strip and a load with a maximum deformation rate of 50 ±5 mm/min (2.00 ±0.15 in/min) is slowly applied across its diametric vertical plane at a constant loading rate until it fails. The peak load is then recorded (P) and used to calculate the indirect tensile stress (S_t) and the fracture energy (G_f) of the sample. Figure 4 shows the set up for the IDT test.

Figure 6: Set up of IDT Testing

Procedures for IDT Data

During loading of the sample the applied load is recorded. The peak load at fracture (P) is recorded and used to calculate the indirect tensile stress using equation 13 below.

$$\text{The horizontal (Indirect) tensile stress} = S_t = \frac{2P}{\pi td} \qquad 13$$

Where

d =the diameter of the specimen,

P =the maximum applied load, and

t =the thickness of the test specimen or core;

The vertical deformation is during loading can be calculated by measuring the displacement in the loading actuator. The total fracture energy at failure is determined by evaluating the area under the Load-Vertical deformation curve as shown in Figure 7. The area under the curve is normalized for the diameter and thickness of the cylinder.

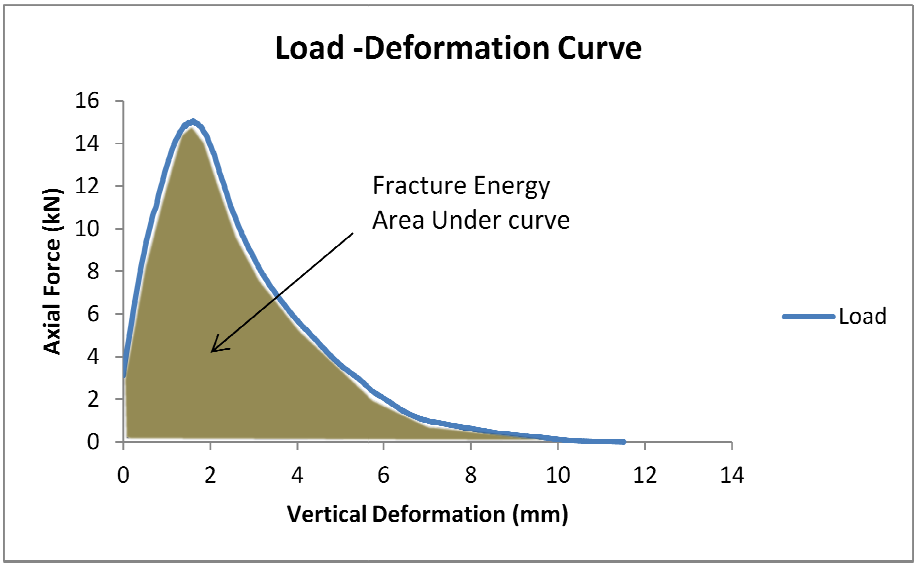

Figure 7: Showing the Accumulation of Fracture Energy during IDT Testing

TESTING PROGRAM

Introduction

The purpose of this study was to determine how much short-term aging beyond the typical industry standard affects the viscosity and potentially the performance of asphalt pavements. Therefore no information used in this research was conducted on virgin material. Viscosities were measured on aged asphalt using the standard binder RTFO aging protocols as the baseline standard from which all other viscosities were related.

The testing program was divided into two stages. In the first stage two virgin asphalt binders were aged to various degrees of temperature and time using the RTFO aging procedure. The viscosities of the aged binders were then measured. The results were then used to select the binder that is most susceptible to aging for the second stage (mixture aging) of the study.

The second stage involved performing STA conditioning on laboratory produced hot mix asphalt (HMA) samples. The samples were produced according to Arizona Department of Transportation (ADOT) dense graded mix specification with 5% binder content. The samples were aged to different degrees of temperature and time then subjected to Dynamic Modulus and Indirect Tensile Strength testing.

BINDER AGING AND TESTING

Materials

Two Arizona performance graded virgin (unmodified) asphalt binders PG 64-22 and PG 76-16 supplied by Holy Asphalt in Arizona samples were tested in this study.

Testing Regime

RTFO aging was first performed on samples of PG 76-16 and PG 64-22 binders at 322ºF for 85 minutes each as prescribed in ASTM D2872. A second set of samples were

aged in the RTFO at 350°F for 85 minutes. In order to evaluate the effect of aging time in the RTFO, a third batch of PG 64-22 binder was aged in the RTFO at 350°F for 175 minutes doubling the prescribed time specified in the ASTM.

Upon completion of the aging process in the RTFO, two replicates samples of each aged asphalt binders were poured into a Brookfield apparatus sample containers, penetration cans and softening point rings. The viscosities of the aged binders were then determined using the Brookfield test, penetration, and ring and ball softening point tests as described earlier in the literature review. Brookfield viscosity was conducted at 250°F, 300°F, 350°F and 375°F for each replicate. Penetration test was conducted using a 1mm diameter needle loaded with a weight of 100g and allowed to drop for 5 seconds into the conditioned binder sample at temperature of 25°C (77°F) per replicate. Penetration results were converted to viscosity values using the Witczak and Mirza equation presented in literature review. The converted values are referred to as "Penetration Viscosity". Table 1 shows a summary of the testing regime used for the first stage of the study. The effect of short term RTFO aging time study was not conducted on the PG 76-16 binder due to time limitations.

Table 1: Summary of Testing Regime and Protocol for Binder Aging Study

	Aging Test		Viscosity Test		
Binder	RTFOT Temp (°F)	RTFOT Time (Minutes)	Penetration Test	Brookfield Test	Softening Point Test
PG 64-22	322	85	2 replicates	2 replicates	2 replicates
PG 64-22	350	85	2 replicates	2 replicates	2 replicates
PG 64-22	350	175	2 replicates	2 replicates	2 replicates
PG76-16	322	85	2 replicates	2 replicates	2 replicates
PG76-16	350	85	2 replicates	2 replicates	2 replicates
PG76-16	350	175	Not Tested	Not Tested	Not Tested

Binder Test Results, Analysis and Discussion

PG 64-22 Binder Results

Table 2 shows the effect of temperature on the viscosity of the PG 64-22 binder after RTFO aging at temperatures 322°F and 350°F for 85 minutes. The table compares the viscosities of the binder aged due to increase in temperature. The base temperature is 322°F representing the standard practice for RTFO binder aging. Viscosities measured at the base temperature represent the base viscosity. Changes in viscosity are measured relative to the base viscosity. The results indicate an average of 9% increase in the overall Brookfield viscosity, 18% increase in the penetration viscosity temperature measured at 77F, and 4% increase softening point due to increased short term aging temperature from 322°F to 350°F.

The trend in the Brookfield viscosity changes show that while the binder becomes stiffer with a 26% increase in viscosity at the lower temperatures (250°F) and it becomes less viscous at higher temperatures (375°F) with a 4% reduction in viscosity. Penetration viscosity measured at 25°C (77F) also increased by 18%.

Table 2: Viscosity and Softening Points of PG 64-22 after 85 Minutes RTFO Aging at Temperature 322°F and 350°F

	Brookfield Viscosity, (cP)				Penetration Viscosity, (cP)	Softening point, (°F)
85 minutes RTFO Temperature	250°F	300 °F	350 °F	375 °F	77 °F	
322°F	1,410	307	94.5	60.9	4.14E+09	129
350°F	1,770	338.0	99.2	58.6	4.89E+09	134.15
Changes	366.0	30.7	4.75	-2.3	7.48E+08	4.95
Percent Change	26%	10%	5%	-4%	18%	4%
Average Percent Change	9%					

Table 3 shows the viscosities of the PG 64-22 binder after RTFO aging at temperatures 350°F for 85 minutes and for 175 minutes. The table compares the viscosities of the binder aged due to increase in short term aging time. The base time is 85 minutes which represents the condition of increased temperature and standard exposure time. Viscosities measured at the base short term aging time under elevated short term aging temperature represent the base viscosity. Changes in viscosity due to extended short-term aging time of 175 minutes are measured relative to the base viscosity at the elevated temperature. The results indicate an average increase of 99% in the overall Brookfield viscosity, 92% increase in the penetration viscosity and 10% increase softening point temperature measured at 77F due to increased aging time from 85 minutes to 175 minutes.

Contrary to the trend observed in increased temperature where Brookfield viscosity changes show the binder to be stiffer at 250°F and less viscous at higher 375°F, increasing the short term aging time made the binder stiffer across all temperatures. Penetration viscosity measured at 25°C (77°F) also increased by 18%.

Table 3: Viscosity and Softening Points of PG 64-22 Binder after RTFO Aging at 359°F for 85 Minutes and 175 Minutes

350°F RTFO Time	Brookfield Viscosity (cP)				Penetration (cP)	Softening point (°F)
	250 °F	300 °F	350 °F	375 °F	77 °F	
85 Minutes	1,770	338	99.2	58.6	4.89E+09	134
175 Minutes	3,380	674	196.8	121	9.41E+09	148.1
Changes	1,610	336	97.6	63	4.52E+09	1.40E+01
Percent Change	90%	100%	98%	107%	92%	10%
Average Percent Change	99%					

Figures 8 and 9 provide graphical representations of the measured Brookfield viscosities and penetration viscosities of the RTFO short-term aged PG 64-22 binder, respectively. The graph show that for all the aging conditions studied, the effect of increasing the aging time from 85 minutes to 175 minutes has more pronounced effect on hardening the PG64-22 binder than increasing the aging temperature from 322°F to 350°F. Figure 10 shows the measured softening points of RTFO short-term aged PG 64-22 binder. The trends in the softening points change due to RTFO short-term aging follow the same trend as that of the changes in viscosities. It indicates that for the PG 64-22 binder, increasing the RTFO aging time from 85 minutes to 175 minutes increased the softening point to a greater extent than the effect of increasing the aging time from 322°F to 350°F.

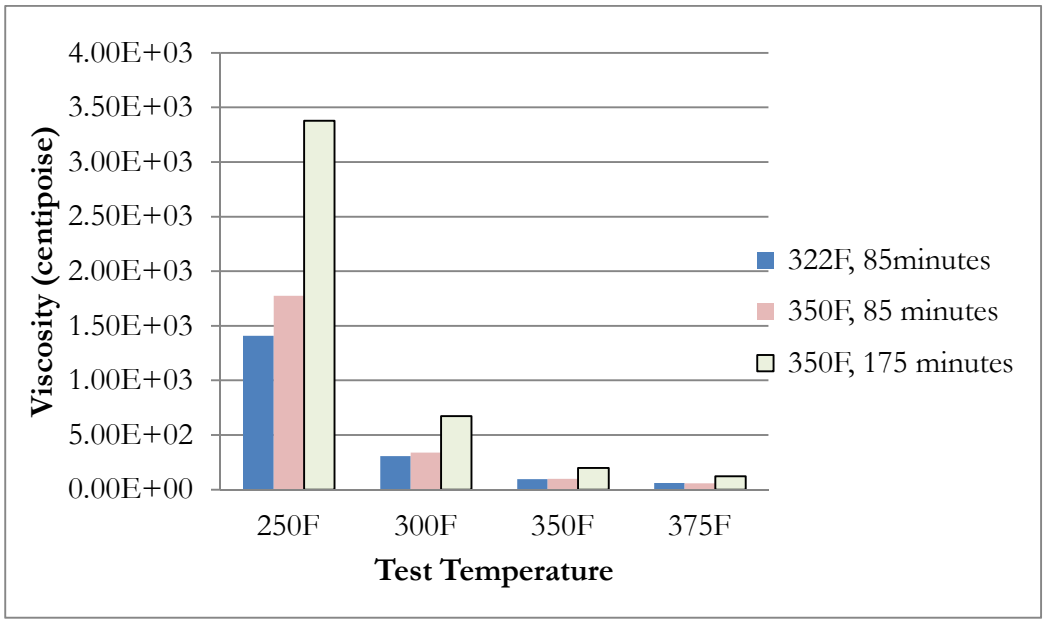

Figure 8: Brookfield Viscosities of Short Term Aged PG 64-22 Binder at Various RTFO Aging Temperatures and Times.

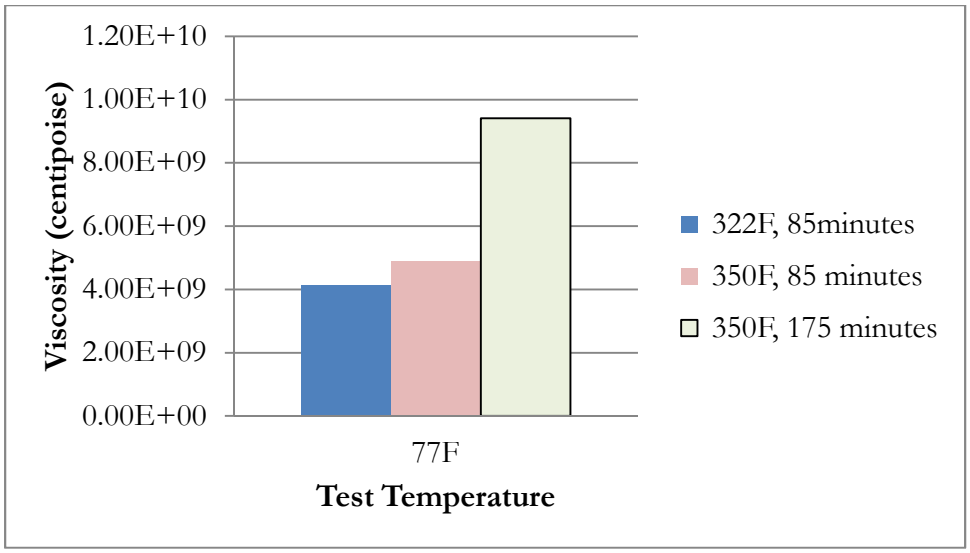

Figure 9: Penetration Viscosities of Short Term Aged PG 64-22 Binder at Various RTFO Temperatures and Times.

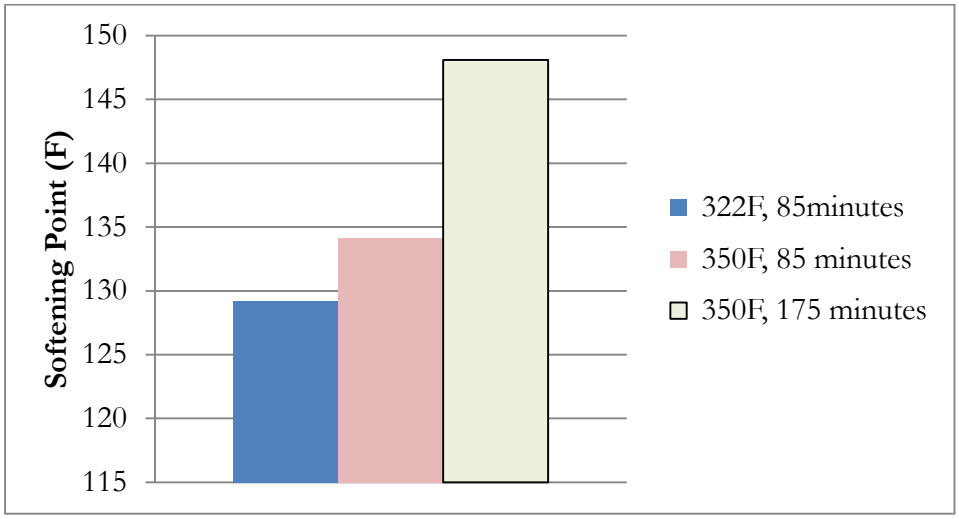

Figure 10: Softening Point of Short Term Aged PG 64-22 Binder at various RTFO temperatures and times.

PG 76-16 Binder Results

Table 4 shows the test results representing effect of temperature on the viscosity of the PG 76-16 binder after RTFOT aging at temperatures 322°F and 350°F for 85 minutes. As previously mentioned, the effect of increasing aging time was not studied for the PG 76-

16 binder. The table compares the viscosities and softening points of the binder aged due increase in temperature. The base temperature is 322°F representing to the standard practice for RTFO binder aging. Viscosities measured at the base temperature represent the base viscosity hence changes in viscosity are measured relative to the base viscosity. The results indicate an average of 4 % increase in the overall Brookfield viscosity, 60% increase in the penetration viscosity measured at 77°F and 4% increase in softening point due to increased short term RTFO aging temperature from 322°F to 350°F at 85 minutes aging time.

Table 4: Viscosity and Softening Points of PG 76-16 after 85 Minutes RTFO Aging at Temperature 322F and 350F

85 mins RTFO Temp.	Brookfield Viscosity (cP)				Penetration (cP)	Softening point (°F)
	250	300	350	375	77	
322°F	3.76E+03	6.54E+02	1.83E+02	1.06E+02	6.70E+09	147
350°F	3.94E+03	6.79E+02	1.88E+02	1.09E+02	1.07E+10	169
Changes	5%	4%	3%	3%	60%	2%
Percent Change	4%					

Figures 11, figure 12 and figure 13 respectively represents the measured Brookfield viscosities, penetration viscosities and softening points of the RTFO short term aged PG 76-16 binder. The graphs show that increasing the aging temperature from 322°F to 350°Fresult in an increase in Brookfield viscosity, penetration viscosity and softening point of the aged binder. The amount of increase in the measured Brookfield viscosity and softening points due to aging are relatively lower than change in penetration viscosity for the PG 76-16 binder. At higher testing temperature (350°F and 375°F), Brookfield viscosity of the short-term aged PG 76-16 binder does not change.

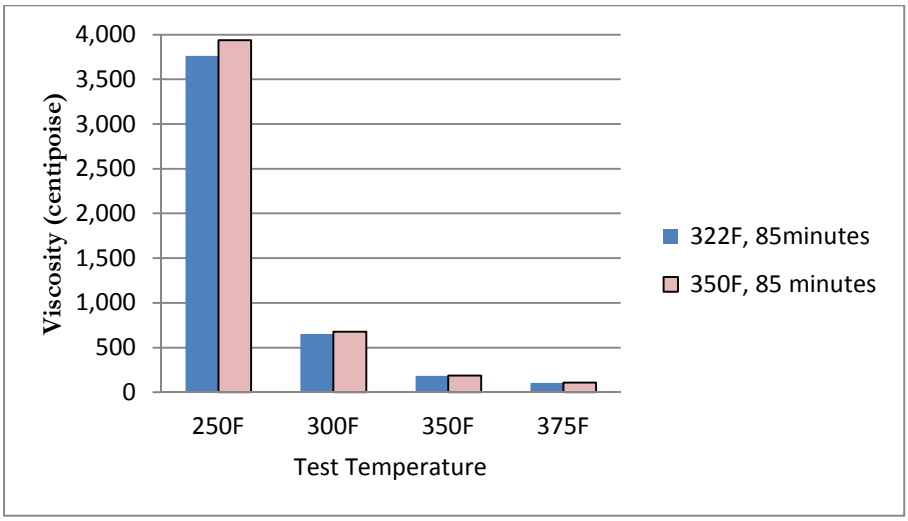

Figure 11: Brookfield Viscosities after Short Term Aged PG 76-16 Binder at Various RTFO Aging Temperatures and Times

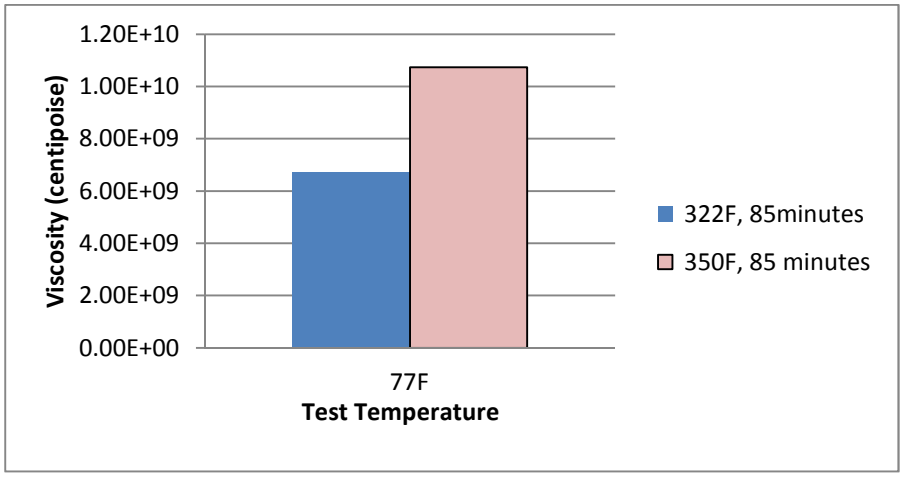

Figure 12: Brookfield Viscosities after Short Term Aged PG 76-16 Binder at various RTFO aging temperatures and times

Penetration viscosity of the PG 76-16 binder increased from 6.70E+09 centipoises to 1.07E+10 centipoises representing an increase of 60%. This result was unexpected and may represent an error in measuring the viscosity because the PG binder was expected to be affected by aging to a lesser degree than the PG 64-22 binder.

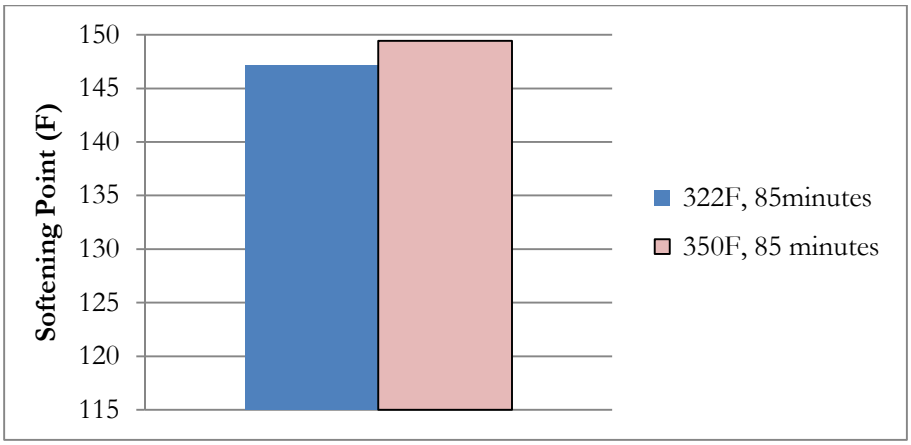

Figure 13: Softening Point of Short Term Aged PG 76-16 Binder at Various RTFO Temperatures and Times

Figure 14 show a graphical representation of the amount of change in Brookfield Viscosity, penetration viscosity and softening point due to all aging conditions above the standard RTFO aging at 322^{O}F and 85 minutes for both binders considered for comparison.

The effect of temperature on both binders was evaluated by comparing viscosity and softening point changes at 350F relative to the standard procedure. The results show that the PG 64-22 binder was most affected by the increase in temperature for both the Brookfield viscosity and softening point. Increase in penetration viscosity was 60% for the PG 70-16 binder which is three times higher than the PG 64-22 binder. However this result was not expected, it demonstrates an anomaly in the general trend of all the test results and may be due to error during testing.

The effect of time on short term aging was evaluated for the PG 64-22 binder by comparing the 85 minutes with 175 minutes aged binder viscosities and softening point changes at 350F RTFO temperature. This condition represents mixing HMA at elevated plant temperatures and hauling over relatively farther construction sites in order to maintain construction

temperatures in cold weather conditions. The results show that the effect of increasing the aging time resulted in the most drastic changed in viscosity and softening points as shown in Figure 14. Both Brookfield viscosities measured at all test temperatures and penetration viscosity approximately doubled due to increased time. Increase in softening point was to a relatively lower degree compared to changes in softening point. However largest increase in viscosity was due to increased time.

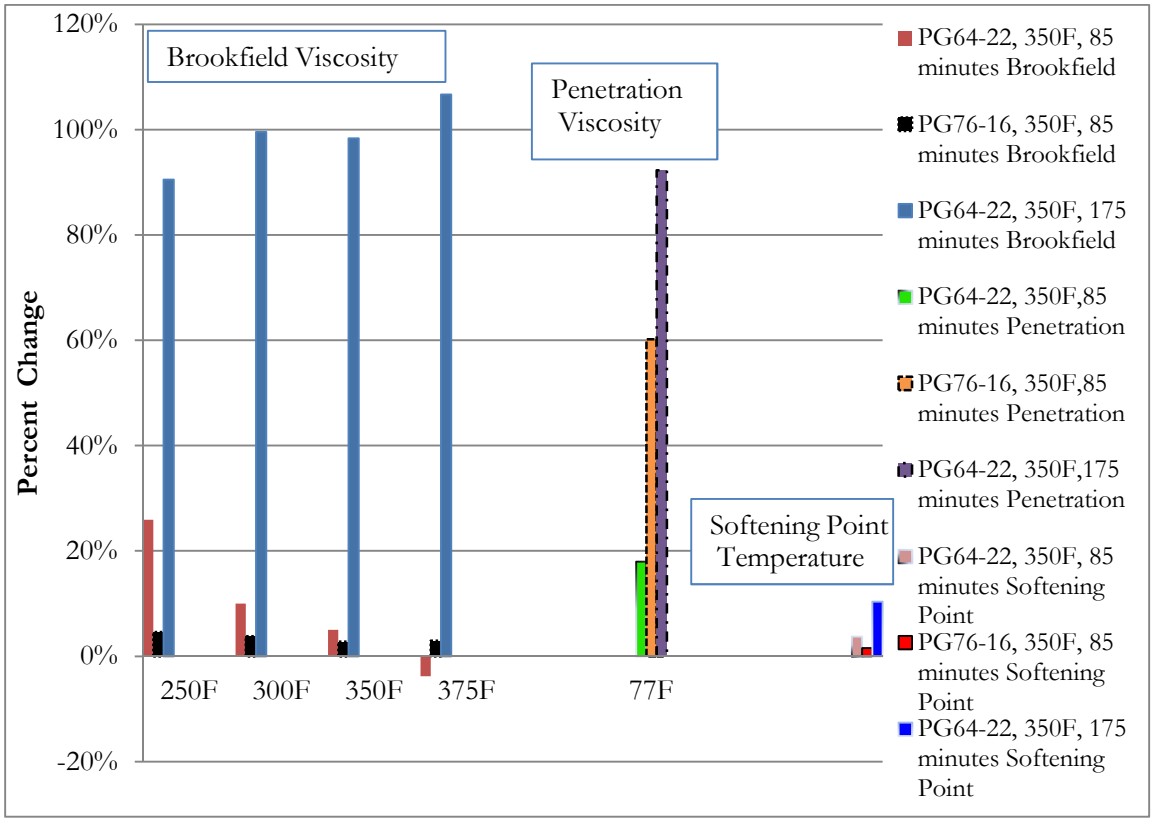

Figure 14: Percent Change in Viscosity and Softening Points of Aged Binders

Statistical Analysis of Binder Aging Test Result

A paired t-test was performed to determine if the increase in temperature and time was significant in changing the Brookfield viscosity of the PG 64-22 binder. For the PG 76-16 binder only the significance of temperature increase was evaluated because the binder was

only aged for 85 minutes at both temperatures. The results of the statistical test are shown in Table 5. Statistical significance evaluation was conducted at a 95% confidence level (C.L.).

For the PG 64-22 binder the mean increase in Brookfield Viscosity due to increase in RTFO temperature from 325°F to 350°F (M=99.66, SD =177.79, N= 4) was not significantly greater than zero, $t_{statistical}$ =-1.12, two-tail p = 0.34, showing that the 25°F increase in RTFO temperature alone is not statistically significant in increasing the Brookfield viscosity of the PG 64-22 binder tested. Also the mean increase in Brookfield Viscosity due to increase in RTFO temperature time from 85 minutes to 170minutes at 350°F (M=525.37, SD =730.06, N= 4) was not statistically significant. ($t_{statistical}$ =-1.44, two-tail p =0.25). It also basically showed that the doubling the RTFO aging time was not statistically significant in increasing the Brookfield viscosity of the PG 64-22 binder tested.

Table 5: Paired t-Test of PG 64-22 and PG 76-16 Binders RTFO Viscosity

	PG 64-22 Binder Effect of RTFO Temp. @ 85 mins (325°F vs. 350°F) Brookfield Viscosity (cP)	PG 64-22 Binder Effect of RTFO Time @ 350°F (85 mins vs. 175 mins) Brookfield Viscosity (cP)	PG 76-16 Binder Effect of RTFO Temp. @ 85 mins (325°F vs. 350°F) Brookfield Viscosity (cP)
Mean change	99.66	525.37	51.49
SD	177.79	730.06	81.60
N	4	4	4
$t_{Statistical}$	-1.12	-1.44	-1.26
Two Tail P value	0.34	0.25	0.30
Two-tail t Critical	3.18	3.18	3.18
Reject or Accept Null Hypothesis	Accept	Accept	Accept
Change	Not Significant	Not Significant	Not Significant

For the PG 76-16 binder the mean increase in Brookfield Viscosity due to increase in RTFO temperature from 325°F to 350°F (M=51.49, SD =81.60, N= 4) was not significantly greater than zero, $t_{statistical}$ =-1.26, two-tail p = 0.30, showing that the 25°F increase in RTFO temperature alone did not cause significant in increase in the Brookfield viscosity of the PG 76-16 binder tested at a 95% confidence level.

The PG 64-22 binder was selected and used to conduct the second stage of this study to evaluate the effect of Short Term Oven Aging of a HMA mix beyond the standard aging temperature and time.

MIXTURE AGING AND TESTING

Materials

A dense graded ADOT 19mm MAG Superpave High Traffic mix with PG 64-22 binder was used for this part of the study. Binder content for the mix was 4.5%. Before samples were prepared, the aggregates were first oven dried, sieved and batched. The mix proportions are presented in Table 6.

Table 6: Gradation and Mixture Proportions

	Sieve Size	Percent Passing
Gradation, % passing	1 in	100
	3/4 in	96
	1/2 in	65
	3/8 in	50
	#4	38
	#8	27
	#30	14
	#100	3.5
	#200	1.8
Asphalt Content, %		4.5
Binder Grade		PG 64-22

Laboratory Mixing, Short Term Aging and Compaction

The purpose of the study was to determine the effect of short term aging due to elevated temperatures beyond typical production mix temperatures of about 330^{O}F. Standard laboratory mixing and short term aging temperatures of 305 ^{O}F and 275^{O}F, respectively, were chosen to simulate aging that occurs at typical production temperatures. In order to simulate the effect of a 25^{O}F increase production temperatures, laboratory mixing and aging temperatures of 330 ^{O}F and 300^{O}F (representing 8% and 9% increase) respectively were used for this study. Samples mixed and aged at standard conditions were designated as LT, and

samples that were mixed and aged at 25^{O}F increased temperature over the standard temperature conditions were designated as HT.

STA times were also chosen to simulate standard laboratory aging conditions of 4 hours and then increased by 2 hours and 4 hours to 6 hours and 8 hours, respectively, to simulate the effect of increased aging time.

Before mixing, the batched aggregates were preheated overnight to ensure drying at the respective mixing temperatures. The binders were also preheated two hours prior to mixing. During mixing, 329.8 grams of preheated binder was introduced to 7000 grams of pre-heated aggregates and thoroughly mixed in a rotating bucket mounted on a motor equipped with a mixing arm.

After each sample was conditioned in the convection oven for 15 minutes, a 6525 gram specimen was used to fill a 150 mm (6 inches) diameter compaction mold in three lifts of approximately equal depth. Each lift when place in the mold was quickly tamped with the scooping tool to ensure that the lifts are well integrated and bonded with each other to from a homogenous sample. After each mold is filled, it was placed in the convection oven for another 15 minutes before compacted in a Servopac Gyratory Compactor into a 150 mm (6 inches) diameter and 175 mm high cylindrical molds. Test samples, 100 mm (4 inches) in diameter by 150 mm (6 inches) high, were cored from the center of the gyratory specimens and prepared for Dynamic Modulus and IDT testing according to AASHTO TP 62-07 procedure (16).

Mixture Aging Matrix and Testing Regime

A total of 24 test samples were manufactured for this study with 12 samples each manufacture under LT and HT conditions. Under LT conditions four samples each were manufactured at aging times of 4 hours, 6 hours and 8 hours for total of 12 samples. Similarly under HT conditions, four samples each were manufactured at aging times of 4, 6 and 8 hours total of 12 more samples. The samples were labeled to identify the mixing and aging condition, their aging time as well as their numerical order of manufacture. For example a sample labeled AG4L1 is the first aging sample manufactured in a group of four that were conditioned under standard conditions of 305^{O}F mixing temperature and 275^{O}F STA temperature for four hours.

Three samples from each group with the same aging temperature and time were use for dynamic modulus testing in accordance with AASHTO TP 62.

One sample (the second sample) from each group was split into two halves and used for Indirect Tensile strength testing (IDT) at room temperature of 77^{o}F.

Table 7 presents a summary of the samples manufactured, their air voids content and testing matrix.

Table 7: A Summary of Mixture Aging Matrix and Testing Regime

Condition	Mixing Temperature	Aging Temperature	Aging Time	Sample ID	Test Performed	% Air Voids
Standard Condition Low Temperature (LT)	305^{O}C	275^{O}C	4 Hours	AG4L1	$\lvert E^* \rvert$	6.83%
				AG4L2	IDT	6.27%
				AG4L3	$\lvert E^* \rvert$	7.30%
				AG4L4	$\lvert E^* \rvert$	6.74%
			6 Hours	AG6L1	$\lvert E^* \rvert$	6.85%
				AG6L2	IDT	6.43%
				AG6L3	$\lvert E^* \rvert$	7.19%
				AG6L4	$\lvert E^* \rvert$	6.15%
			8 Hours	AG8L1	$\lvert E^* \rvert$	6.70%
				AG8L2	IDT	6.39%
				AG8L3	$\lvert E^* \rvert$	7.72%
				AG8L4	$\lvert E^* \rvert$	6.94%
Elevated Condition High Temperature (HT)	330^{O}C	300^{O}C	4 Hours	AG4H1	$\lvert E^* \rvert$	7.60%
				AG4H2	IDT	6.18%
				AG4H3	$\lvert E^* \rvert$	6.49%
				AG4H4	$\lvert E^* \rvert$	7.25%
			6 Hours	AG6H1	$\lvert E^* \rvert$	7.54%
				AG6H2	IDT	6.28%
				AG6H3	$\lvert E^* \rvert$	7.68%
				AG6H4	$\lvert E^* \rvert$	7.20%
			8 Hours	AG8H1	$\lvert E^* \rvert$	7.19%
				AG8H2	IDT	6.41%
				AG8H3	$\lvert E^* \rvert$	7.25%
				AG8H4	$\lvert E^* \rvert$	7.80%

Dynamic Modulus Testing

Dynamic modulus $\lvert E^* \rvert$ tests were performed in accordance with AASHTO TP 62-07 utilizing a servo-hydraulic testing machine. Results from the test was used to predict the $\lvert E^* \rvert$ master curves for each combination of STA and mixing temperature and time. The results were also used to analyze the effect of STA and mixing temperature and STA time on the dynamic modulus of the mixture.

Three samples from each group with the same aging temperature and time were used for dynamic modulus testing in accordance with AASHTO TP 62 at a full sweep of loading frequencies (25, 10, 5, 1, 0.5 and 0.1 Hz) and temperatures (-10, 4.4, 21.1, 37.8 and 54.4°C). In order to minimize bias due to loading, all samples utilized for the $|E^*|$ testing were capped on both end with sulfur to ensure a smooth and leveled contact surface to apply dynamic load. The applied dynamic load was applied in continuous wave form resulting in a haversine stress. Testing was conducted in an order of increasing temperature and decreasing loading frequency in order to minimize any potential damage to any specimen before the next sequential test. The magnitudes of the applied dynamic loads were varied with temperature such that the recoverable micro-stains of each specimen were maintained within the viscoelastic range of 40 to 100. The resulting applied dynamic haversine stress was measured through the load cell. The deformations in the sampled being tested were measured with spring-loaded Linear Variable Differential Transducers (LVDTs) mounted on brackets, studs and aligning guiding rods secured to the samples with glue as was shown in Figure 3 earlier.

Indirect Tensile Strength Testing

One sample from each group was split into two halves and used for Indirect Tensile strength testing (IDT) in accordance with ASTM D6931-07 conducted at room temperature of 77°F. The samples used for the test consist of the second samples in each group. For each test the samples were split diametrically into two half to form two smaller cylindrical samples of approximately similar lengths and diameter. The samples were then labeled and tested as the top and bottom samples. IDT data for the top and bottom samples were then averaged to represent the IDT results for each sample. Results of the IDT test is used to determine

the effect of the change in the STA and mixing temperatures as well as the STA time on the indirect tensile strength and the fracture energy of the samples. Analysis of the result can be used to predict the relative fatigue performance of the aged mixtures.

Production of Mixture, Testing and Analysis of Results

Results of the IDT and $|E^*|$ testing of the samples are presented in this section. In order to determine the effect of various STA and mixing condition on compaction data from the gyratory compactor was also retrieved for analysis.

Laboratory Compaction Data

Compaction data from the IPC gyratory compaction equipment was retrieved and compared to ascertain the effect of the change in the STA and mixing conditions and time on the number of gyration and shear stress required to produce a 150 mm (6 inches) diameter and 175 mm high cylindrical sample from a 6525 gram sample. Table 8 shows compaction data gathered for all samples manufactured. The table summarizes the number of gyrations and maximum shear stress obtained from the IPC gyratory compaction equipment after compaction was complete within each group. Groups LT-4Hrs, HT-4Hrs, HT-6Hrs and HT-8Hrs each had high outliers in the number of gyrations. These outliers introduced high variances within each group.

Table 8: Gyratory Compaction Data for all STA and Mixing Conditions

	Sample ID	Number of Gyrations	Max Shear Stress per IPC, KPa
LT-4Hrs	AG4L1	27	580
	AG4L2	**[78]**	590
	AG4L3	24	580
	AG4L4	33	610
	Mean	40.5	590
	Standard Dev	25.3	14.14
LT-6Hrs	AG6L1	33	605
	AG6L2	36	604
	AG6L3	38	602
	AG6L4	37	605
	Mean	36	604
	Standard Dev	2.2	1.41
LT-8Hrs	AG8L1	30	600
	AG8L2	31	601
	AG8L3	52	600
	AG8L4	49	600
	Mean	40.50	600.25
	Standard Dev	11.62	0.50
HT-4Hrs	AG4H1	47	559
	AG4H2	28	600
	AG4H3	**[73]**	600
	AG4H4	26	585
	Mean	43.5	586
	Standard Dev	21.8	19.34
HT-6Hrs	AG6H1	**[86]**	580
	AG6H2	38	600
	AG6H3	29	600
	AG6H4	33	590
	Mean	46.5	592.5
	Standard Dev	26.59	9.57
HT-8Hrs	AG8H1	58	600
	AG8H2	37	580
	AG8H3	**[82]**	630
	AG8H4	36	610
	Mean	53.25	605
	Standard Dev	21.69	20.82

[ ] - Outliers were not included in statistical analysis.

Statistical Analysis and Comparison of Laboratory Compaction Data

A series of paired t-test was performed on the data set to determine if either temperature or time was effective in influencing a change in the compaction effort. The null hypothesis (H_O) used states that the changes in the number of gyrations and shear stresses due to varying mixture aging and mixing were not significant. The test was conducted at a 95% confidence level (α=0.05). The null hypothesis was rejected if the two tail P-values is less than 0.05, or when the absolute value of $t_{statistical}$ is greater or equal to than the absolute value Two Tail T-critical. If the null hypothesis is accepted, then the changes produced are not significant, however if the null hypothesis is rejected, then the alternate hypothesis (H_a) that the changes in the shear tress and number of gyrations are significant is accepted.

The results of the paired t-test are summarized in table 9. Table 9 also shows the mean and standard deviation and percent change in number of gyration and shear stress for each data set compared. Results of the statistical analysis show that the null hypothesis was accepted in all cases except for the change in shear stress due to increasing the STA time from 4 hours to 6 hours. The exception could be considered as a statistical anomaly and may be due to errors introduced during laboratory compaction.

Effect of Temperature on Compaction

A comparison of the number of gyrations and maximum shear stress was conducted between samples manufactured under LT temperatures and HT temperature. The results shown in Table 9 indicates that the increase in temperature caused an average of 22.4% increase number of gyrations and an average of 0.6% reduction in the maximum shear stress. However, the statistical analysis using the t-paired test showed that neither change in the

number of gyrations and maximum shear stress is statistically significant at 95% confidence level.

Effect of STA Time on Compaction

A similar comparison of the number of gyrations and maximum shear stress was conducted between samples manufactured at 4, 6 and 8 hours STA time. 4 hours STA time was used as the base time from which all comparisons were made. The results are shown in table 9 as % change.

The 4 versus 6 hours comparison represent the results a 2 hour increase in STA time from 4 hours in the compaction data. The results showed that a 2 hours increase in STA time caused a 1.8% reduction in the number of gyration and a 1.7% increase in the maximum shear stress. Statistical analysis of the results using the t-paired test showed that while the reduction in the number of gyration is not significant, the increase in the maximum shear stress was significant at 95% confidence level.

The 4 versus 8 hours comparison represent the results an 8 hour increase in STA time from 4 hours in the compaction data. The results showed that 4 hours increase in STA time caused an 11% increase in the number of gyration and a 2.5% increase in the maximum shear stress. Statistical analysis of the results using the t-paired test showed that both increases in the number of gyration and maximum shear stress were not significant at a 95% confidence level.

Table 9: Results of Paired t-test and Analysis of Changes in Number of Gyration and Maximum Shear Stress on Compaction Data

	Effect of Temperature (LT vs. HT)		Effect of Time (4Hrs vs. 6Hrs)		Effect of Time (4Hrs vs. 8Hrs)	
	Gyrations	Max Shear Stress	Gyrations	Max Shear Stress	Gyrations	Max Shear Stress
Mean change	-8.75	3.58	0.75	-10.25	-4.88	-14.63
SD	28.97	18.40	28.32	11.68	22.20	20.41
N	12	12	8	8	8	8
$t_{Statistical}$	-1.05	0.67	0.07	-2.48	-0.62	-2.03
Two Tail P value	0.32	0.51	0.94	0.04	0.55	0.08
Two-tail t Critical	2.20	2.20	2.36	2.36	2.36	2.36
Reject or Accept Null Hypothesis	Accept	Accept	Accept	Reject	Accept	Accept
% Change	22.4%	-0.6%	-1.8%	1.7%	11.6%	2.5%
Was Change Significant?	Not Significant	Not Significant	Not Significant	Significant	Not Significant	Not Significant

Test Results and Analysis of Dynamic Modulus Data

Table 10 shows an example of the table of results for three replicates conditioned at 25°F increase in mixing and STA temperatures and 4 hours STA time (AG4H). The test procedure produced large volume of data. The information recorded was mainly the input sweep parameters including the frequency (HZ), cycle period (ms), number of cycles, rest period(s), static stress level (kPa), positive dynamic stress (kPa), negative dynamic stress (kPa), confining pressure (kPa) and the temperature (°C). The analysis and computation performed in the servo equipment yielded the data to be used for further analysis and development of the master curve.

Table 10: Example Table of Results Showing Average |E*| and Phase Angle of the Three Replicates for Condition AG4H

Average Dynamic Modulus and Phase Angle (HT- 4 Hours STA) **Binder Grade: 64-22 Binder Content: 4.50%** **Date: 09/30/2012 Average Air Voids: 7.11%**													
		Dynamic Modulus E*						Phase Angle, ϕ					
Temp (°F)	Freq. (Hz)	Rep 1 (ksi)	Rep 2 (ksi)	Rep 3 (ksi)	Ave (ksi)	Std. Dev	Coeff. of Var. (%)	Rep 1 (Deg)	Rep 2 (Deg)	Rep 3 (Deg)	Ave (Deg)	Std. Dev	Coeff. of Var. (%)
14	25	3298	2715	3415	3143	375	11.9	0.4	0.8	3.2	1.5	1.5	101.7
	10	3224	2586	3369	3060	417	13.6	3.9	3.6	6.6	4.7	1.6	34.5
	5	3167	2510	3266	2981	411	13.8	4.4	4.8	7.9	5.7	1.9	33.9
	1	2932	2303	3029	2755	394	14.3	5.4	5.7	8.9	6.7	1.9	28.8
	0.5	2841	2230	2946	2672	387	14.5	5.5	7.3	9.5	7.4	2.0	26.8
	0.1	2605	2016	2638	2420	350	14.5	6.6	7.5	11.9	8.7	2.9	33.2
40	25	2264	1874	2644	2261	385	17.0	3.3	4.9	7.1	5.1	1.9	37.6
	10	2212	1821	2479	2171	331	15.2	6.6	8.1	11.7	8.8	2.6	30.0
	5	2098	1694	2307	2033	312	15.3	8.2	9.5	12.5	10.1	2.2	21.9
	1	1816	1431	1928	1725	261	15.1	9.7	11.8	15.7	12.4	3.0	24.3
	0.5	1719	1331	1779	1610	243	15.1	10.7	12.8	17.0	13.5	3.2	23.7
	0.1	1486	1125	1431	1347	195	14.5	13.3	14.5	19.9	15.9	3.5	22.2
70	25	1563	1162	1361	1362	201	14.7	10.5	10.9	15.8	12.4	2.9	23.6
	10	1383	1044	1217	1215	169	13.9	15.5	16.3	21.8	17.8	3.4	19.2
	5	1227	940	1095	1087	144	13.2	17.2	17.9	24.7	19.9	4.1	20.7
	1	883	666	761	770	109	14.1	21.4	22.4	29.8	24.5	4.6	18.7
	0.5	759	586	658	667	87	13.1	25.7	23.6	31.9	27.1	4.4	16.1
	0.1	531	411	478	473	60	12.7	28.0	26.9	36.7	30.5	5.4	17.6
100	25	632	472	596	566	84	14.8	25.0	22.6	27.7	25.1	2.6	10.2
	10	515	370	472	452	75	16.5	26.2	27.1	29.0	27.4	1.4	5.2
	5	425	304	386	372	62	16.6	28.0	28.8	32.2	29.7	2.3	7.6
	1	266	181	209	219	44	20.0	31.7	32.9	39.2	34.6	4.0	11.5
	0.5	213	141	160	171	38	22.0	32.6	34.6	39.4	35.5	3.5	9.9
	0.1	133	87	100	107	23	22.0	31.5	32.9	37.7	34.0	3.3	9.6
130	25	205	162	263	210	51	24.2	29.4	30.0	31.7	30.3	1.2	3.9
	10	143	111	185	146	37	25.5	28.9	29.9	30.8	29.8	1.0	3.3
	5	111	86	139	112	26	23.4	29.7	28.3	28.8	28.9	0.7	2.4
	1	61	43	67	57	12	21.8	28.0	27.4	25.9	27.1	1.1	4.1
	0.5	46	32	54	44	11	24.8	26.7	25.5	24.5	25.6	1.1	4.2
	0.1	33	24	45	34	11	31.3	22.3	17.5	19.2	19.7	2.4	12.3

The information obtained and recorded from the servo equipment includes dynamic modulus (MPa), phase angle (Degrees), dynamic stress (kPa), recoverable axial micro-strain, permanent axial micro-strain, temperatures (°C) and the confining pressure (kPa) (however, unconfined tests were conducted). The summary data in Table 9 was obtained for each LVDT at each frequencies, and temperature for the three replicates. The averages for the three replicates for each sample were obtained and extracted for further analysis. The results show that coefficient of variation increases for $|E^*|$ values as temperature increases and frequency decreases. This suggests that as temperature increases and traffic speed reduces, there is a tendency for increased material displacement in the pavement matrix which tends to increase variability in the results obtained. In contrast to $|E^*|$, the results in Table 9 shows that the coefficient of variation of the Phases decreases as temperature increases and frequency of applied load increases.

Development of Shift Factors and Master Curves

The master curve was developed using the shift factor at reference temperature of 70°F, the measured dynamic modulus and phase angle data. Microsoft excel 2007 was used to develop and optimize the sigmoidal function as follows;

The shift factor is defined by a parabolic equation given by equation 11 developed from previous research of large volumes of existing data.

$$Log\ a(T) = aT_i^2 + bT_i + c \qquad (11)$$

Where

a, b and c are parameters to be determined by optimization using the excel solver.

$a(T)$ is the shift factor at any temperature T.

When the shift factor is obtained, the reduced frequency f_r can be determine from equation 12 as follows;

$$\text{Log}(f_r)=\text{Log}\left(f^{*}a(T)\right) \quad (12)$$

Where f is the frequency and the reduced frequency f_r is the frequency of loading at the reference temperature of 70°F.

The value of the frequency obtained from the equation above is substituted into the sigmoidal function as shown in equation 13 below.

$$\text{Log}\left|E_p^{*}\right|=\delta+\frac{\alpha}{1+e^{(\beta+\gamma(\log f_r))}} \quad (13)$$

Where $\left|E_p^{*}\right|$ is the predicted dynamic modulus and α, β, δ and γ are as defined in equation 10 above. The values for α, β, δ and γ are determined by optimization using the Microsoft excel 2007 solver.

Optimization of the Predictive Sigmoidal Function using Microsoft Excel 2007

Initial values of a, b, c, α, β, δ and γ were assumed for the solver. These values were used to estimate the dynamic modulus at the testing temperatures where the dynamic modulus has been determined. The error determined by the difference between the measured dynamic modulus ($|E_M^{*}|$) and the predicted dynamic modulus $\left|E_p^{*}\right|$ was computed. The sum of the squares of the errors was then determined. Minimization of the sum of the square of the errors is used as the objective in the solver based on changing the values of a, b, c, α, β, δ and γ subject to certain constraints as shown below.

$\text{Objective} = \text{minmize}\sum(|E_{\text{M}}^{*}| - |E_{\text{P}}^{*}|)^2$ Subject to the conditions in table 11

Optimization was performed by running the solver function multiple times until the final values for all parameters ceased to change. After optimization in the solver, the values of all the parameters (a, b, c, α, β, δ and γ) were determined and used to establish the master curve for each condition.

Figure 15 shows an example of a shifted and optimized dynamic modulus master curve for aged sample at 25°F increased temperature and 4 hour STA time (AG4H). It shows a plot of the actual measured data and the predicted data.

After the shift factor is applied to the measured dynamic modulus, the measured $|E^*|$ aligns with the predictive curve.

Table 11: Initial Values and Constraints of Parameters for Development of Master Curves in Excel Solver

		Constraints	
Parameter	Starting Values	Minimum Value	Maximum value
α	4.2521	None	None
β	2.6829	None	None
δ	1.2459	None	None
γ	0.4493	None	None
a	0.0001	-0.022925	0.061447
b	-0.0733	None	None
c	4.7618	None	12.24376
$\log a(70^o F)$	None	0	0

Figure 15 shows that the dynamic modulus of the mix decreases with increase in the test temperature at a given loading frequency or rate. It also shows that the dynamic modulus of a mix increases with frequency at a given temperature. Similar graphs plotted for all the testing conditions are shown in appendix B. The graphs were then compared in the

following section to determine the effect of the various mixing and STA conditions on the predicted values of the dynamic modulus.

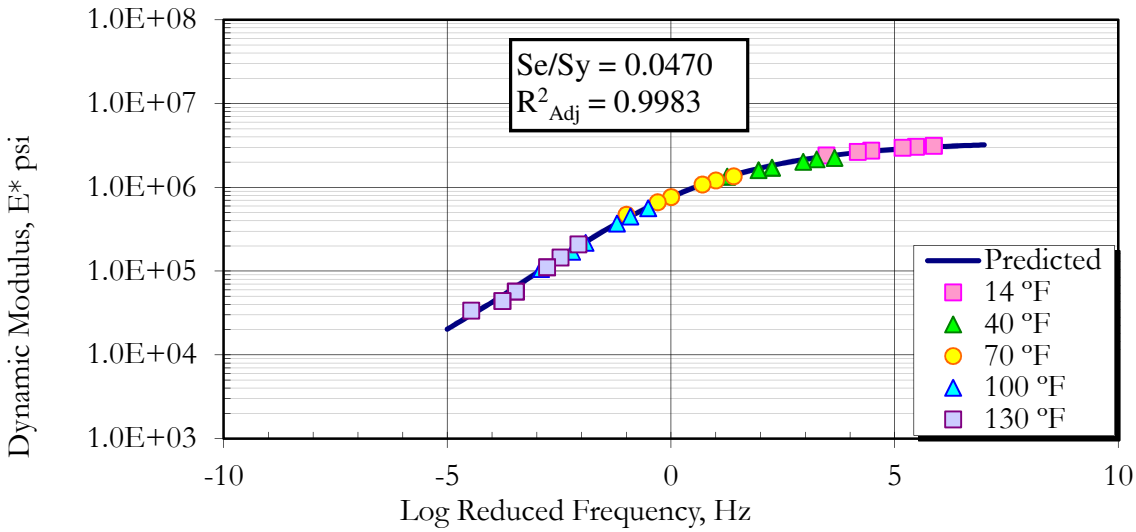

Figure 15: Samples Shifted $|E^*|$ Master Curve for Aged Sample at 25°F Increased Temperature and 4 hours STA Time (AG4H)

Comparison of $|E^*|$ Master Curves

This section presents a comparison of the predictive $|E^*|$ master curves produced from shifting and optimization of data obtained from each sample. The comparisons are necessary to assess the impact of changing STA and mixing conditions on dynamic modulus of the mixture. The desired results is to have higher $|E^*|$ values at low frequencies and high temperature (on the left side of the graph) and relatively lower $|E^*|$ values at higher frequencies and lower temperature (on the right side of the $|E^*|$ master curve). This means that the mix is likely stiffer at higher temperatures to resist rutting and more flexible at lower temperatures to resist thermal cracking. The detrimental effect of short term aging is of concern in low temperature environments due to the associated higher likelihood of thermal

cracking of the aged asphalt mixtures. Particular attention should be given to relative changes in $|E^*|$ at lower temperatures.

Effect of Temperature on Predicted $|E^*|$

Comparison of predictive $|E^*|$ master curves based on data set for samples with different mixing and STA temperatures are presented in Figures 14 through 16. All three graphs indicate that there is generally no noticeable change in the dynamic of the samples due to increased mixing and STA temperatures.

Figure 16 and 17 show comparisons of master curves for samples aged under LT and HT conditions with the same STA time of 4 and 6 hours, respectively. The graphs show that at very low frequencies (low vehicular speeds) and higher temperatures, the samples aged at the standard LT conditions have higher predictive $|E^*|$ and hence will perform better than the samples aged under HT conditions. However, at high frequency and low temperatures, there seem to be no difference in the predicted $|E^*|$ for both samples. Therefore based on the results shown in Figures 16 and 17, it appears that a 25°F increase in Mixing and STA temperatures does not affect the low temperature $|E^*|$ for samples with 4 hours and 6 hours STA time. Figure 18 compares samples aged under LT and HT conditions for 8 hours and shows no practical difference in the predictive $|E^*|$ values.

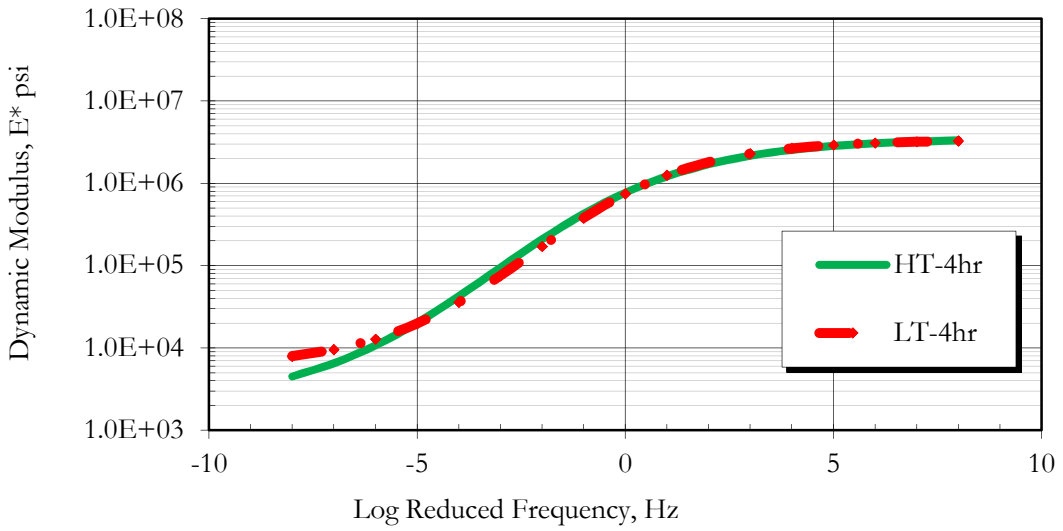

Figure 16: Effect of Temperature on Predicted $|E^*|$ at 4 Hours STA Time High Temperature vs. Low Temperature

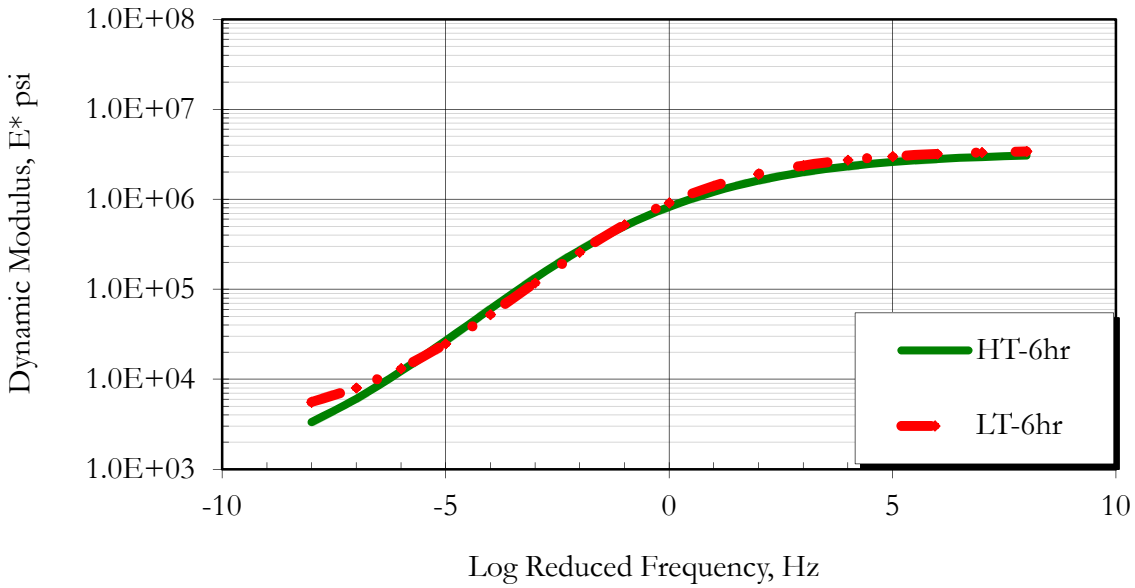

Figure 17: Effect of Temperature on Predicted $|E^*|$ at 6 Hours STA Time High Temperature vs. Low Temperature

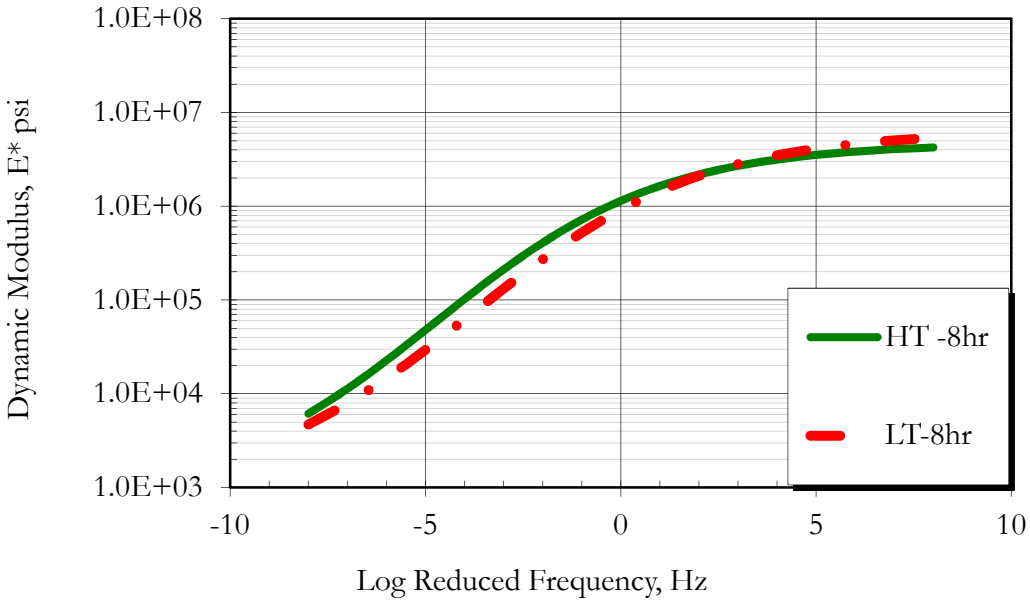

Figure 18: Effect of Temperature on Predicted $|E^*|$ at 8 Hours STA Time High Temperature vs. Low Temperature

Effect of STA Time on Predicted |E*|

In order to assess the effect of increasing short-term aging time on the properties of the asphalt mixture, the master curves of mixtures with STA time of 4, 6 and 8 hours were compared. The comparisons are shown in Figures 19 and 20. The effect of temperature was eliminated by separating samples aged under LT condition from HT conditions. The result show that for both LT and HT conditions, an 8 hour STA time representing a 4hour increase over the standard laboratory temperature resulted in a noticeable increase in the low temperature stiffening of the asphalt mixture.

Figure 19 represents a comparison of master curves for samples aged under LT conditions for 4, 6, and 8 hours of STA time. It can be seen from the graphs that at lower frequencies

(high temperature), the curve for the 4hours aged samples have the highest predictive $|E^*|$ values, whilst the curve for the 8 hours aged samples have the lowest $|E^*|$ values. At high frequency (lower temperature) the curve for the 8 hours aged samples have the higher predictive $|E^*|$ values than the curve for the 4 hours aged samples. Therefore it can be said that under typical STA and mixing temperatures (LT conditions), the samples aged for 4 hours are stiffer at higher temperature and more flexible at lower temperature than samples aged for 8 hours. Hence both the low temperature and high temperature predicted performance of the asphalt mixture will be potentially affected when the short term aging time is increased by 4 hours. For samples aged for 6 hours, the moderate to high temperature (low frequency) predictive $|E^*|$ master curve coincides with the master curve for the 8 hours aged samples but the low temperature (high frequency) predictive $|E^*|$ master curve coincides with the master curve for the 4 hours aged samples. Hence a 2 hour increase in aging time only will likely affect the high temperature performance of the mixture, but did not affect the low temperature predictive $|E^*|$ for samples aged under LT conditions.

1

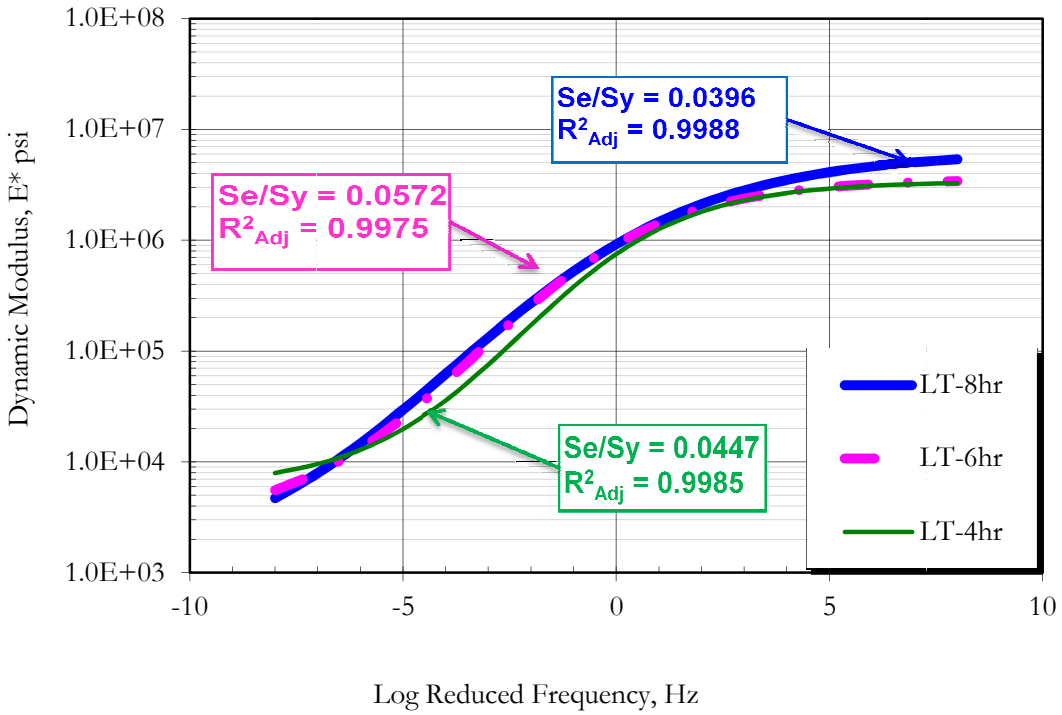

Figure 19: Effect of Short Term Aging Time on Predicted $|E^*|$ at Standard Aging Temperature (LT)

Figure 20 represents a comparison of master curves for samples ages under HT conditions for 4, 6, and 8 hours of STA time. The graphs show that at both lower and higher frequencies (high and low temperature environments), the curve for the 8 hours aged samples have the highest predictive $|E^*|$ values whilst the curve for the 6 hours aged samples have the lowest $|E^*|$ values. For all practical purposes it can be said that the predictive $|E^*|$ master curve for the 4 hours and 6 hours aged samples are similar at higher and lower temperature condition. Therefore under elevated STA and mixing temperatures (HT conditions), samples aged for 8 hours are stiffer at higher temperature and lower temperature conditions. Hence only the low temperature properties of the asphalt mixture is

adversely affected when the short term aging time is increased by 2 and 4 hours under HT condition.

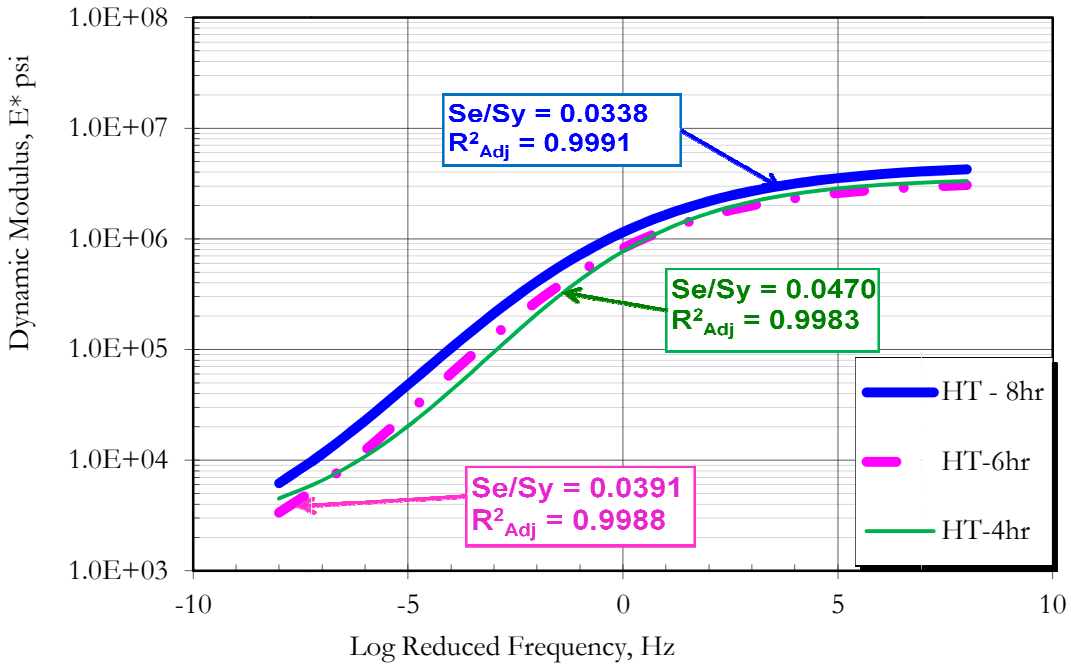

Figure 20: Effect of Short Term Aging Time on Predicted $|E^*|$ at Elevated Aging Temperatures (HT)

Comparison of Measured $|E^*|$ Data

In addition to comparing predictive $|E^*|$ master curves, a comparison of measured $|E^*|$ is presented in this section to ascertain the effect of the various aging and mixing condition on the measured values. Subsequently t paired statistical analysis of the measured $|E^*|$ is also conducted to determine if the change in the measured $|E^*|$ is significant enough to affect the predicted performance of the mixture and hence limit potential changes in the standard practice.

Effect of Increased Temperature at 4 Hours STA Time on Measured $|E^*|$

The Figures 21 through 25 present changes and trends in measured $|E^*|$ of samples that were conditioned for 4 hours of STA time. It compares LT with HT conditions across all frequencies and temperatures. It shows that for all temperatures, the measured $|E^*|$ decreases as the frequency of dynamic load application increases for both LT and HT conditions. It also shows that measured $|E^*|$ for LT condition is greater than that for HT condition at temperatures below 70^{O}F. Measured $|E^*|$ are essentially equal at 70^{O}F across all the frequencies. For temperatures above 70^{O}F the measured $|E^*|$ for HT are greater than that for LT condition. However, it is worthy to note that the differences between the average $|E^*|$ values for both LT and HT condition are within the maximum and minimum values of each other. This gives an indication that the effect of a 25^{O}F increase in temperature does not significantly change $|E^*|$ of the mixture when aged for 4 hours.

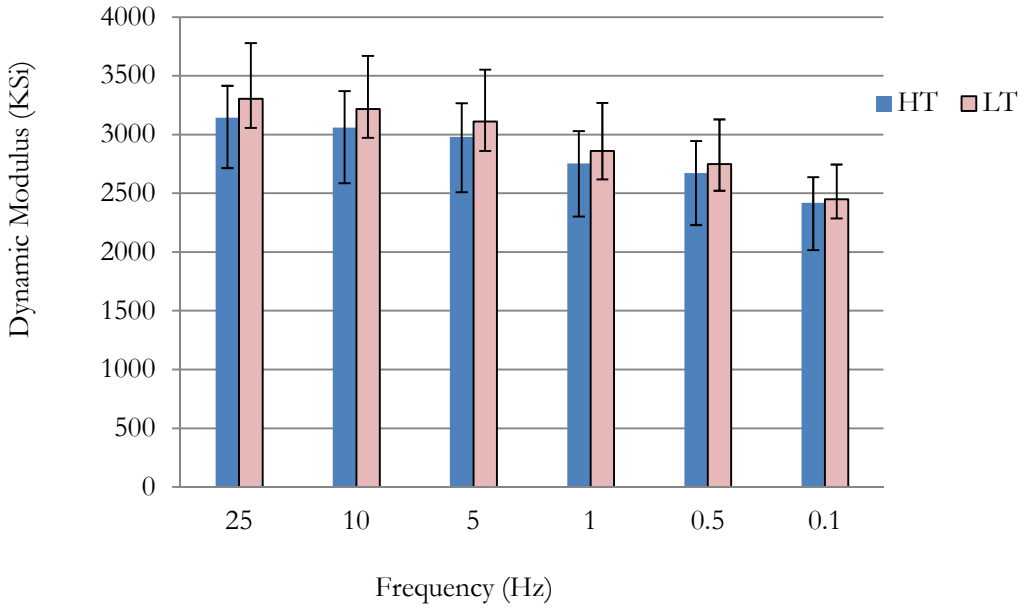

Figure 21: Measured $|E^*|$ at 14^{o}F for Normal (LT) and 25^{o}F Elevated (HT) STA and Mixing Temperatures and 4 Hours STA

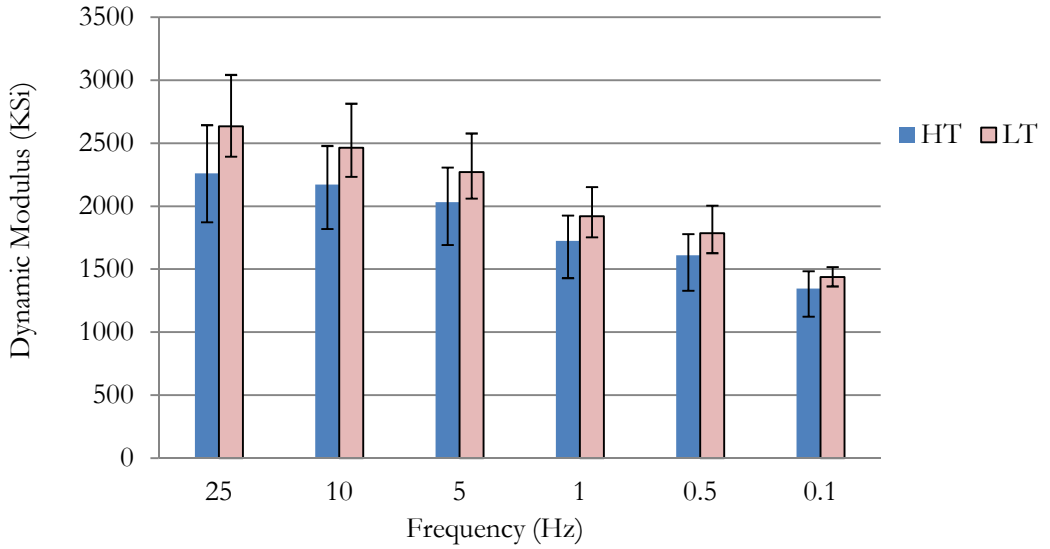

Figure 22: Measured $|E^*|$ at 40°F for Standard (LT) and 25°F Elevated (HT) STA and Mixing Temperatures and 4 Hours STA

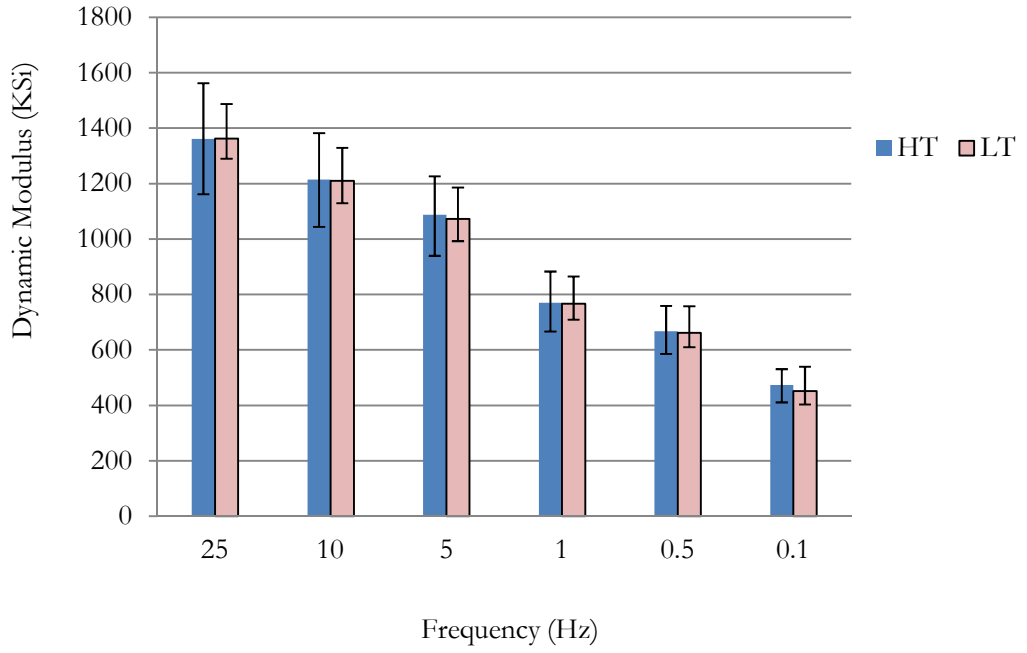

Figure 23: Measured $|E^*|$ at 70°F for Normal (LT) and 25°F Elevated (HT) STA and Mixing Temperatures and 4 Hours STA

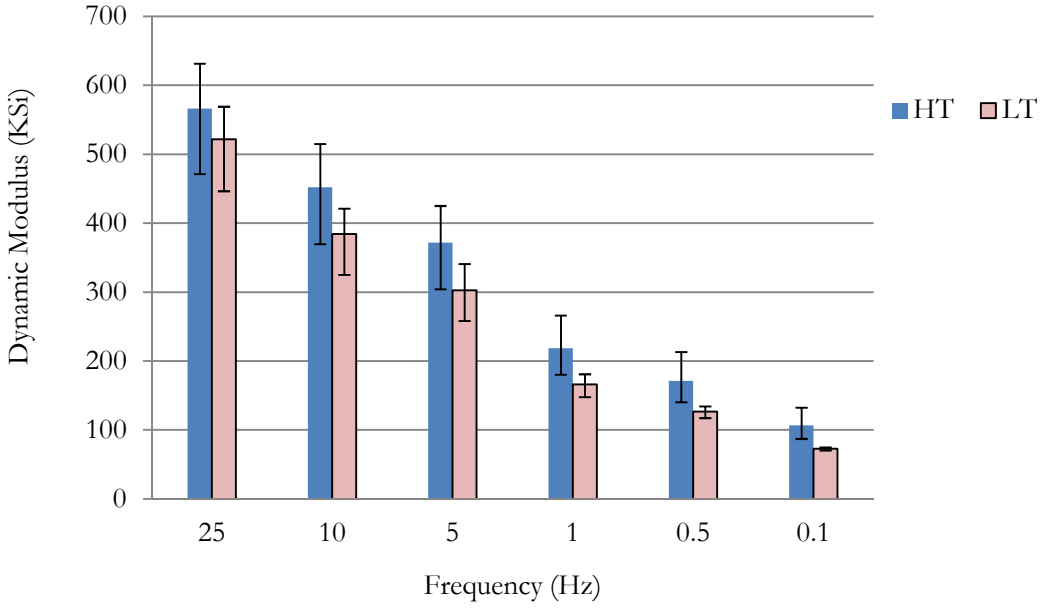

Figure 24: Measured $|E^*|$ at 100°F for Normal (LT) and 25°F Elevated (HT) STA and Mixing Temperatures and 4 Hours STA

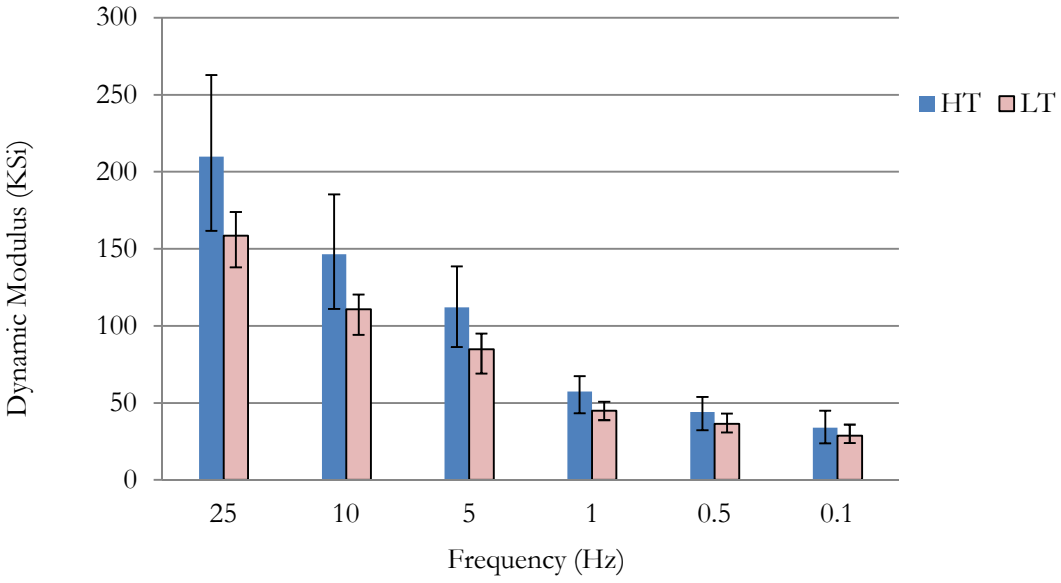

Figure 25: Measured $|E^*|$ at 130°F for Normal (LT) and 25°F Elevated (HT) STA and Mixing Temperatures and 4 Hours STA

Effect of Increased Temperature at 8 Hours STA Time on Measured $|E^*|$

Figures 26 through 30 present the changes and trends in measured $|E^*|$ for sample conditioned for 8 hours of STA time. It compares LT conditions with HT conditions across all frequencies and temperatures. They also show that for all temperatures, the measured $|E^*|$ decreases as the frequency of dynamic load application increases for both LT and HT conditions. It also shows that measured $|E^*|$ for LT condition is great than that for HT condition at temperatures below 70^{O}F. At temperatures of 70^{O}F and above, the measured $|E^*|$ for HT are greater than that for LT condition. Differences between the average $|E^*|$ values for LT and HT condition are also within the maximum and minimum values of each other as observed for 4 hours aging . This also gives the indication that a 25^{O}F increase in temperature over LT conditions does not significantly change the $|E^*|$ of a mixture with 8 hours of STA time.

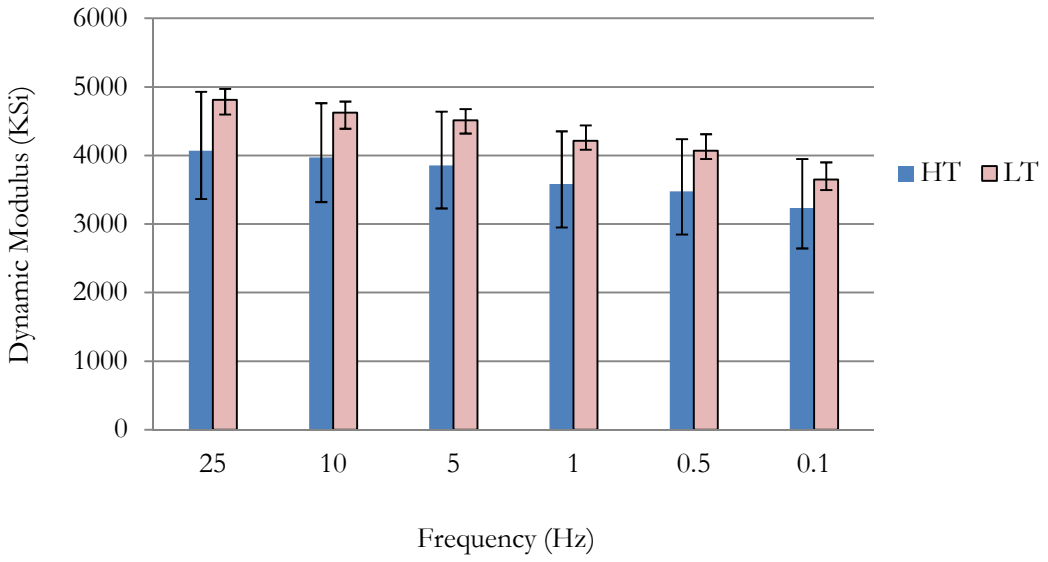

Figure 26: Measured $|E^*|$ at 14^{o}F for Normal (LT) and 25^{o}F Elevated (HT) STA and Mixing Temperatures and 8 Hours STA Time

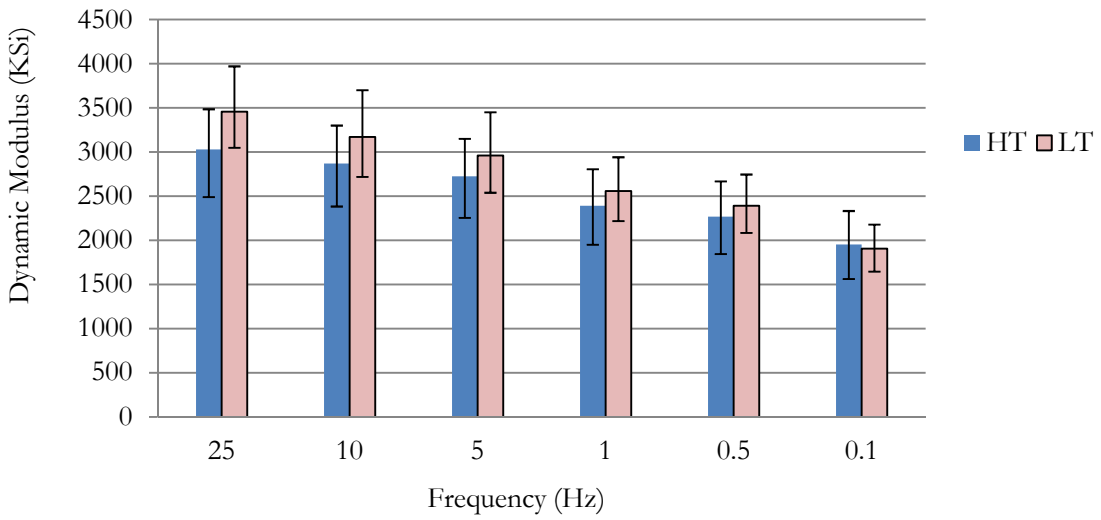

Figure 27: Measured $|E^*|$ at 40°F for Normal (LT) and 25°F Elevated (HT) STA and Mixing Temperatures and 8 Hours STA Time

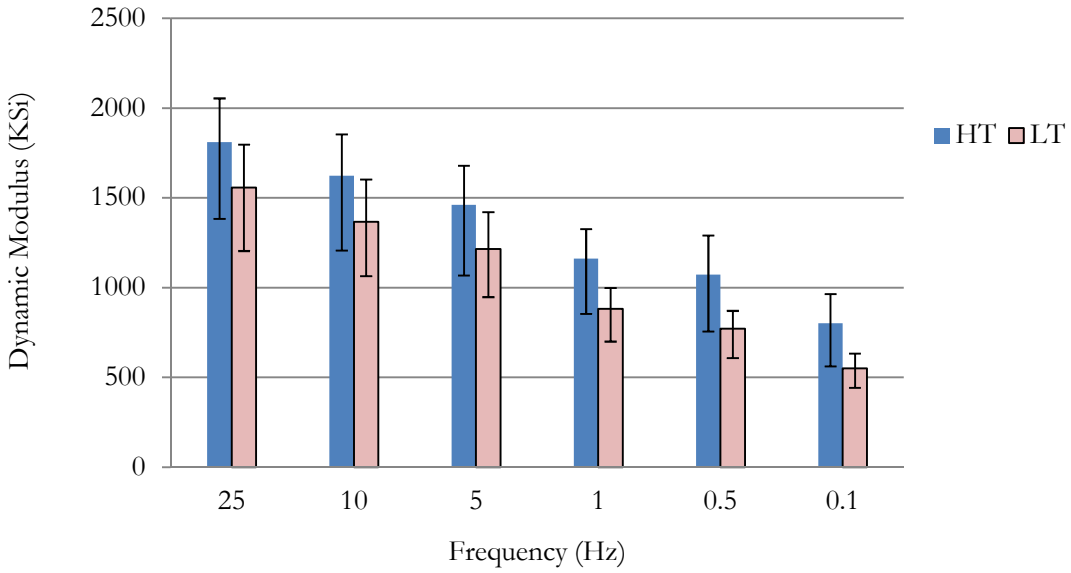

Figure 28: Measured $|E^*|$ at 70°F for Normal (LT) and 25°F Elevated (HT) STA and Mixing Temperatures and 8 Hours STA Time

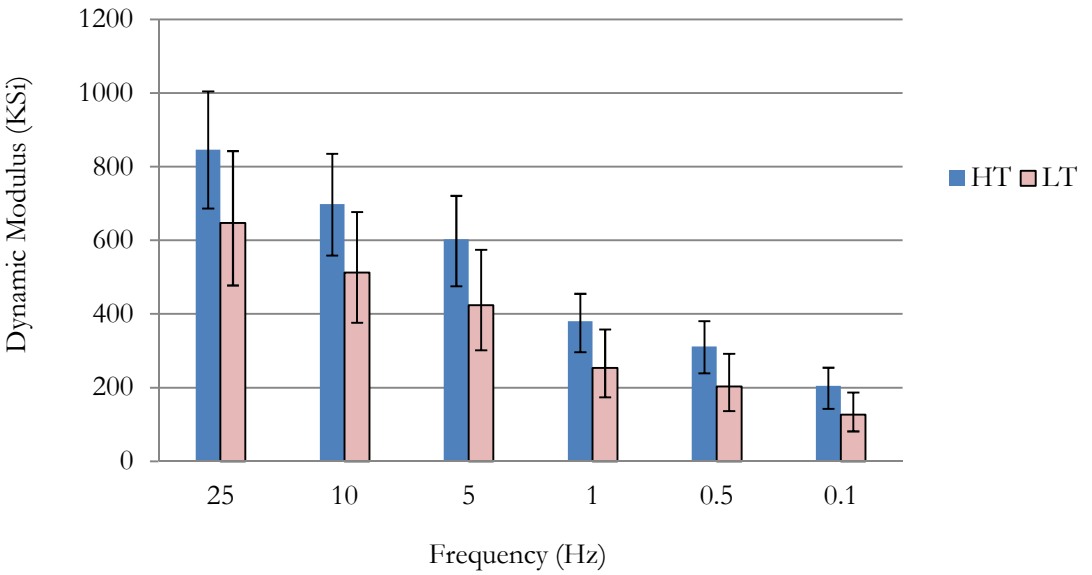

Figure 29: Measured $|E^*|$ at 100°F for Normal (LT) and 25°F Elevated (HT) STA and Mixing Temperatures and 8 Hours STA Time

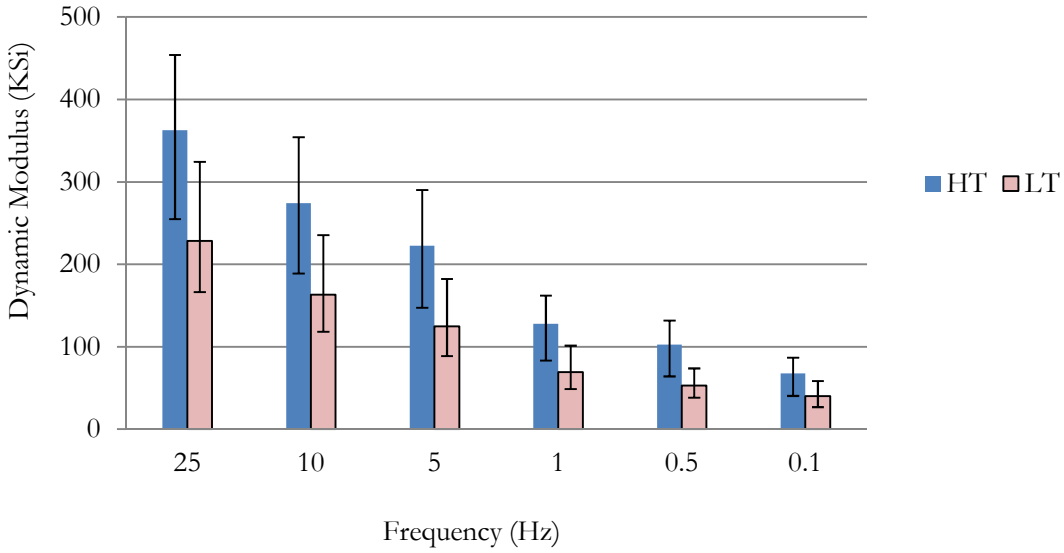

Figure 30: Measured $|E^*|$ at 130°F for Normal (LT) and 25°F Elevated (HT) STA and Mixing Temperatures and 8 Hours STA Time

Effect of STA Time on Measured $|E^*|$

The effect of increased STA time on the dynamic modulus of the mixture was explored by comparing measured $|E^*|$ of samples aged under similar temperature conditions, but different aging times. Figures 31 through 35 compare samples aged under LT conditions for 4 hours, 6 hours and 8 hours; Figures 36 through 40 compare samples aged under HT conditions for 4 hours, 6 hours and 8 hours. Statistical paired t test is use to determine the significance level of the increase in stiffness due to increasing STA time.

Effect of Increased STA Time on Measured $|E^*|$ Under Standard (LT) Conditions

Figures 31 and 32 show that in a low temperatures environment (below 70^{O}F), the $|E^*|$ of the mixture aged for 6 hours are similar to those of the mixtures aged for 4 hours; whiles an 8 hours STA time mixture show a noticeable increase in the $|E^*|$ with values outside the range of error bars of the 4 hours and 6 hours aged mixtures. This gives the indication that a 4 hour increase in STA time may increase the stiffness of a mixture in a low temperature environment. Statistical analysis of the paired data using the paired t test is later conduct to determine if the increase in $|E^*|$ is statistically significant.

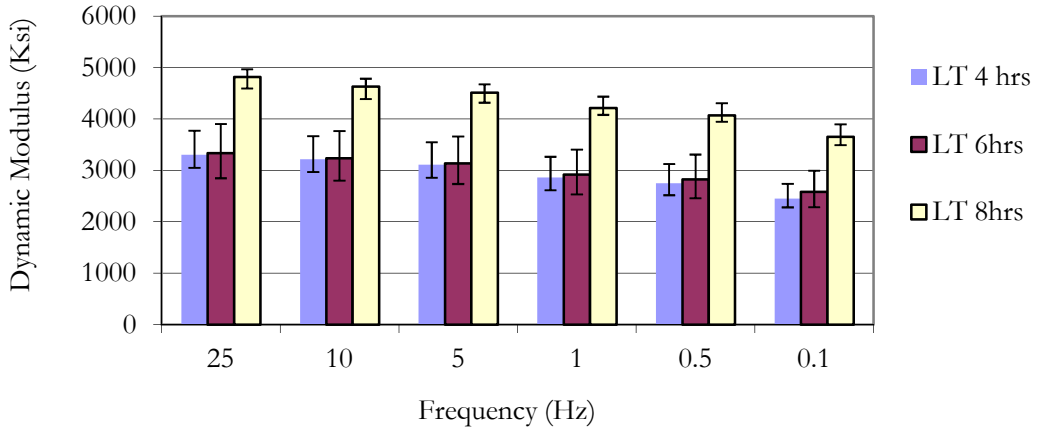

Figure 31: Measured $|E^*|$ at 14^{o}F at Different STA Aging Times for Normal (LT) STA and Mixing Temperatures

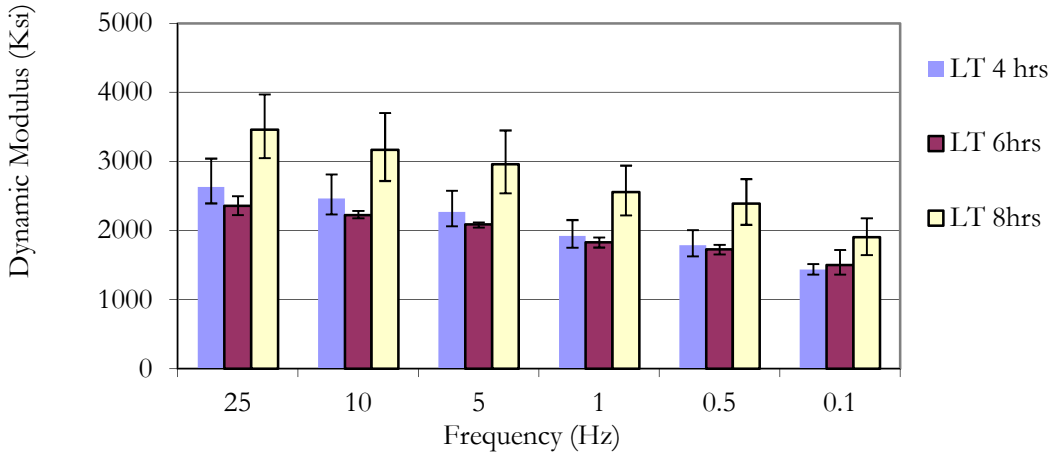

Figure 32: Measured $|E^*|$ at 40°F at Different STA Aging Times for Normal (LT) STA and Mixing Temperatures

Figures 33 to 35 show that in normal and high temperature environment (70°F, 100°F and 130°F), the $|E^*|$ of the 8 hours and 6 hours aged mixtures are higher the E* data for 4 hour STA time mixture. This show that a 2 hour and 4 hour increase in STA time will result in a stiffness increase of the mixture in a higher temperature environment. However the values of $|E^*|$ for all the STA times are within range of error bars of each other, suggesting there is no statistical difference.

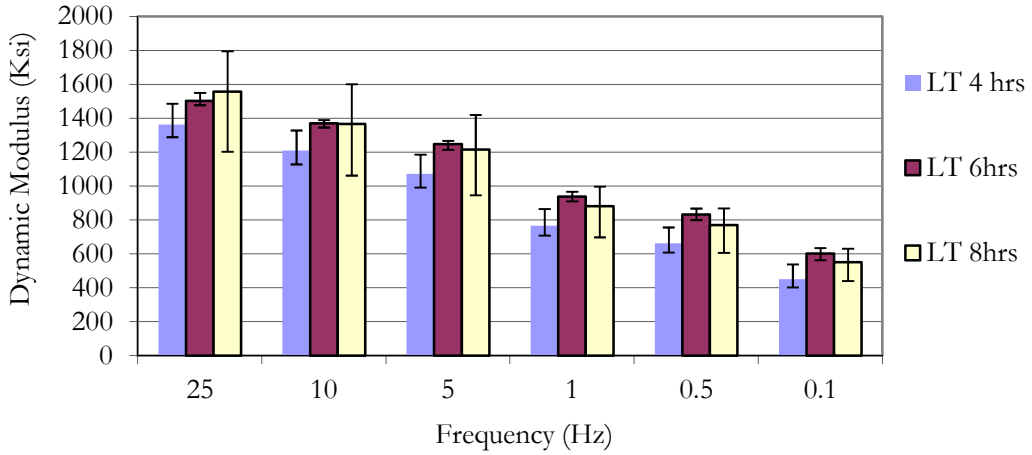

Figure 33: Measured $|E^*|$ at 70°F at Different STA Aging Times for Normal (LT) STA and Mixing Temperatures

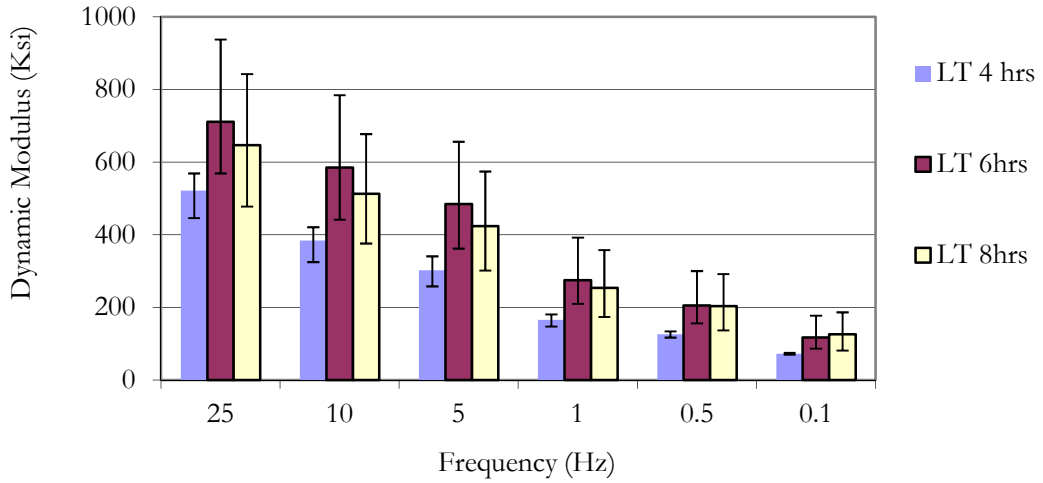

Figure 34: Measured $|E^*|$ at 100°F at Different STA Aging Times for Normal (LT) STA and Mixing Temperatures

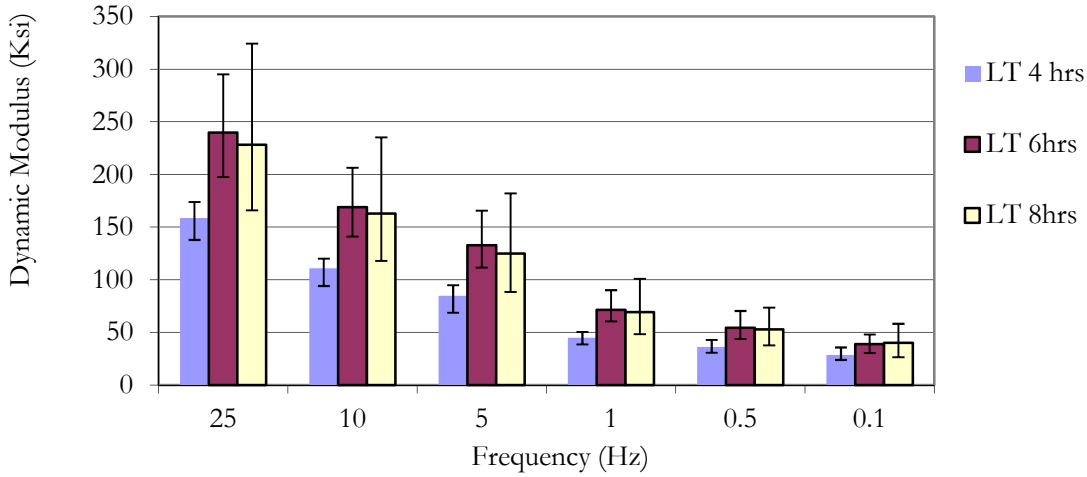

Figure 35: Measured $|E^*|$ at 130°F at Different STA Aging Times for Normal (LT) STA and Mixing Temperatures

Effect of Increased STA Time on Measured $|E^*|$ Under Elevated HT Conditions

Figures 36 through 40 show that the measured $|E^*|$ of the mixtures aged for 4 and 6 hours are essentially similar in values and noticeably lower than measured $|E^*|$ for mixture aged for 8 hours. This shows that a 4 hour increase in STA time may increase the stiffness of the mixture for all temperature environments.

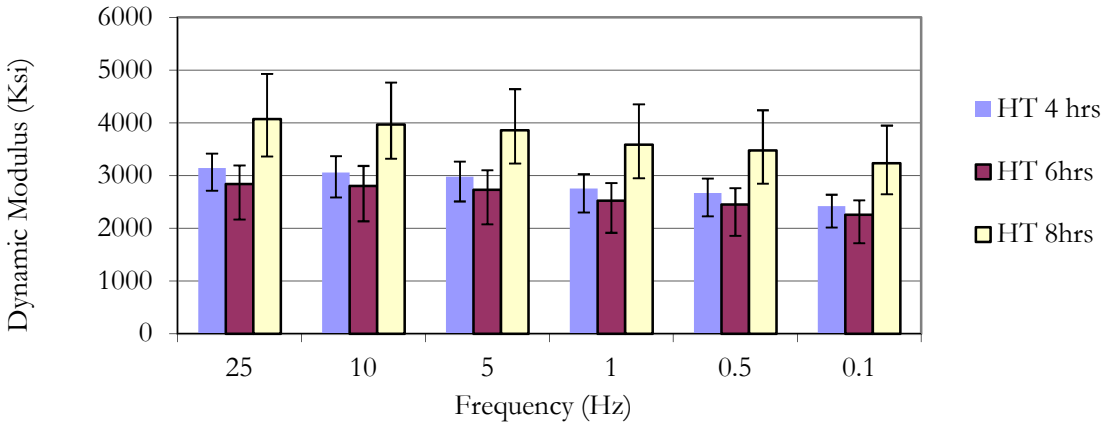

Figure 36 : Measured $|E^*|$ at 14°F at Different STA Aging Times for 25°F Elevated (HT) STA and Mixing Temperatures

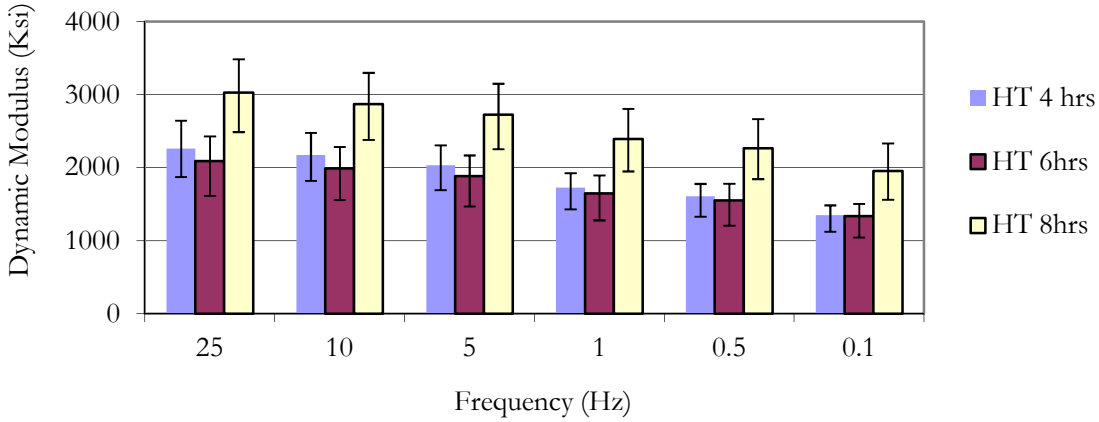

Figure 37 : Measured $|E^*|$ at 40°F at Different STA Aging Times for 25°F Elevated (HT) STA and Mixing Temperatures

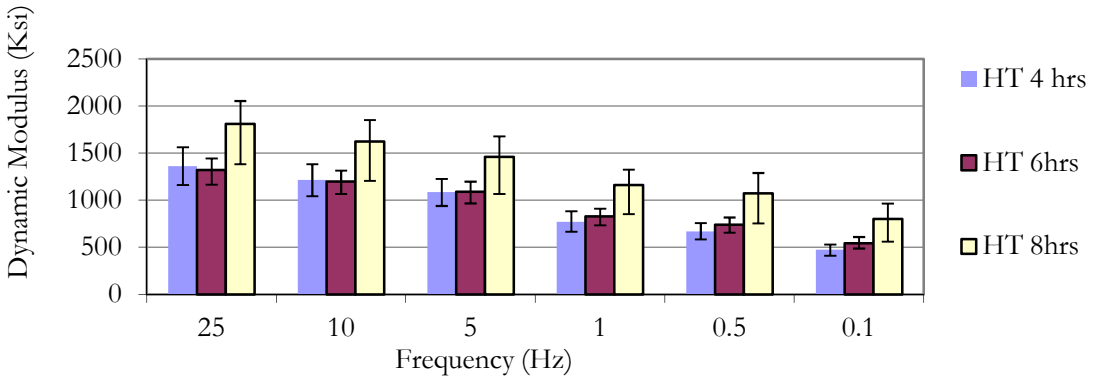

Figure 38: Measured $|E^*|$ at 70°F at Different STA Aging Times for 25°F Elevated (HT) STA and Mixing Temperatures

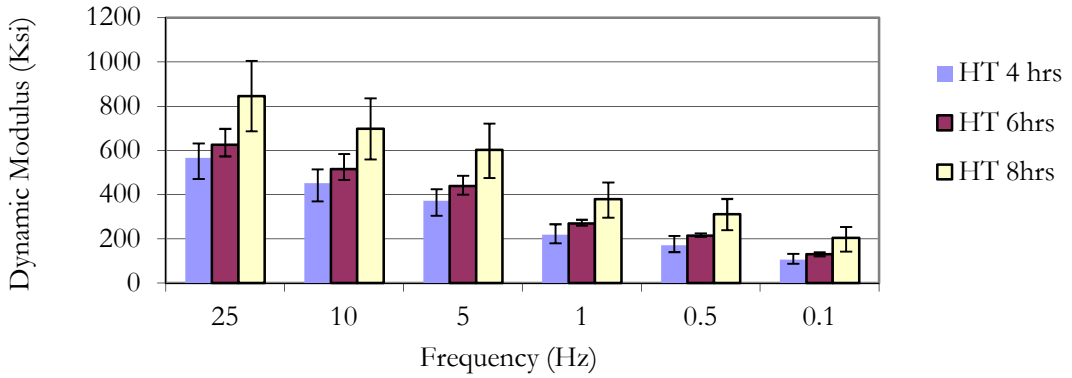

Figure 39: Measured $|E^*|$ at 100°F at Different STA Aging Times for 25°F Elevated (HT) STA and Mixing Temperatures

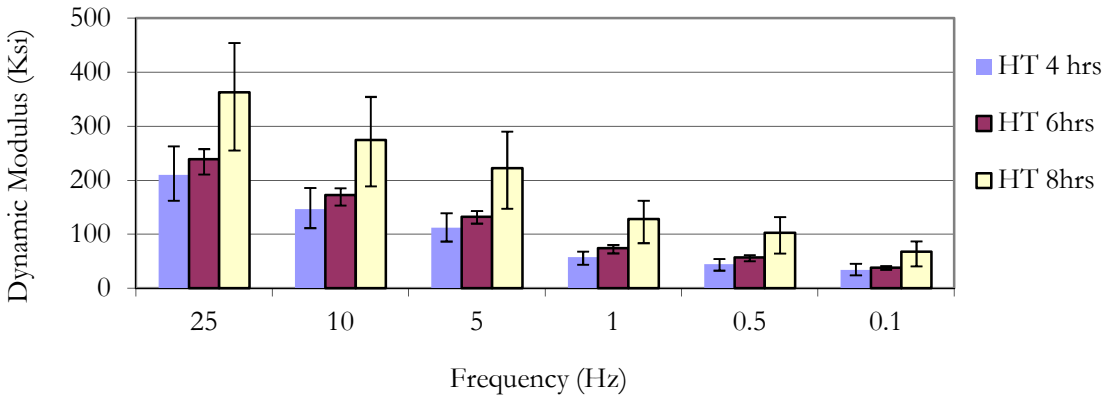

Figure 40: Measured $|E^*|$ at 130°F at Different STA Aging Times for 25°F Elevated (HT) STA and Mixing Temperatures

Statistical Analysis of $|E^*|$ Test Results

The t-Paired test was used to analyze the result of the dynamic modulus to determine if there were significant changes in $|E^*|$ the dynamic modulus due to changes in temperature and time. The t paired test was conducted at the 95% confidence level with a null hypothesis that the increase in mixing temperature, STA temperature and STA times did not cause significant changes in the dynamic modulus of the asphalt concrete mixture. Results of the statistical analysis are shown in Tables 12, 13 and 14. Paired data was compared for each replicate and at every frequency and temperature at which $|E^*|$ was measured. The data was grouped into LT and HT regardless of STA time to evaluate the effect of temperature, and then grouped into 4, 6 and 8 hours groups regardless LT and HT condition to evaluate the effect of the time on the change in dynamic modules.

Statistical Analysis of the Effect of Temperature on Dynamic Modulus (LT vs. HT)

The effect of a 25^{O}F increased STA and Mixing temperature was evaluated by pairing samples from LT and HT conditions and performing the paired t-test on $|E^*|$ measured at similar chamber temperatures and frequencies for each replicate. The critical t-values, t-statistical and P-values are shown in table 12. The results shown in table 12 indicates that at a 95% confidence level increasing the mixing and STA temperatures by 25^{o}F did not yield a significant change in measured $|E^*|$ at all frequencies and temperatures of measurement.

Statistical Analysis of the Effect of Time on dynamic Modulus (4 Hrs vs. 6 Hrs)

The significance of the effect of a 2 hour increase in STA time was evaluated by paring samples with 4 hours STA times to samples 6 hours STA times with $|E^*|$ measured at similar chamber temperatures and frequencies for each paired replicate. The paired t-test analysis was conducted on the paired replicate data. The critical t-values, t-statistical and P-values are shown in Table 13.

Table 12: t-Paired Test Results for the Effect of Increasd Temperature on $|E^*|$ (HT Versus LT) at 95% Confidence Level

FRQ	TEMP (°F)	Ave Δ $\|E^*\|$ (Ksi)	% Ave Change	$t_{Critical}$ two-tail	$t_{Statistical}$	P(T<=t) two-tail	Statistical Significance
0.1	14	-255	-8%	2.31	1.59	0.151	Not Significant
0.1	40	-69	-3%	2.31	0.53	0.609	Not Significant
0.1	70	72	17%	2.31	-1.02	0.339	Not Significant
0.1	100	42	55%	2.31	-1.85	0.101	Not Significant
0.1	130	11	43%	2.31	-1.26	0.242	Not Significant
0.5	14	-349	-10%	2.31	1.99	0.081	Not Significant
0.5	40	-160	-7%	2.31	1.07	0.317	Not Significant
0.5	70	73	13%	2.31	-0.79	0.455	Not Significant
0.5	100	55	42%	2.31	-1.71	0.126	Not Significant
0.5	130	20	53%	2.31	-1.66	0.135	Not Significant
1	14	-376	-10%	2.31	2.12	0.067	Not Significant
1	40	-184	-8%	2.31	1.16	0.280	Not Significant
1	70	57	9%	2.31	-0.63	0.546	Not Significant
1	100	58	36%	2.31	-1.52	0.167	Not Significant
1	130	24	51%	2.31	-1.65	0.137	Not Significant
5	14	-397	-10%	2.31	2.10	0.069	Not Significant
5	40	-226	-8%	2.31	1.21	0.261	Not Significant
5	70	34	5%	2.31	-0.30	0.770	Not Significant
5	100	68	25%	2.31	-1.18	0.273	Not Significant
5	130	41	49%	2.31	-1.61	0.145	Not Significant
10	14	-416	-11%	2.31	2.12	0.066	Not Significant
10	40	-276	-9%	2.31	1.39	0.202	Not Significant
10	70	31	4%	2.31	-0.25	0.807	Not Significant
10	100	61	19%	2.31	-0.95	0.369	Not Significant
10	130	50	44%	2.31	-1.68	0.131	Not Significant
25	14	-467	-11%	2.31	2.28	0.052	Not Significant
25	40	-357	-11%	2.31	1.70	0.127	Not Significant
25	70	23	3%	2.31	-0.18	0.859	Not Significant
25	100	53	14%	2.31	-0.71	0.496	Not Significant
25	130	62	39%	2.31	-1.63	0.141	Not Significant

The results shown in Table 13 indicates that there was no significant change in measured $|E^*|$ at the highest frequency of 25/sec for all temperature. Significant increase in measured $|E^*|$ however occurred at frequencies of 0.1, 0.5,1,5 and 10 measured at temperatures of 70°F and higher.

Table 13: t-Paired Significance Test Results for 2 Hours Increased STA Time on $|E^*|$ (4 Hours Versus 6 Hours) at 95% Confidence Level

FRQ	TEMP (^{O}F)	Ave Δ $\|E^*\|$ (Ksi)	% Ave Change	$t_{Critical}$ two-tail	$t_{Statistical}$	P(T<=t) two-tail	Statistical Significance
0.1	14	-15	-1%	2.57	0.191	0.856	Not Significant
0.1	40	26	2%	2.57	-0.376	0.722	Not Significant
0.1	70	110	25%	2.57	-5.027	0.004	Significant
0.1	100	34	44%	2.57	-2.260	0.073	Not Significant
0.1	130	7	31%	2.57	-1.569	0.178	Not Significant
0.5	14	-72	-3%	2.57	0.797	0.461	Not Significant
0.5	40	-59	-3%	2.57	0.846	0.436	Not Significant
0.5	70	122	19%	2.57	-4.725	0.005	Significant
0.5	100	62	46%	2.57	-2.588	0.049	Significant
0.5	130	16	45%	2.57	-2.874	0.035	Significant
1	14	-86	-4%	2.57	0.963	0.380	Not Significant
1	40	-85	-4%	2.57	1.152	0.301	Not Significant
1	70	114	15%	2.57	-3.758	0.013	Significant
1	100	80	46%	2.57	-2.675	0.044	Significant
1	130	22	48%	2.57	-3.486	0.018	Significant
5	14	-111	-4%	2.57	1.218	0.278	Not Significant
5	40	-166	-7%	2.57	2.014	0.100	Not Significant
5	70	89	9%	2.57	-1.993	0.103	Not Significant
5	100	125	40%	2.57	-2.734	0.041	Significant
5	130	34	43%	2.57	-2.477	0.056	Not Significant
10	14	-120	-4%	2.57	1.265	0.262	Not Significant
10	40	-211	-9%	2.57	2.205	0.079	Not Significant
10	70	72	6%	2.57	-1.490	0.196	Not Significant
10	100	132	33%	2.57	-2.577	0.050	Significant
10	130	42	39%	2.57	-2.637	0.046	Significant
25	14	-135	-5%	2.57	1.218	0.278	Not Significant
25	40	-225	-9%	2.57	1.733	0.144	Not Significant
25	70	50	4%	2.57	-0.890	0.414	Not Significant
25	100	124	24%	2.57	-2.248	0.075	Not Significant
25	130	55	36%	2.57	-2.409	0.061	Not Significant

Statistical Analysis of the Effect of 2 Hours Increase STA Time on $|E^*|$ (4 Hrs vs. 8 Hrs)

The significance of a 4 hour increase in STA time on $|E^*|$ the was evaluated by comparing samples with 4 hours STA to samples 8 hours STA and performing the paired t-test on $|E^*|$ measured at similar chamber temperatures and frequencies for each replicate. The critical t-values, t-statistical and P-values are shown in Table 14. The results shown in Table 14 indicate that there are significant increases in the dynamic modulus of the mixture particularly at lower temperatures (Below 70^{O}F) across all frequencies. The results also show that for all frequencies, there is no significance change in $|E^*|$ measured at 70^{o}F and also at higher temperature (130^{O}F) for almost all frequencies except 1/sec.

Table 14: t-Paired Significance Test Results for 4 Hours Increased STA Time on $|E^*|$ (4 Hrs vs. 8 Hrs) at 95% Confidence Level

FRQ	TEMP (^{O}F)	Ave Δ $\|E^*\|$ (Ksi)	% Ave Change	$t_{Critical}$ two-tail	$t_{Statistical}$	P(T<=t) two-tail	Statistical Significance
0.1	14	1009	44%	2.57	-3.489	0.017	Significant
0.1	40	536	42%	2.57	-3.075	0.028	Significant
0.1	70	213	49%	2.57	-2.358	0.065	Not Significant
0.1	100	76	91%	2.57	-2.790	0.038	Significant
0.1	130	22	84%	2.57	-2.155	0.084	Not Significant
0.5	14	1064	42%	2.57	-3.302	0.021	Significant
0.5	40	631	41%	2.57	-3.018	0.029	Significant
0.5	70	257	42%	2.57	-2.134	0.086	Not Significant
0.5	100	109	77%	2.57	-2.934	0.032	Significant
0.5	130	37	102%	2.57	-2.419	0.060	Not Significant
1	14	1092	42%	2.57	-3.342	0.020	Significant
1	40	652	39%	2.57	-2.967	0.031	Significant
1	70	253	35%	2.57	-2.115	0.088	Not Significant
1	100	125	68%	2.57	-2.936	0.032	Significant
1	130	47	100%	2.57	-2.582	0.049	Significant
5	14	1138	40%	2.57	-3.488	0.018	Significant
5	40	690	35%	2.57	-2.710	0.042	Significant
5	70	259	26%	2.57	-1.817	0.129	Not Significant
5	100	176	54%	2.57	-2.822	0.037	Significant
5	130	75	84%	2.57	-2.370	0.064	Not Significant
10	14	1159	39%	2.57	-3.574	0.016	Significant
10	40	703	34%	2.57	-2.614	0.047	Significant
10	70	283	25%	2.57	-1.794	0.133	Not Significant
10	100	187	47%	2.57	-2.731	0.041	Significant
10	130	90	78%	2.57	-2.415	0.060	Not Significant
25	14	1218	40%	2.57	-3.609	0.015	Significant
25	40	797	36%	2.57	-2.854	0.036	Significant
25	70	322	26%	2.57	-1.899	0.116	Not Significant
25	100	202	39%	2.57	-2.518	0.053	Not Significant
25	130	111	66%	2.57	-2.441	0.059	Not Significant

Indirect Tensile Strength Test (IDT) Results

Indirect tensile strength (IDT) test was conducted at 70^{O}F for all the samples tested. The test results a shown in table 15. A graphical representations and comparison of the IDT strength and fracture energy are shown in figures 41 and 42. The results lead to show that increasing the manufacturing temperature of the mix by 25^{O}F as well as increasing the STA time by 2 and 4 hours both leads to increases in tensile strength and reduction in fracture energy potential attributed of the mixture.

Figure 41 compares the tensile strength of samples manufactured under LT and HT temperatures as well 4, 6 and 8 hours STA time. The results show an increase in tensile strength with increasing aging temperature as well as increasing STA time. Under HT conditions, the indirect tensile strength increased from 231 psi to 302 psi with an increase in STA time from 4 to 8 hours. Similar trends are observed for LT condition. Figure 41 also show that there is a noticeable increase in the indirect tensile strength of the mixture at 6 and 8 hours STA time for a 25^{O}F increase in manufacturing temperature (LT to HT).

Figure 42 compares the fracture energy potential of samples manufactured under LT and HT temperatures as well 4, 6 and 8 hours STA time. It shows a noticeable decrease in the fracture energy potential with increasing STA time to 6 and 8 hours from the standard 4 hour STA time. The results also show that when the STA time is increased to 6 and 8 hours then a 25^{O}F increase in manufacturing temperature (LT to HT) caused a noticeable reduction in the fracture energy potential of the sample.

Table 15: Indirect Tensile Strength Results measure at $70^{O}F$ for Samples Manufactured at LT and HT Conditions for 2, 4, and 8 Hours STA Time.

	Sample ID	Air Voids			IDT (S_t)						Fracture Energy					
					Kpa			psi			J/m^2			in-lbf/in^2		
		μ (%)	σ (%)	CV (%)	μ	σ	CV (%)	μ	σ	CV (%)	μ	σ	CV (%)	μ	σ	CV (%)
LT	LT-4Hrs	6.27	0.01	0.1	1605	36.27	2.26	233	5.26	2.3	8224	376	4.6	46.96	2.15	4.6
	LT-6Hrs	6.43	0.22	3.4	1749	85.56	4.89	254	12.41	4.9	7719	821	10.6	44.07	4.69	10.6
	LT-8Hrs	6.39	0.28	4.3	1679	61.45	3.66	243	8.91	3.7	7744	913	11.8	44.22	5.21	11.8
HT	HT-4Hrs	6.28	0.17	2.7	1591	59.82	3.76	231	8.68	3.8	8109	1314	16.2	46.30	7.51	16.2
	HT-6Hrs	6.18	0.37	6.0	1919	18.60	0.97	278	2.70	1.0	6373	177	2.8	36.39	1.01	2.8
	HT-8Hrs	6.41	0.03	0.5	2085	0	0	302	0.00	0.0	6602	0	0.0	37.70	0.00	0.0

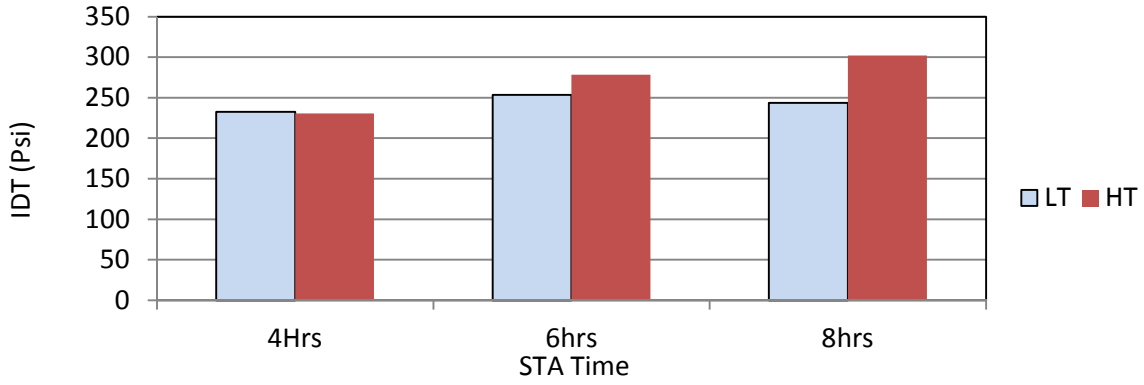

Figure 41: IDT Measured at 70°F for Aged Samples at LT and HT Conditions for 4, 6 and 8 Hours STA times

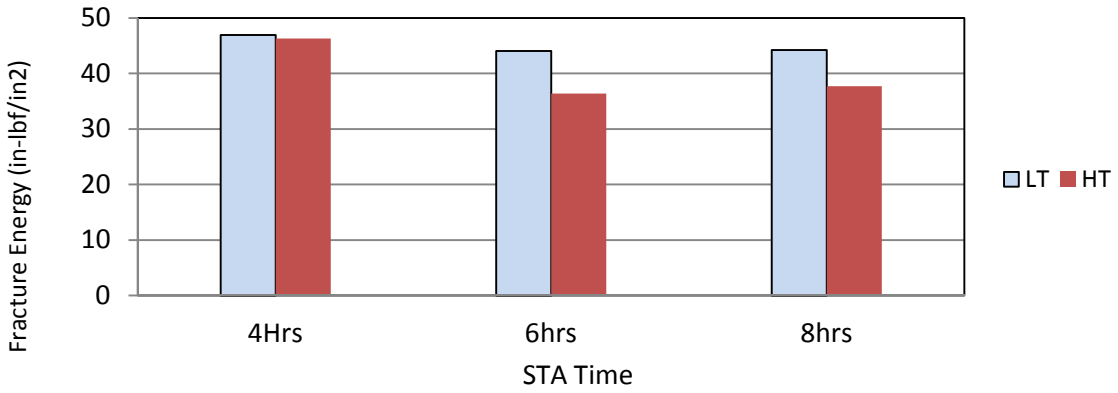

Figure 42: Fracture Energy Measured at 70°F for Aged Samples at LT and HT Conditions for 4, 6 and 8 Hours STA times

Statistical Analysis of IDT data

Results of the statistical analysis using the t-paired test evaluate the significance of the changes in IDT strength and fracture energy are presented in tables 16 and 17. The results show a significant increase in IDT strength and a significant decrease in fracture energy potential of the asphalt mixture in all cases. Therefore increasing the short term aging time by 2 and 4 hours as well as increasing mixing temperature of the HMA mix resulted in significantly increased brittleness and reduced potential to resist the onset of cracking in the

mixture. These changes are likely to adversely affect the ability of the mixture to withstand thermal cracking.

Table 16: Statistical Analysis of IDT Results using the t-Paired Test

	Effect of Temperature (LT vs. HT) IDT (KPa)	Effect of Time (4Hrs vs. 6Hrs) IDT (KPa)	Effect of Time (4Hrs vs. 8Hrs) IDT (KPa)
Mean change	112.47	336.35	171.23
SD	158.20	122.88	152.89
$t_{Statistical}$	-1.74	-3.64	-1.36
Two Tail P value	1.42E-01	3.57E-02	2.68E-01
Two-tail t Critical	2.57	3.18	3.18
Reject or Accept Null Hypothesis	Reject	Reject	Reject
% Change	6.70%	15%	11%
Significance	Significant	Significant	Significant

Table 17: Statistical Analysis of Fracture Energy Results using the t-Paired Test

	Effect of Temperature (LT vs. HT) Fracture Energy (J/m^2)	Effect of Time (4Hrs vs. 6Hrs) Fracture Energy (J/m^2)	Effect of Time (4Hrs vs. 8Hrs) Fracture Energy (J/m^2)
Mean change	-569.53	-1120.57	-993.46
SD	1021.60	1145.54	1217.07
$t_{Statistical}$	1.37	1.96	1.63
Two Tail P value	2.30E-01	1.45E-01	2.01E-01
Two-tail t Critical	2.57	3.18	3.18
Reject or Accept Null Hypothesis	Reject	Reject	Reject
Change	Significant	Significant	Significant

SUMMARY, CONCLUSIONS AND RECOMMENDATIONS FOR FUTURE RESEARCH

Summary

Heating of asphalt during production causes the volatilization and oxidation of the binders used in the asphalt mixtures. Volatilization and oxidation causes the degradation of the asphalt pavements by increasing the stiffness of the binders, which in turn causes it to be more susceptible to thermal cracking. This results in the likelihood of negatively affecting the predicted functional and structural performance of the pavement. Degradation of asphalt binders caused by volatilization and oxidation of asphalt mixtures due to high production temperature occurs during the early stages of the pavement life is known as short term aging (STA). Elevated temperatures and increased exposure time to elevated temperatures results in an increase in the degree of short term aging of asphalt.

The objective of this research was to investigate how elevated mixing temperatures and exposure time to elevated temperatures affects aging and stiffening of asphaltic binders, thus potentially influencing the performance of pavements.

While thus far, most studies on have focused on long term aging, this study focused only on the effects of short term aging and how it performs on asphalt binders and pavements.

The study was conducted in two stages. The first stage evaluated the short term aging effect on asphalt binders. It involved aging two performance graded (PG) virgin asphalt binders (PG 76-16) and PG 64-22) at two different temperatures as well as times: (standard and elevated aging temperatures and aging times and then measuring their viscosities). The result showed that in all cases, there was an expected increase in viscosity due to increased

temperature and time. Results showed the highest increase in viscosity resulted from increase in the aging time. The result also indicated the expected results that PG 64-22 was more susceptible to elevated short term aging temperature and time than PG 76-16 binders.

The second stage involved evaluating the effects of elevated short term aging temperature and time on the properties of the asphalt mix. It involved short term aging of asphalt mixes produced in the lab with the PG 64-22 binder at mixing and STA temperatures elevated 25^{O}F above the standard practice. The STA time was also increased by 2 and 4 hours longer than standard practice of 4 hours in the lab and then compacted in a gyratory compactor. Dynamic modulus (E*) and Indirect Tensile Strength (IDT) testing was measured for the aged mixtures for each temperature and time. The effect of different aging times and temperatures on the stiffness and fatigue properties of the aged asphalt mixtures was then measured and evaluated. The results confirmed the expected outcome that for the mixtures tested; increasing the STA and mixing temperature by 25^{o}F changed the stiffness and strength of the mixtures. However, for the mixture tested, the results showed that the most significant change in the dynamic modulus, indirect tensile strength and fracture energy potential occurs with the four hour increase in short term aging time regardless of the mixing and STA temperature.

Conclusions of the Binder Aging Study

Two asphalt binders PG 64-22 and PG 76-16 binders were short term aged in an RTFO at 322^{O}F and 350^{O}F for 85 minutes, representing approximately 8.6% increase in temperature. New samples of the PG 64-22 binder were then aged at 350^{o}F for 175 minutes to evaluate the effect of time on aging. The following conclusion can be drawn from the results.

- Increasing the RTFO short aging temperature above the standard 322^{O}F to 350^{O}F for both binders increases the viscosity hence stiffness of both binders.
- The PG 64-22 binder was aged to a greater degree than the PG 76-16 binder when the Brookfield Viscosity and softening point temperatures were compared. It is believed that the penetration viscosity of the PG 76-16 binder was measured in error. Therefore, the PG 64-22 binder is considered more susceptible to higher degree of stiffness due to short aging when exposed to the same temperature increase as the PG 76-16 binder during aging.
- Increasing the aging time from 85 minutes to 175 minutes can increase the amount of stiffening of a given binder. The increase in viscosity can be up to double when aged for an additional 85 minutes at the same temperature.
- The significance of the results of increasing aging time for the PG 64-22 binder is that, during construction of an HMA pavement, the potential effect of increasing mixing temperature on stiffening the binder may be further exacerbated by keeping the HMA mixture at the elevated temperature for prolonged periods over longer hauling distances with the goal of achieving compaction temperatures.
- The statistical analysis conducted on the results of the PG 64-22 binder concluded that the increase in viscosity due to increasing RTFO short term aging temperature by 8.6% is not significant at 95% confidence level. The effect of doubling the RTFO aging time was also not significant at the 95% confidence level.

Conclusions of STA Study

Twenty four HMA samples were manufactured in the laboratory with 4.5% PG 64-22 binder content in accordance with Arizona Department of Transportation mix design.

Standard industry and laboratory mixing and short term aging temperatures and times as well as 25^{O}F elevated mixing temperature, 2 and 4 hours extended aging times were used. The samples were the subjected to dynamic modulus testing as well as IDT testing to determine the effect of short-term aging associated with elevated mixing temperatures and STA time by comparing the testing results. Paired t- test was used to analyze the significance of the changes in $|E^*|$ and compaction. The following conclusions are a summary drawn from the test results on the asphalt mixture;

- A 25°F (8%) Increase in the mixing temperature resulted in a noteworthy change in $|E^*|$, IDT, and fracture energy.
- A 4 hours increase in aging time had a significant increase on E* and IDT, as well as decreased the fracture energy potential of the mixture.
- A 2 hour increase in aging time had only a minor increase on stiffness.
- Therefore, increasing the storage, transportation and waiting time at the construction site will have adverse effects on increasing the stiffness of the mix.

Conclusion of Compaction Data Analysis

The conclusion drawn from the statistical analysis of the compaction data is that at a 95% confidence level, increasing the STA and mixing temperature by 25°F from 275°F and 305°F to 300^{O}F and 330^{O}F as well as increasing STA time by 2 hours and 4 hours does not cause significant changes in the number of gyrations and shear stress during compaction.

Conclusion of the Dynamic Modulus Data Study

Conclusion drawn from that data presented and statistical analysis of the $|E^*|$ data are as follows;

- The predicted dynamic modules used for design is unlikely to be changed by a 25°F increase in mixing temperature and a 2 hour increase STA aging time. However a 4 hour increase short-term aging will cause a change in the dynamic modulus.
- Increasing the mixing and short-term aging temperature of the mix by 25°F resulted in increase in the low temperature dynamic modulus and increase in the high temperature dynamic of the asphalt concrete mixture. However changes in dynamic modulus due to the temperature increase alone was not significant at a 95% confidence level. Therefore it can be concluded that a 25°F increase in the mixing temperature will not significantly affect the dynamic module of the asphalt mixture.
- The effect of increasing STA time on the dynamic modulus was analyzed by comparing the change dynamic modulus due to 4, 6 and 8 hours of short-term aging time in the asphalt mix representing standard, 2 and 4 hours increase in STA time. The result show that a 2 hour increase in STA time significantly increases the higher temperature dynamic modulus of the mix at frequencies between 0.1 and 10. At very higher frequencies of traffic load application, the dynamic modulus of the mix is not significantly affected by a 2 hour increase in mixing temperature. It can therefore be concluded that the dynamic modulus of the mixture in a low temperature environment will not be affected by a 2 hour increase in STA time.
- A four hour increase in mixing and STA time significantly increased both the low temperature and high temperature dynamic modulus of the mixture. This indicates that the hauling distance and waiting times which contributes to increased aging time could significantly affect the dynamic modulus of a mix. It can be concluded that a 4 hour

increase in STA time over the standard will significantly increase the dynamic modulus of the mixture.

Conclusion of IDT Data Analysis

The results of the IDT data analysis lead to the conclusion that, increasing the plant mixing temperature and/or increasing exposure time of a mix to higher mixing temperatures could result in pavements with significantly increased degree of brittleness and reduced ability to resist crack initiations. Such pavements could have problems with thermal cracking.

Recommendation for Future Research

The study conducted was limited in its extent of asphalt binder type and the HMA mix type used as well as the testing conducted. Before suggesting changes to standard practices, the following are recommended for further evaluation;

- It is recommended that the findings of this study should be validated with additional HMA mixtures and binder types from all regions in Arizona. It is conceived that test results, findings and the relations in this study may be different depending on the binder and mixture types (grade and stiffness characteristics).
- Consider including other material characterization tests, such as crack propagation and fatigue. This is necessary for a comprehensive understanding of the alterations in the material properties and potential performance associated with the proposed changes in production practice.
- A pavement design and performance analysis should be conducted with the DARWin-ME software using the different properties measured to evaluate how the effect of the material changes due to STA will affect the design of pavements.

REFERENCES

AASHTO Designation TP62-07. Standard Method of Test for Determining Dynamic Modulus of Hot-Mix.

Asphalt Concrete Mixtures. AASHTO Provisional Standards, Washington, D.C., USA, 2007.

AASHTO Designation R30. STANDARD PRACTICE FOR MIXTURE CONDITIONING OF HOT MIX ASPHALT.

ASTM Designation D6931-07. Standard Test Method for Indirect Tensile (IDT) Strength of Bituminous Mixture**.**

ASTM Designation D4402. Standard Test Method for Viscosity Determination of Asphalt at Elevated Temperatures Using a Rotational Viscometer.

ASTM-D5-06 Designation. Standard Test Method for Penetration of Bituminous Materials.

ASTM D36/D36M Designation. Standard Test Method for Softening Point of Bitumen (Ring-and-Ball Apparatus).

ASTM D2872-04 Designation Standard Test Method for Effect of Heat and Air on a Moving Film of Asphalt (Rolling Thin-Film Oven Test).

Airey, G.D., and Brown, S.K. Rheological Performance of Aged Polymer Modified Bitumen. In Journal of the Association of Asphalt Technologists, Volume. 67, 1998.

Azari, H. Analysis of the Effect of Laboratory Short-Term Conditioning on Mechanical Properties of Asphalt Mixture, Transportation Research Board 90th Annual Meeting, Washington DC 2011 Report Number 11-1427.

Baek, C., Underwood, S. and Kim, Y.R. Effects of Oxidative Aging on Asphalt Mixture Properties, TRB Annual Meeting, 2012.

Bell, C.A., Weider, A.J. and Fellin, M.J. Laboratory Aging of Asphalt-Aggregate Mixtures: Field Validation, Oregon State University Corvallis, OR 97331, Strategic Highway Research Program, SHRP-A-390, National Research Council, Washington, DC 1994.

Brown, K., Roberts, K. and Lee, K. Hot Mix Asphalt Material, mixture design and construction, 3rd Edition, National Asphalt Pavement Association, (2009).

Christensen, D. W., Bonaquist, R. F. Evaluation of Indirect Tensile Test(IDT) Procedures for Low-Temperature Performance of Hot Mix Asphalt, NCHRP REPORT 530, WASHINGTON, D.C. 2004.

Clark, R.G. Practical Results of Asphalt hardening on Pavement life. AAPT Vol.27, 1958

Huang, S.-C., and Grimes. W. Influence of aging temperature on the Rheological and Chemical properties of Asphalt Binder. In Transportation Research Record 2179, TRB, National Research Council, Washington, D.C.2010, Volume 1, pp. 29-48.

Lee, J. S., Amirkhanian, N. S., Shatanawi, K. and Kim, W. K. Short-term aging characterization of asphalt binders using gel permeation chromatography and selected Superpave binder tests. In Science Direct, Construction and Building Materials, August 2007.

Maricopa Association of Governments (MAG). Uniform Standard Specification for Public Construction, Arizona, 2012.

Mirza, M. W. Development of A Global Aging System for Short and Long Term Aging of Asphalt Cements, Dissertations submitted to the faculty of the Graduate School of the University of Maryland Partial Fulfillment of the Requirements for the Degree of Doctor of Philosophy, 1993

Read, J., Whiteoak and D. Hunter, R. The Shell Bitumen Handbook, 5th revised edition, Thomas Telford Ltd, London, 2009.

University of California at Berkeley, Oregon State University Austin Research Engineers, Inc., Accelerated Performance-Related Tests for Asphalt-Aggregate Mixes and Their Use in Mix Design and Analysis Systems, Strategic Highway Research Program, SHRP-A-417, National Research Council ,Washington, DC 1994

Witczak, M.W. and Mirza, M.W., Development of a Global Aging System for Short and Long Term Aging of Asphalt Cements, Journal of the Association of the Asphalt Paving Technologists, Vol. 64, 1995

APPENDIX A

BINDER RESULTS

Viscosity of Binder PG:PG 64-22- 322°F aged at 325°F Aged for 85 minutes

Test #	Temp (F)	Temp (R)	Log(Temp) (R)	Penetration (0.1mm)	Average Viscosity (P)	Average Viscosity (cP)	Loglog (Viscosity) (cP)
Penetration	77	536.7	2.730	19.0	4.14E+07	4.14E+09	0.983
Softening point	129	588.9	2.770	-	13,000	1.30E+06	0.786
Brookfield 1	250	709.7	2.851	-	-	1.41E+03	0.498
Brookfield 2	300	759.7	2.881	-	-	3.07E+02	0.396
Brookfield 3	350	809.7	2.908	-	-	9.45E+01	0.296
Brookfield 4	375	834.7	2.922	-	-	6.09E+01	0.252

Viscosity of Binder PG:PG 64-22- 322°F aged at 350 °F Aged for 85 minutes

Test #	Temp (F)	Temp (R)	Log(Temp) (R)	Penetration (0.1mm)	Average Viscosity (P)	Average Viscosity (cP)	Loglog (Viscosity) (cP)
Penetration	77	536.7	2.730	17.7	4.89E+07	4.89E+09	0.986
Softening point	134	593.8	2.774	-	13,000	1.30E+06	0.786
Brookfield 1	250	709.7	2.851	-	-	1.77E+03	0.512
Brookfield 2	300	759.7	2.881	-	-	3.38E+02	0.403
Brookfield 3	350	809.7	2.908	-	-	9.92E+01	0.300
Brookfield 4	375	834.7	2.922	-	-	5.86E+01	0.247

Viscosity of Binder PG:PG 64-22- Aged at 350 °F for 175 Minutes

Test #	Temp (F)	Temp (R)	Log(Temp) (R)	Penetration (0.1mm)	Average Viscosity (P)	Average Viscosity (cP)	Loglog (Viscosity) (cP)
Penetration	77	536.7	2.730	13.2	9.41E+07	9.41E+09	0.999
Softening point	148	607.8	2.784	-	13,000	1.30E+06	0.786
Brookfield 1	250	709.7	2.851	-	-	3.38E+03	0.548
Brookfield 2	275	734.7	2.866			1.47E+03	0.501
Brookfield 3	300	759.7	2.881	-	-	6.74E+02	0.452
Brookfield 4	350	809.7	2.908	-	-	1.97E+02	0.361
Brookfield 5	375	834.7	2.922	-	-	1.21E+02	0.319

Viscosity of Binder PG:PG 76-16 Aged at 325^{O}F for 85 minutes

Test #	Temp (F)	Temp (R)	Log(Temp) (R)	Penetration (0.1mm)	Average Viscosity (P)	Average Viscosity (cP)	Loglog (Viscosity) (cP)
Penetration	77	536.7	2.730	15.4	6.70E+07	6.70E+09	0.992
Softening point	147	606.9	2.783	-	13,000	1.30E+06	0.786
Brookfield 1	250	709.7	2.851	-	-	3.76E+03	0.553
Brookfield 2	300	759.7	2.881	-	-	6.54E+02	0.450
Brookfield 3	350	809.7	2.908	-	-	1.83E+02	0.354
Brookfield 4	375	834.7	2.922	-	-	1.06E+02	0.307

Viscosity of Binder PG:PG 76-16 Aged at 350^{O}F for 85 minutes

Test #	Temp (F)	Temp (R)	Log(Temp) (R)	Penetration (0.1mm)	Average Viscosity (P)	Average Viscosity (cP)	Loglog (Viscosity) (cP)
Penetration	77	536.7	2.730	12.5	1.07E+08	1.07E+10	1.001
Softening point	149	609.1	2.785	-	13,000	1.30E+06	0.786
Brookfield 1	250	709.7	2.851	-	-	3.94E+03	0.556
Brookfield 2	300	759.7	2.881	-	-	6.79E+02	0.452
Brookfield 3	350	809.7	2.908	-	-	1.88E+02	0.357
Brookfield 4	375	834.7	2.922	-	-	1.09E+02	0.309

APPENDIX B

DYNAMIC MODULUS TEST RESULTS

Average Dynamic Modulus and Phase Angle, LT-4 HOURS STA

Binder 64-22 Binder 4.50%
Date: 9/30/2012 Air Voids: 6.96%

Temp.	Freq	Dynamic Modulus E*						Phase Angle, ϕ					
		Rep 1	Rep 2	Rep 3	Ave	Std. Dev.	Coeff. of Var.	Rep 1	Rep 2	Rep 3	Ave	Std. Dev.	Coeff. of Var.
(°F)	(Hz)	(ksi)	(ksi)	(ksi)	(ksi)			(Deg)	(Deg)	(Deg)	(Deg)		
14	25	3778	3077	3056	3304	411	12.4	1.8	0.5	1.8	1.3	0.8	57.5
	10	3670	3012	2972	3218	392	12.2	5.5	6.2	4.8	5.5	0.7	12.7
	5	3552	2922	2860	3111	382	12.3	6.6	6.0	5.2	5.9	0.7	11.3
	1	3269	2692	2617	2860	357	12.5	8.0	6.9	6.8	7.2	0.7	9.5
	0.5	3129	2595	2522	2748	332	12.1	8.0	7.2	7.1	7.4	0.5	7.1
	0.1	2745	2317	2285	2449	257	10.5	8.6	8.8	8.5	8.7	0.1	1.3
40	25	2394	3043	2463	2633	356	13.5	6.1	4.8	3.6	4.8	1.2	25.8
	10	2235	2815	2339	2463	309	12.5	9.6	10.4	10.1	10.0	0.4	4.1
	5	2063	2579	2172	2271	272	12.0	10.6	11.5	10.6	10.9	0.5	5.0
	1	1755	2153	1856	1921	207	10.8	13.2	12.7	12.8	12.9	0.2	1.8
	0.5	1629	2006	1725	1787	196	11.0	15.7	15.1	14.5	15.1	0.6	3.9
	0.1	1365	1518	1427	1437	77	5.4	17.1	18.2	17.5	17.6	0.6	3.2
70	25	1309	1290	1488	1362	109	8.0	10.9	11.5	10.6	11.0	0.5	4.2
	10	1171	1129	1329	1210	106	8.7	17.0	16.7	16.1	16.6	0.4	2.7
	5	1037	993	1187	1072	102	9.5	18.9	19.7	20.1	19.6	0.6	3.0
	1	726	709	865	767	86	11.2	25.0	25.4	25.0	25.1	0.2	1.0
	0.5	617	610	758	662	83	12.6	26.5	27.7	27.6	27.3	0.6	2.3
	0.1	412	403	540	452	76	16.8	29.7	32.2	33.7	31.9	2.0	6.4
100	25	549	447	569	521	66	12.6	29.0	26.1	25.1	26.7	2.0	7.6
	10	406	325	421	384	52	13.4	29.4	30.4	31.7	30.5	1.2	3.8
	5	308	258	341	303	42	13.8	30.3	31.0	33.2	31.5	1.5	4.8
	1	169	148	181	166	17	10.1	31.2	31.4	37.7	33.4	3.7	11.0
	0.5	127	117	135	126	9	6.8	31.7	32.2	39.4	34.4	4.3	12.6
	0.1	71	75	72	73	2	3.1	27.1	26.9	37.8	30.6	6.2	20.4
130	25	138	164	174	159	19	11.7	32.8	28.5	32.8	31.3	2.5	8.0
	10	94	120	118	111	14	13.0	30.8	26.9	33.8	30.5	3.5	11.4
	5	69	95	90	85	14	16.3	29.2	24.4	33.3	29.0	4.4	15.3
	1	39	51	45	45	6	13.2	24.7	20.5	33.4	26.2	6.5	24.9
	0.5	31	43	35	36	6	17.1	21.4	17.9	31.7	23.6	7.2	30.3
	0.1	24	36	26	29	6	22.2	11.9	15.7	23.6	17.1	6.0	35.0

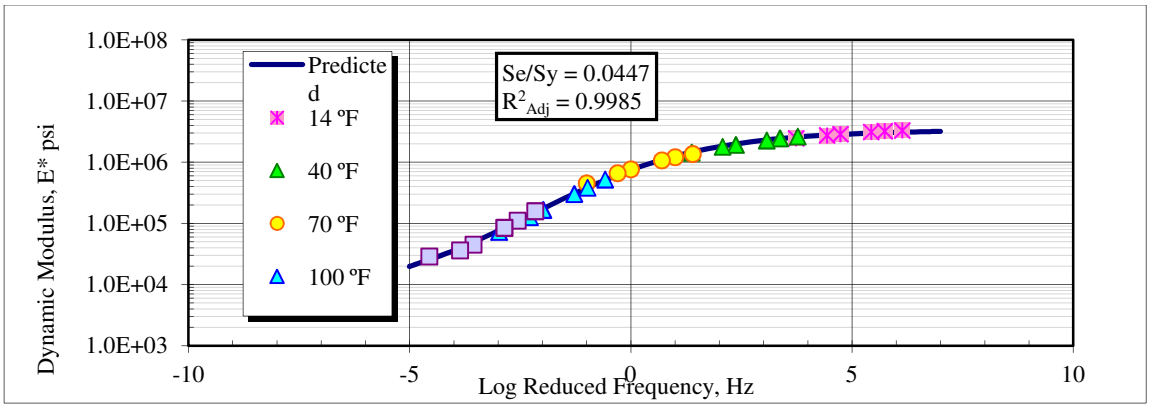

Average Dynamic Modulus and Phase Angle (LT-6Hours)

Binder Grade: 64-22 **Binder Content:** 4.50%

Date: 09/30/2012 **Ave Air Voids:** 6.73%

Temp	Freq	Dynamic Modulus E*						Phase Angle, ϕ					
(°F)	(Hz)	Rep 1 (ksi)	Rep 2 (ksi)	Rep 3 (ksi)	Ave (ksi)	Std. Dev.	Coeff. of Var.	Rep 1 (Deg)	Rep 2 (Deg)	Rep 3 (Deg)	Ave (Deg)	Std. Dev	Coeff. of Var.
14	25	3908	2851	3248	3336	534	16.0	3.3	1.8	4.8	3.3	1.5	44.9
	10	3771	2806	3125	3234	492	15.2	7.0	4.8	7.8	6.5	1.6	24.3
	5	3663	2740	3013	3139	474	15.1	7.7	5.2	8.5	7.1	1.7	23.6
	1	3411	2539	2801	2917	447	15.3	9.5	6.2	9.6	8.4	1.9	22.7
	0.5	3312	2464	2706	2827	437	15.5	9.0	6.9	9.8	8.5	1.5	17.6
	0.1	2999	2290	2449	2579	372	14.4	9.3	8.0	9.9	9.1	1.0	10.6
40	25	2498	2225	2349	2357	136	5.8	3.7	5.1	2.9	3.9	1.1	28.4
	10	2287	2178	2209	2225	56	2.5	6.9	9.2	8.7	8.3	1.2	14.2
	5	2118	2045	2102	2088	38	1.8	6.1	9.3	8.6	8.0	1.7	21.1
	1	1900	1755	1839	1831	73	4.0	10.3	11.6	10.0	10.6	0.9	8.4
	0.5	1794	1656	1732	1727	69	4.0	12.8	13.2	11.7	12.5	0.8	6.4
	0.1	1719	1421	1362	1501	191	12.8	13.9	11.1	11.5	12.2	1.5	12.4
70	25	1551	1479	1479	1503	42	2.8	11.1	8.9	8.5	9.5	1.4	14.7
	10	1390	1346	1373	1370	22	1.6	16.5	14.7	14.0	15.1	1.3	8.5
	5	1262	1215	1268	1248	29	2.3	18.8	17.7	16.0	17.5	1.4	7.9
	1	932	911	968	937	29	3.1	22.8	21.7	21.8	22.1	0.6	2.7
	0.5	825	801	869	832	34	4.1	24.9	23.8	24.1	24.2	0.6	2.3
	0.1	603	564	636	601	36	6.0	30.3	28.0	31.1	29.8	1.6	5.4
100	25	937	569	627	711	198	27.8	21.6	22.8	28.0	24.1	3.4	14.0
	10	785	442	530	585	178	30.4	23.1	28.1	31.8	27.7	4.3	15.7
	5	656	362	434	484	153	31.7	26.4	28.9	33.9	29.7	3.8	12.8
	1	392	210	221	275	102	37.2	30.7	32.1	36.5	33.1	3.0	9.2
	0.5	301	156	160	206	82	40.0	32.6	32.8	35.3	33.6	1.5	4.5
	0.1	178	87	87	117	52	44.7	26.8	32.9	32.5	30.7	3.4	11.0
130	25	295	198	227	240	50	20.9	29.9	34.2	32.3	32.1	2.2	6.7
	10	207	141	159	169	34	20.1	27.6	33.1	29.9	30.2	2.8	9.1
	5	166	112	121	133	29	21.8	24.6	30.9	29.7	28.4	3.3	11.8
	1	90	61	64	72	16	22.9	22.0	26.2	26.2	24.8	2.4	9.8
	0.5	71	44	49	54	14	26.1	20.0	25.9	24.4	23.4	3.1	13.1
	0.1	48	31	38	39	9	22.8	14.5	20.9	18.6	18.0	3.2	17.9

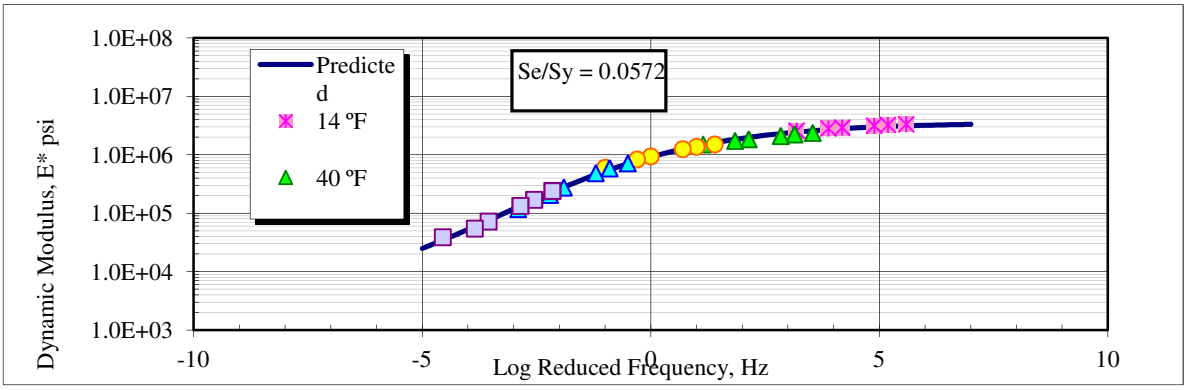

Average Dynamic Modulus and Phase Angle (LT-8 Hours)

Binder Grade: 64-22 **Binder Content:** 4.50%

Date: 09/30/2012 **Air Voids:** 7.12%

Temp.	Freq	Dynamic Modulus E*						Phase Angle, ϕ					
		Rep 1	Rep 2	Rep 3	Ave	Std.	Coeff.	Rep 1	Rep 2	Rep 3	Ave	Std.	Coeff.
(°F)	(Hz)	(ksi)	(ksi)	(ksi)	(ksi)	Dev.	of Var.	(Deg)	(Deg)	(Deg)	(Deg)	Dev.	of Var.
14	25	4874	4596	4970	4813	194	4.0	1.8	0.7	1.3	1.3	0.6	45.1
	10	4704	4390	4787	4627	209	4.5	6.1	3.1	3.0	4.1	1.8	43.7
	5	4536	4320	4678	4512	180	4.0	7.9	4.3	4.7	5.6	2.0	35.0
	1	4119	4085	4439	4214	195	4.6	9.2	5.2	6.2	6.9	2.1	30.2
	0.5	3954	3950	4310	4071	207	5.1	9.4	5.9	6.3	7.2	1.9	26.3
	0.1	3559	3496	3899	3652	217	5.9	10.8	7.3	8.0	8.7	1.9	21.8
40	25	3971	3049	3354	3458	469	13.6	5.4	4.6	4.3	4.8	0.5	11.3
	10	3702	2719	3087	3169	496	15.7	8.8	7.5	7.2	7.8	0.8	10.8
	5	3450	2539	2889	2959	460	15.5	10.0	8.7	9.4	9.4	0.6	6.7
	1	2941	2219	2516	2559	363	14.2	12.3	10.5	10.8	11.2	1.0	8.5
	0.5	2746	2084	2346	2392	334	13.9	12.8	11.6	11.9	12.1	0.6	5.1
	0.1	2179	1646	1888	1904	267	14.0	17.0	14.3	13.7	15.0	1.7	11.6
70	25	1797	1204	1672	1557	313	20.1	13.8	10.6	10.4	11.6	2.0	16.9
	10	1602	1064	1434	1366	275	20.2	18.5	14.7	15.0	16.0	2.1	13.2
	5	1421	947	1280	1216	243	20.0	19.8	17.0	16.5	17.7	1.8	9.9
	1	998	699	947	882	160	18.1	25.2	21.5	21.8	22.9	2.1	9.1
	0.5	870	607	834	770	143	18.5	26.7	23.6	23.9	24.8	1.7	7.0
	0.1	632	441	578	550	98	17.9	29.9	31.2	30.0	30.4	0.8	2.5
100	25	842	478	621	647	184	28.4	22.4	22.8	24.1	23.1	0.9	3.7
	10	677	376	484	512	153	29.8	24.2	27.2	25.3	25.5	1.5	5.9
	5	574	302	395	424	138	32.6	25.7	28.1	27.6	27.2	1.3	4.6
	1	358	174	229	254	94	37.2	28.8	31.0	29.4	29.7	1.1	3.7
	0.5	292	137	181	203	80	39.3	29.1	31.1	30.2	30.1	1.0	3.4
	0.1	187	82	111	126	55	43.2	27.3	31.1	27.8	28.7	2.1	7.4
130	25	324	166	194	228	84	37.0	25.0	31.3	30.3	28.9	3.4	11.8
	10	235	118	136	163	63	38.8	23.3	29.3	28.0	26.8	3.1	11.7
	5	182	89	104	125	50	40.3	24.8	28.8	28.1	27.2	2.1	7.9
	1	101	49	58	69	28	40.5	25.7	26.2	24.4	25.5	0.9	3.6
	0.5	74	38	47	53	19	35.3	38.6	25.9	21.4	28.6	8.9	31.1
	0.1	58	27	35	40	16	41.2	20.0	20.3	16.2	18.8	2.3	12.1

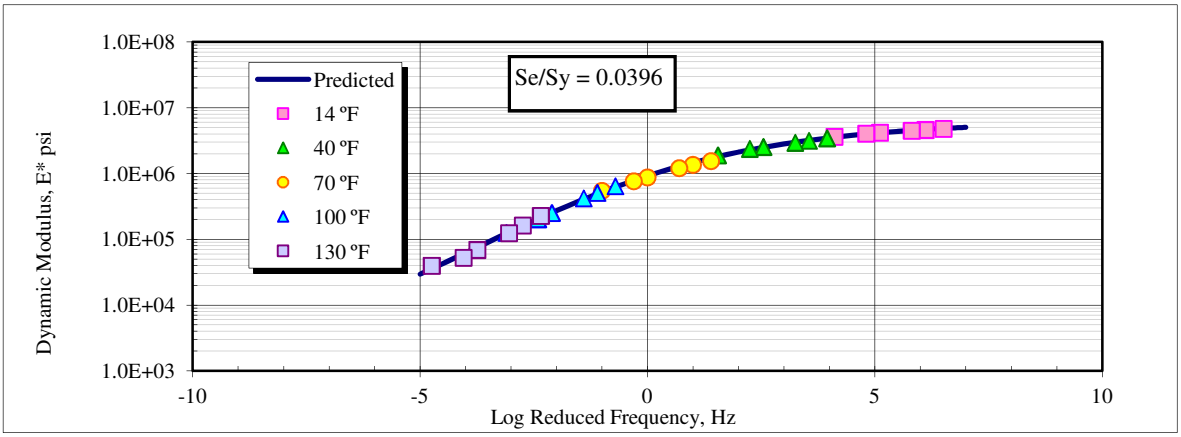

Average Dynamic Modulus and Phase Angle -AG4HT

Binder 64-22 **Binder Content: 4.50%**

Date: 09/30/2012 **Air Voids: 7.11%**

Temp	Freq	Dynamic Modulus E*						Phase Angle, φ					
		Rep 1	Rep 2	Rep 3	Ave	Std. Dev.	Coeff. of Var.	Rep 1	Rep 2	Rep 3	Ave	Std. Dev.	Coeff. of Var.
(°F)	(Hz)	(ksi)	(ksi)	(ksi)	(ksi)			(Deg)	(Deg)	(Deg)	(Deg)		
14	25	3298	2715	3415	3143	375	11.9	0.4	0.8	3.2	1.5	1.5	101.7
	10	3224	2586	3369	3060	417	13.6	3.9	3.6	6.6	4.7	1.6	34.5
	5	3167	2510	3266	2981	411	13.8	4.4	4.8	7.9	5.7	1.9	33.9
	1	2932	2303	3029	2755	394	14.3	5.4	5.7	8.9	6.7	1.9	28.8
	0.5	2841	2230	2946	2672	387	14.5	5.5	7.3	9.5	7.4	2.0	26.8
	0.1	2605	2016	2638	2420	350	14.5	6.6	7.5	11.9	8.7	2.9	33.2
40	25	2264	1874	2644	2261	385	17.0	3.3	4.9	7.1	5.1	1.9	37.6
	10	2212	1821	2479	2171	331	15.2	6.6	8.1	11.7	8.8	2.6	30.0
	5	2098	1694	2307	2033	312	15.3	8.2	9.5	12.5	10.1	2.2	21.9
	1	1816	1431	1928	1725	261	15.1	9.7	11.8	15.7	12.4	3.0	24.3
	0.5	1719	1331	1779	1610	243	15.1	10.7	12.8	17.0	13.5	3.2	23.7
	0.1	1486	1125	1431	1347	195	14.5	13.3	14.5	19.9	15.9	3.5	22.2
70	25	1563	1162	1361	1362	201	14.7	10.5	10.9	15.8	12.4	2.9	23.6
	10	1383	1044	1217	1215	169	13.9	15.5	16.3	21.8	17.8	3.4	19.2
	5	1227	940	1095	1087	144	13.2	17.2	17.9	24.7	19.9	4.1	20.7
	1	883	666	761	770	109	14.1	21.4	22.4	29.8	24.5	4.6	18.7
	0.5	759	586	658	667	87	13.1	25.7	23.6	31.9	27.1	4.4	16.1
	0.1	531	411	478	473	60	12.7	28.0	26.9	36.7	30.5	5.4	17.6
100	25	632	472	596	566	84	14.8	25.0	22.6	27.7	25.1	2.6	10.2
	10	515	370	472	452	75	16.5	26.2	27.1	29.0	27.4	1.4	5.2
	5	425	304	386	372	62	16.6	28.0	28.8	32.2	29.7	2.3	7.6
	1	266	181	209	219	44	20.0	31.7	32.9	39.2	34.6	4.0	11.5
	0.5	213	141	160	171	38	22.0	32.6	34.6	39.4	35.5	3.5	9.9
	0.1	133	87	100	107	23	22.0	31.5	32.9	37.7	34.0	3.3	9.6
130	25	205	162	263	210	51	24.2	29.4	30.0	31.7	30.3	1.2	3.9
	10	143	111	185	146	37	25.5	28.9	29.9	30.8	29.8	1.0	3.3
	5	111	86	139	112	26	23.4	29.7	28.3	28.8	28.9	0.7	2.4
	1	61	43	67	57	12	21.8	28.0	27.4	25.9	27.1	1.1	4.1
	0.5	46	32	54	44	11	24.8	26.7	25.5	24.5	25.6	1.1	4.2
	0.1	33	24	45	34	11	31.3	22.3	17.5	19.2	19.7	2.4	12.3

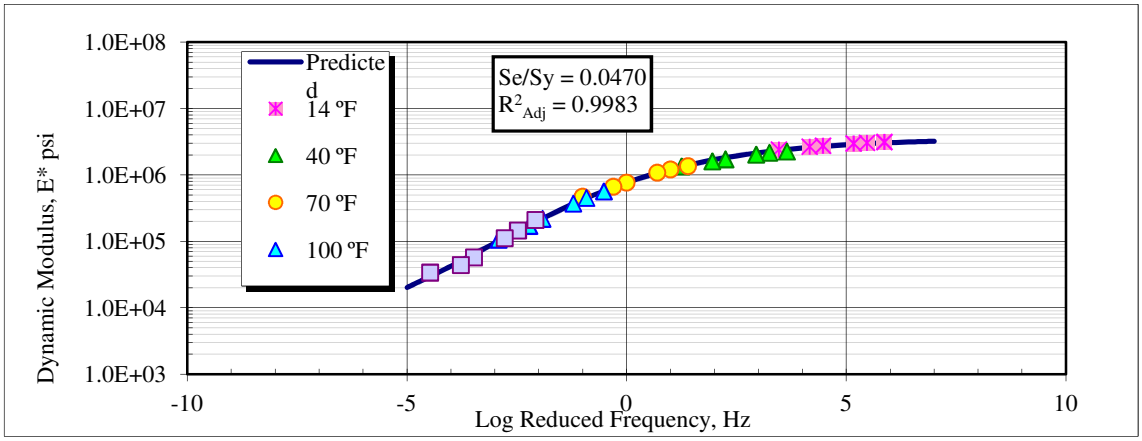

Average Dynamic Modulus and Phase Angle (HT-6 Hours)

Binder Grade: 64-22 **Binder Content:** 4.50%

Date: 09/30/2012 **Air Voids:** 7.47%

Temp	Freq	Dynamic Modulus E*						Phase Angle, φ					
		Rep 1	Rep 2	Rep 3	Ave	Std.	Coeff.	Rep 1	Rep 2	Rep 3	Ave	Std.	Coeff.
(°F)	(Hz)	(ksi)	(ksi)	(ksi)	(ksi)	Dev.	of Var.	(Deg)	(Deg)	(Deg)	(Deg)	Dev.	of Var.
14	25	3191	2169	3159	2840	581	20.5	2.7	4.1	-0.2	2.2	2.2	100.5
	10	3184	2135	3092	2803	581	20.7	5.1	6.7	2.6	4.8	2.1	43.8
	5	3102	2078	3018	2733	568	20.8	6.0	7.7	4.0	5.9	1.9	31.6
	1	2860	1916	2797	2524	528	20.9	6.9	8.6	4.9	6.8	1.9	27.3
	0.5	2762	1857	2730	2449	513	21.0	7.5	9.0	5.3	7.2	1.9	25.7
	0.1	2527	1719	2531	2259	468	20.7	8.3	9.5	5.9	7.9	1.8	23.1
40	25	2215	1616	2431	2088	422	20.2	4.6	2.8	3.0	3.5	1.0	28.8
	10	2120	1558	2285	1987	381	19.2	8.6	6.1	6.7	7.2	1.3	17.8
	5	2011	1472	2169	1884	366	19.4	9.3	6.7	7.1	7.7	1.4	18.4
	1	1760	1280	1895	1645	323	19.6	10.5	8.4	9.2	9.3	1.1	11.5
	0.5	1659	1208	1783	1550	303	19.5	10.8	9.0	10.2	10.0	0.9	9.0
	0.1	1458	1044	1504	1336	253	19.0	12.4	10.5	12.6	11.8	1.1	9.6
70	25	1445	1165	1351	1320	143	10.8	8.5	9.0	8.7	8.7	0.3	3.0
	10	1314	1067	1218	1200	125	10.4	13.6	13.6	14.0	13.7	0.2	1.6
	5	1198	967	1104	1090	116	10.6	16.2	15.1	15.3	15.5	0.5	3.5
	1	910	735	836	827	88	10.6	19.1	14.6	19.3	17.7	2.7	15.2
	0.5	817	656	749	741	81	10.9	20.4	19.8	20.4	20.2	0.4	1.8
	0.1	610	488	533	544	62	11.4	23.4	23.9	25.1	24.2	0.9	3.6
100	25	697	573	605	625	65	10.3	24.1	20.9	23.1	22.7	1.6	7.1
	10	584	467	494	515	61	11.9	24.0	22.4	24.9	23.8	1.3	5.5
	5	485	400	433	440	43	9.8	26.4	25.3	27.0	26.2	0.9	3.3
	1	287	260	262	270	15	5.5	29.9	29.9	30.8	30.2	0.5	1.7
	0.5	225	212	209	215	9	4.0	34.2	32.5	31.7	32.8	1.3	3.9
	0.1	140	122	131	131	9	6.9	30.1	28.5	31.8	30.1	1.7	5.5
130	25	258	211	248	239	25	10.4	27.3	23.0	30.1	26.8	3.6	13.4
	10	185	153	180	173	17	10.0	29.8	28.7	31.0	29.8	1.1	3.8
	5	143	120	134	132	12	9.0	28.3	29.0	31.0	29.4	1.4	4.7
	1	78	64	80	74	8	11.3	30.2	30.1	29.1	29.8	0.6	2.0
	0.5	60	50	61	57	6	11.0	29.7	31.1	28.4	29.7	1.3	4.5
	0.1	41	34	40	38	4	9.8	22.6	27.3	21.4	23.8	3.1	13.1

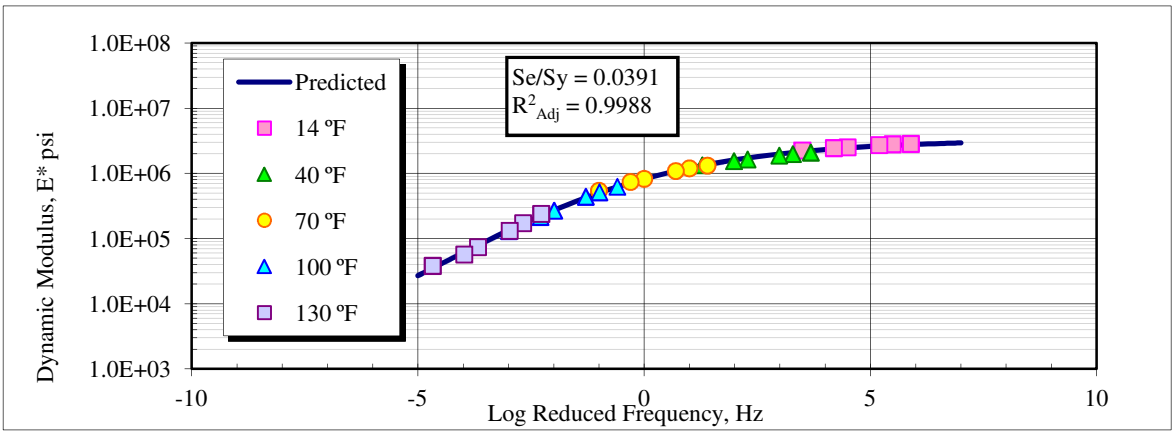

Average Dynamic Modulus and Phase Angle (HT 8-Hours)

Binder Grade: 64-22 **Binder Content:** 4.50%

Date: 07/30/2010 **Average Air Voids:** 7.41%

Temp	Freq	Dynamic Modulus E*						Phase Angle, φ					
		Rep 1	Rep 2	Rep 3	Ave	Std.	Coeff.	Rep 1	Rep 2	Rep 3	Ave	Std.	Coeff.
(°F)	(Hz)	(ksi)	(ksi)	(ksi)	(ksi)	Dev.	of Var.	(Deg)	(Deg)	(Deg)	(Deg)	Dev.	of Var.
14	25	3364	4928	3916	4070	793	19.5	3.0	1.8	2.6	2.5	0.6	24.7
	10	3322	4763	3823	3969	732	18.4	5.9	4.6	5.7	5.4	0.7	13.3
	5	3228	4641	3702	3857	719	18.6	6.3	5.8	7.2	6.4	0.7	11.2
	1	2951	4353	3449	3584	711	19.8	7.7	6.5	7.7	7.3	0.7	9.7
	0.5	2848	4239	3348	3478	705	20.3	8.1	7.1	7.7	7.6	0.5	6.7
	0.1	2645	3949	3115	3236	660	20.4	8.9	8.0	8.8	8.6	0.5	5.8
40	25	2490	3485	3113	3029	503	16.6	4.6	3.4	6.1	4.7	1.4	29.2
	10	2384	3300	2929	2871	461	16.1	8.4	7.2	8.7	8.1	0.8	9.8
	5	2255	3151	2769	2725	450	16.5	9.3	7.7	10.6	9.2	1.5	15.9
	1	1951	2806	2415	2391	428	17.9	10.8	8.8	11.8	10.5	1.5	14.6
	0.5	1845	2668	2286	2267	412	18.2	11.6	9.3	12.5	11.1	1.6	14.7
	0.1	1562	2333	1961	1952	385	19.7	13.4	11.2	14.8	13.1	1.8	13.8
70	25	1383	1994	2054	1810	371	20.5	9.7	6.4	11.7	9.3	2.7	28.9
	10	1206	1813	1853	1624	362	22.3	13.9	11.9	14.5	13.5	1.4	10.1
	5	1067	1636	1678	1460	341	23.4	14.6	13.5	17.2	15.1	1.9	12.5
	1	853	1326	1304	1161	267	23.0	18.3	16.1	19.5	18.0	1.7	9.4
	0.5	755	1290	1175	1073	282	26.2	20.4	20.2	21.8	20.8	0.8	4.1
	0.1	561	964	879	802	212	26.5	23.1	24.3	25.9	24.4	1.4	5.9
100	25	686	1005	847	846	159	18.8	22.9	17.2	21.0	20.4	2.9	14.3
	10	559	835	700	698	138	19.8	26.6	19.1	22.1	22.6	3.8	16.7
	5	475	721	612	603	123	20.4	27.2	22.7	26.4	25.4	2.4	9.4
	1	296	455	390	380	80	21.0	30.8	27.7	32.6	30.4	2.5	8.2
	0.5	239	381	316	312	71	22.7	33.6	29.8	35.3	32.9	2.8	8.6
	0.1	143	254	218	205	57	27.8	32.8	28.5	35.5	32.3	3.5	10.9
130	25	255	454	379	363	101	27.7	26.9	26.1	28.8	27.3	1.4	5.0
	10	189	354	280	274	83	30.2	31.6	26.3	29.9	29.3	2.7	9.1
	5	147	290	230	222	72	32.3	31.6	26.0	31.5	29.7	3.2	10.7
	1	83	162	138	128	40	31.6	30.5	28.2	33.5	30.8	2.7	8.6
	0.5	64	132	112	102	35	34.0	29.8	30.4	32.2	30.8	1.3	4.1
	0.1	40	87	76	68	24	35.8	26.2	28.6	30.7	28.5	2.3	8.0

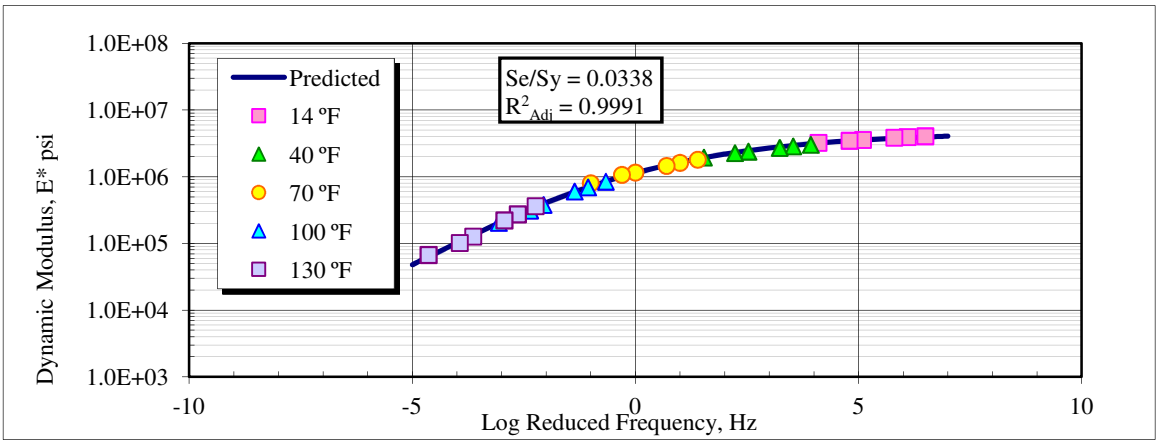

	|*E**| Predictive Model Final Parameter Values					
	Standard Temperature Conditioned (LT) Samples			Elevated Temperature Conditioned (HT) Samples		
Parameter	LT -4Hrs	LT -6Hrs	LT -8Hrs	HT -4Hrs	HT -6Hrs	HT -8Hrs
δ	3.7706	3.4149	2.9277	3.2964	2.7341	2.8648
α	2.7574	3.1377	3.8701	3.2503	3.7878	3.8077
β	1.1681	1.4622	1.2910	1.3632	1.6568	1.6489
γ	0.5229	0.4500	0.3405	0.4323	0.3736	0.3482
a	0.0002	0.0001	0.0002	0.0002	0.0002	0.0003
b	-0.1029	-0.0861	-0.1123	-0.0958	-0.0941	-0.1132
c	6.1329	5.3690	6.6364	5.7756	5.7799	6.6350
Log a(14°F)	4.7355	4.1894	5.1133	4.4716	4.4951	5.1014
Log a(40°F)	2.3734	2.1447	2.5514	2.2535	2.2860	2.5343
Log a(70°F)	0.0000	0.0000	0.0000	0.0000	0.0000	0.0000
Log a(100°F)	-1.9802	-1.9013	-2.1007	-1.9111	-1.9896	-2.0588
Log a(130°F)	-3.5589	-3.5501	-3.7423	-3.4713	-3.6735	-3.6341
Se/Sy	0.0447	0.0572	0.0396	0.0470	0.0391	0.0338
R2	0.9985	0.9975	0.9988	0.9983	0.9988	0.9991

APPENDIX C

IDT RESULTS

IDT test results for top and bottom portions of each samples							
Temperature	Specimen ID		Air Voids	S_t		Fracture Energy	
				kPa	psi	J/m^2	in-lbf/in^2
21.1^{0C}	AG4HT	Top	6.39%	1632.80	236.82	9,038.60	51.61
	AG4HB	Bottom	6.45%	1548.20	224.55	7,179.77	41.00
21.1^{0C}	AG4LT	Top	6.26%	1630.20	236.44	7,958.12	45.44
	AG4LB	Bottom	6.27%	1578.90	229.00	8,489.77	48.48
21.1^{0C}	AG6HT	Top	6.58%	1932.20	280.24	6,248.04	35.68
	AG6HB	Bottom	6.87%	1905.90	276.43	6,498.58	37.11
21.1^{0C}	AG6LT	Top	6.28%	1688.20	244.85	7,138.48	40.76
	AG6LB	Bottom	6.59%	1809.20	262.40	8,298.89	47.39
21.1^{0C}	AG8HT	Top	6.71%		Lost Sample		
	AG8HB	Bottom	6.67%	2084.50	302.33	6,601.99	37.70
21.1^{0C}	AG8LT	Top	6.40%	1635.40	237.19	8,389.56	47.91
	AG8LB	Bottom	7.54%	1722.30	249.80	7,098.89	40.54